

FLUORESCENCE DIP SPECTROSCOPY
OF COPPER AND SILVER
AS A DIAGNOSTIC TOOL
IN SEVERAL ATOMIZATION RESERVOIRS

By

DONNA JEAN ROBIE

A DISSERTATION PRESENTED TO THE GRADUATE SCHOOL
OF THE UNIVERSITY OF FLORIDA IN PARTIAL FULFILLMENT
OF THE REQUIREMENTS FOR THE DEGREE OF
DOCTOR OF PHILOSOPHY

UNIVERSITY OF FLORIDA

1993

ACKNOWLEDGEMENTS

I want to express my gratitude to many people at the University of Florida for their insight and suggestions regarding the work presented in this dissertation especially Ben Smith and Giuseppe Petrucci. The entire Winefordner group deserves recognition, since, at some time or another, each person has given me their support in some way. I am especially grateful to Jim Winefordner for giving me the opportunity to learn from the best.

In addition to professional support, I was lucky enough to have an emotional support system including my parents and my sister. I want to give a much deserved thank you to Stefanie Pagano for always being there to tell me what I needed to hear, whether I wanted to hear it or not. I also want to acknowledge Mike Naughton for several years of support through graduate school. And I want to say thank you to Rafael Vargas, without whom I never would have made it through my last months at the University of Florida.

I especially want to acknowledge my brother, Daniel Robie, without whose support and love I would not be receiving this degree. Through his constant optimism and patience, he has walked me through some difficult times, and there is no way I can completely express my gratitude. He has been a constant inspiration to me, and I hope he will continue to share his strength with me throughout my life.

TABLE OF CONTENTS

ACKNOWLEDGEMENTS	ii
ABSTRACT	v
CHAPTER 1 INTRODUCTION	1
CHAPTER 2 ATOMIC FLUORESCENCE SPECTROSCOPY	4
Conventional Source Atomic Fluorescence Spectroscopy	4
History	4
Theory	6
Types of atomic fluorescence	6
Theoretical treatment of atomic fluorescence spectroscopy	39
Applications of Conventional Source AFS	42
Advantages and Disadvantages	43
Laser Excited Atomic Fluorescence Spectroscopy (LEAFS)	44
History of Flame LEAFS	45
History of Furnace LEAFS	52
History of ICP-LEAFS	54
History of LEAFS in Other Atomization Reservoirs	56
History of Two Photon LEAFS	57
History of Two-Color Excitation Fluorescence	59
Advantages and Disadvantages of LEAFS	60
CHAPTER 3 DIAGNOSTIC APPLICATIONS OF LEAFS	62
Diagnostic Characterization of Atom Sources	62
Investigation of Atomic Parameters Using LEAFS	64
Investigation of Atomic Parameters Using Two-Color LEAFS	65
Advantages and Disadvantages of LEAFS as a Diagnostic Tool	70
CHAPTER 4 INSTRUMENTATION USED IN LEAFS	72
Excitation Sources	72
Principles of Lasers	75
Types of Lasers	81
Atomization Reservoirs used in LEAFS	84

Flames	88
Plasmas	92
Electrothermal Atomizers	96
Other Atomization Reservoirs used in LEAFS	97
Wavelength Selection Devices	98
Detection Methods used in LEAFS	101
CHAPTER 5 RATE EQUATIONS THEORETICAL TREATMENT OF	
LEAFS	105
Two Level Atomic System	105
Three Level Atomic System	115
Fluorescence Dip Spectroscopy	122
Three Level Atom System	122
Five Level Atom System	129
Negative/Inverse Fluorescence Dip	133
Time Dependent Fluorescence Dips	148
CHAPTER 6 EXPERIMENTAL	167
Instrumentation	167
Analyte Solutions	174
Experimental Procedure	175
CHAPTER 7 RESULTS AND DISCUSSION	179
Experiments Performed	179
Theoretical Modeling	205
Excitation at $\lambda_{1 \rightarrow 3}$ and $\lambda_{3 \rightarrow 4}$	207
Excitation at $\lambda_{1 \rightarrow 2}$ and $\lambda_{2 \rightarrow 4}$	210
Excitation at $\lambda_{1 \rightarrow 2}$ and $\lambda_{3 \rightarrow 4}$	212
Excitation at $\lambda_{1 \rightarrow 3}$ and $\lambda_{2 \rightarrow 4}$	214
Saturation Through Laser Excitation	215
CHAPTER 8 CONCLUSIONS	246
REFERENCE LIST	249
BIOGRAPHICAL SKETCH	250

Abstract of Dissertation Presented to the Graduate School
of the University of Florida in Partial Fulfillment of the
Requirements for the Degree of Doctor of Philosophy

FLUORESCENCE DIP SPECTROSCOPY
OF COPPER AND SILVER
AS A DIAGNOSTIC TOOL
IN SEVERAL ATOMIZATION RESERVOIRS

By

Donna Jean Robie

December 1993

Chairperson: James D. Winefordner
Major Department: Department of Chemistry

The application of two-step laser excited atomic fluorescence spectroscopy (LEAFS) to the field of analytical chemistry has proven to be a method demonstrating unprecedented sensitivity and selectivity as well as being quite useful as a diagnostic tool in the examination of atom reservoirs and processes involved in the atom systems being studied. One variation on two-step LEAFS is fluorescence dip spectroscopy which involves the monitoring of the fluorescence signal, from a directly excited level or from an excited level populated through thermal means, as the result of one-step excitation and two step excitation with the second step tuned to deplete the population of the monitored level and, therefore, the fluorescence signal.

This kind of study can be used to examine relationships between excited atomic levels in much the same way saturated one-step fluorescence has been implemented in

the determination of physical parameters for transitions involving the ground state. The work performed for this dissertation was designed to examine the collisional relationship between two intermediate, excited state atomic levels and the effect this relationship has on the fluorescence dip measurement. Through one-step excitation, fluorescence is monitored from both the directly populated level and the collisionally coupled level. A second laser is then added while monitoring the fluorescence from the same level and calculating the difference. This decrease in signal is affected by several experimental parameters including the electronic spacing between these intermediate levels as well as the atom reservoir implemented in the experiment. Different atoms were examined in different collisional environments and the results compared to theoretical results following a rate equations approximation, which is discussed and outlined in detail in this dissertation.

CHAPTER 1 INTRODUCTION

Atomic fluorescence was first studied by Wood in 1902¹ and then in 1924 by Nichols and Howes,² both of these studies dealing with possible diagnostic applications of the technique. In 1963, Alkemade³ suggested the application of resonance fluorescence in flames as an analytical technique. Winefordner and Vickers⁴ then explored the application possibility and in doing so obtained sensitivities on the order of 1 $\mu\text{g/ml}$ for several elements causing them to comment that "... it [atomic fluorescence spectrometry] may prove superior to either atomic emission or atomic absorption flame spectrometry..." (161) as an analytical tool. Since these preliminary studies, the field of atomic fluorescence spectroscopy has quickly developed, the main goal being to obtain better detection limits, greater linear ranges, etc. than previous studies. In contrast, the growth in the field of analytical fluorescence spectroscopy as applied to diagnostic techniques, resulting in physical information about both the atom being studied as well as the atom cell of interest in the investigation, has fallen behind despite the fact that the results of such studies are crucial for the complete understanding of analytical spectroscopic techniques.

Many diagnostic studies have been performed in both the inductively coupled plasma (ICP) and an air/acetylene flame, the atom reservoirs of interest in the studies presented in this dissertation, as well as other atom cells, yet it is without argument that further study is necessary for physical characterization of flames and plasmas.^{5,6} In

fact, improvement upon previous analytical studies requires the understanding of the atom reservoir that is only possible through diagnostic studies to determine such parameters as the spatial distribution and temperature profile of the atom source. The availability of such information can facilitate the choices a chemist has to make as pertains to experimental conditions in a subsequent experiment employing a similar atomization environment.

In addition to information about the atom reservoir being employed in a study, it is also necessary for chemists to know as much as possible about the atom they are performing the studies on in order to select the best possible experimental conditions and procedure to yield the desired results. The need for fundamental atomic reference data was the study of a questionnaire distributed by P.W.J.M. Boumans and A. Scheeline.⁷ Several well recognized analytical chemists responded to the questionnaire^{8,9,10,11} with the consensus being that more reference data was needed about atomic systems since "...any information regarding the basic mechanism of excitation and deexcitation of selectively excited states will be of general usefulness to all techniques." (5)⁸ In Seliskar's response to the questionnaire,¹¹ he mentions that while fundamental physical information is incomplete for one-photon absorption studies, the same information for two-photon and multi-photon studies is practically nonexistent.

With the advent of these multi-photon excitation fluorescence studies, and subsequent growth in this field since the results of the above questionnaire were published has resulted in substantial routine use of such techniques, the need for physical information about transitions between excited states has become an even more pressing

one. This is the void in fundamental atomic information that the work presented in this dissertation will serve a small role in filling. Two atoms (Ag and Cu), approximated as five level systems, were studied using a two-photon excitation fluorescence technique resulting in information about the collisional relationships between excited state levels. These studies were performed in three different atomization reservoirs, namely an air/acetylene flame, the inductively coupled plasma (ICP), and a reduced pressure inductively coupled plasma to determine the effect that the different environments would have on the fluorescence measurements and, therefore, on the relationship of the excited state levels themselves.

CHAPTER 2 ATOMIC FLUORESCENCE SPECTROSCOPY

Conventional Source Atomic Fluorescence Spectroscopy

History

Atomic fluorescence spectroscopy involves the absorption of a photon at a certain wavelength by an atom resulting in an excited state atom and the subsequent de-excitation of this atom. This de-excitation results in the release of a photon of a certain wavelength usually of equal or lesser energy than the originally absorbed photon. Both the wavelengths of the absorbed and emitted radiation are characteristic of the atom species present.

The fluorescence of atomic vapors has been studied by 19th and 20th century physicists. These investigations have been discussed in detail by Mitchell and Zemansky¹² and Pringsheim¹³ and will not be addressed in this dissertation. In 1905, Wood¹⁴ observed the phenomenon of "...non-luminous sodium vapor radiating a brilliant yellow light when illuminated by the light from a very intense sodium flame." (513). Wood¹⁵ further studied sodium in a sealed glass tube with the excitation of the sodium D-doublet emission of a flame naming the resulting fluorescence resonance radiation. Atomic fluorescence was then explored by other spectroscopists in a similar manner for sodium,^{16,17,18,19} magnesium,²⁰ and lithium,²¹ In 1923, Nichols and

Howes^{22,23} suggested the implementation of a flame as the atom cell in atomic fluorescence experiments. In doing so, they were able to detect strontium, lithium, sodium, calcium, barium, and thallium.

The next substantial advance in the field of atomic fluorescence spectroscopy came in 1956 with the suggestion from Boers *et al.*²⁴ that these techniques could be used to study the analyte atom, not simply detect its presence. This suggestion was expanded upon by Alkemade³ at the Tenth International Spectroscopy Colloquium in 1963 where he described methods resulting in excited state atoms in flames. At this time Alkemade also suggested the use of atomic fluorescence spectroscopy as an analytical tool.

In 1964, Winefordner and Vickers⁴ investigated the possibility of the application of atomic fluorescence flame spectroscopy as discussed by Alkemade. They utilized metal vapor discharge tubes as excitation sources for mercury, zinc, cadmium, and thallium in an acetylene/oxygen flame eventually detecting these elements at concentrations as low as 1 $\mu\text{g/ml}$. This technique was further explored^{25,26,27,28,29} with the goal of these investigations being the development of a more sensitive technique through the optimization of optics, instrumentation, and flame conditions. In fact, these studies resulted in detection limits that established atomic fluorescence spectroscopy as a technique rivalling atomic emission and atomic absorption techniques in sensitivity.

Further improving upon atomic fluorescence spectroscopy was the suggestion of the usefulness of a continuum source for the excitation of the analyte species in the atom cell eliminating the need for a different line source for the investigation of each

element.³⁰ This introduction made it possible to evaluate atoms not determinable through previous excitation methods, and the field of atomic fluorescence spectroscopy virtually exploded with these previously undetectable atoms being examined at the same time as improvements were constantly being made on the experimental procedure to obtain the best sensitivity possible.

Theory

Types of atomic fluorescence

Atomic fluorescence spectroscopy is a technique in which the emission collected and measured is the direct result of radiational, rather than thermal, excitation. Fluorescence techniques have been defined based on their different excitation and fluorescence schemes,^{31,32,33} and this discussion of the types of atomic fluorescence will be based on these previous designations. There are two basic types of atomic fluorescence spectroscopy, resonance fluorescence and non-resonance fluorescence.

Resonance fluorescence (Figure 2-1) involves the same two levels in the excitation and de-excitation processes, meaning that the wavelength of the absorbed photon responsible for the excitation of the atom species is identical to that of the emitted photon involved in the atom's relaxation. This type of fluorescence has been found to be the most useful as pertains to analytical applications since the transition probabilities for these transitions are usually greater than those for other transitions. Resonance fluorescence techniques do not necessarily involve the ground state in the excitation and de-excitation process. If the atom probed by the excitation radiation is already in an

excited state, absorbs a photon at a given wavelength, and relaxes back to its original ground state fluorescing at that same wavelength, this is still considered a resonance fluorescence process, but is designated as excited state resonance fluorescence (Figure 2-2) to distinguish it from conventional resonance fluorescence.

The term non-resonance fluorescence is applied to all transitions where the wavelength of the photon absorbed is different than that of the emitted photon with the energy of the photon involved in the fluorescence process usually, but not always, being lower than the energy corresponding to the excitation process. This type of fluorescence can be divided into two categories : direct-line fluorescence and stepwise line fluorescence.

Direct-line fluorescence results when the excitation and de-excitation processes have a common upper level. Again, this process does not necessarily involve the ground state in either the absorption or emission processes, and has, therefore been divided into Stokes and anti-Stokes categories. Stokes processes involve the emission of a wavelength at a lower energy than the absorbed photon (Figure 2-3) while anti-Stokes fluorescence pertains to a process where the emitted photon is of a wavelength corresponding to an energy greater than that used for the excitation process (Figure 2-4). If these processes occur between two excited states, the terms excited state Stokes and excited state anti-Stokes are applied (Figures 2-5 & 2-6).

Stepwise-line fluorescence is said to occur when the upper levels involved in the excitation and emission steps are different. This can occur in several variations involving either a radiationless transition to a level lower than the initially excited one, or

thermally-assisted excitation to a higher excited level than that reached through absorption as a result of the excitation step prior to the fluorescence takes place. The many types of stepwise-line fluorescence include Stokes stepwise-line fluorescence (Figure 2-7), excited state Stokes stepwise-line fluorescence (Figure 2-8), anti-Stokes stepwise-line fluorescence (Figure 2-9), excited state anti-Stokes stepwise-line fluorescence (Figure 2-10), thermally assisted Stokes and anti-Stokes stepwise-line fluorescence (Figure 2-11), and excited state thermally assisted Stokes and anti-Stokes stepwise line fluorescence (Figure 2-12).

In addition to the types of fluorescence techniques just discussed, sensitized fluorescence can also occur in analytical studies. This type of fluorescence occurs when an excited state atom or molecule, the "donor", transfers its excitation energy to another atom species present, the "acceptor", in the atom cell through collisions. The acceptor then undergoes radiative de-excitation resulting in atomic fluorescence (Figure 2-13). This type of fluorescence requires a high population of "donor" atoms, however, and this is not normally the case especially in flame atom cells where energy transfer fluorescence mechanisms are of virtually no use because of the collisional deactivation of these "donors" resulting in an inadequate concentration to fulfill its intended purpose.

Another type of fluorescence is multi-photon excitation fluorescence in which two photons of the same wavelength are absorbed by the analyte atom through a virtual level (Figure 2-14). This type of fluorescence is not of much analytical use because the improbability of the transitions involved makes it an unlikely choice for analytical studies. Two-photon excitation techniques have since been extended to, more

Figure 2-1 : Resonance fluorescence (either process)

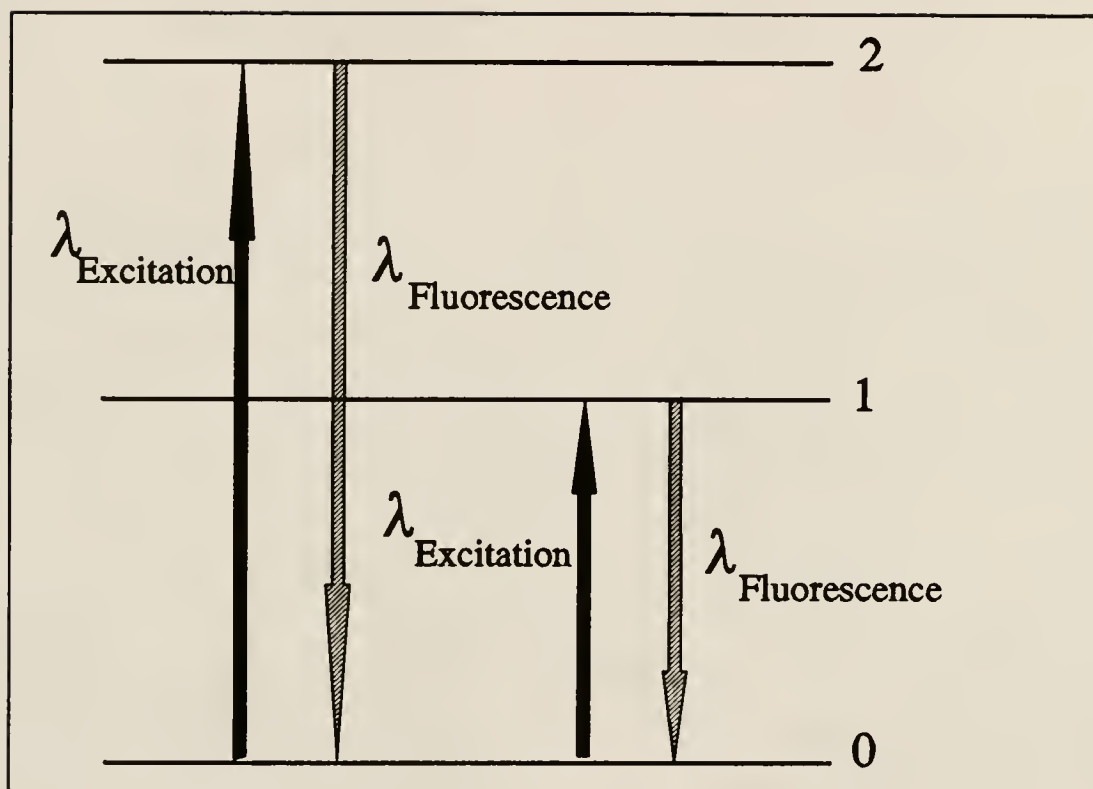


Figure 2-2 : Excited state resonance fluorescence

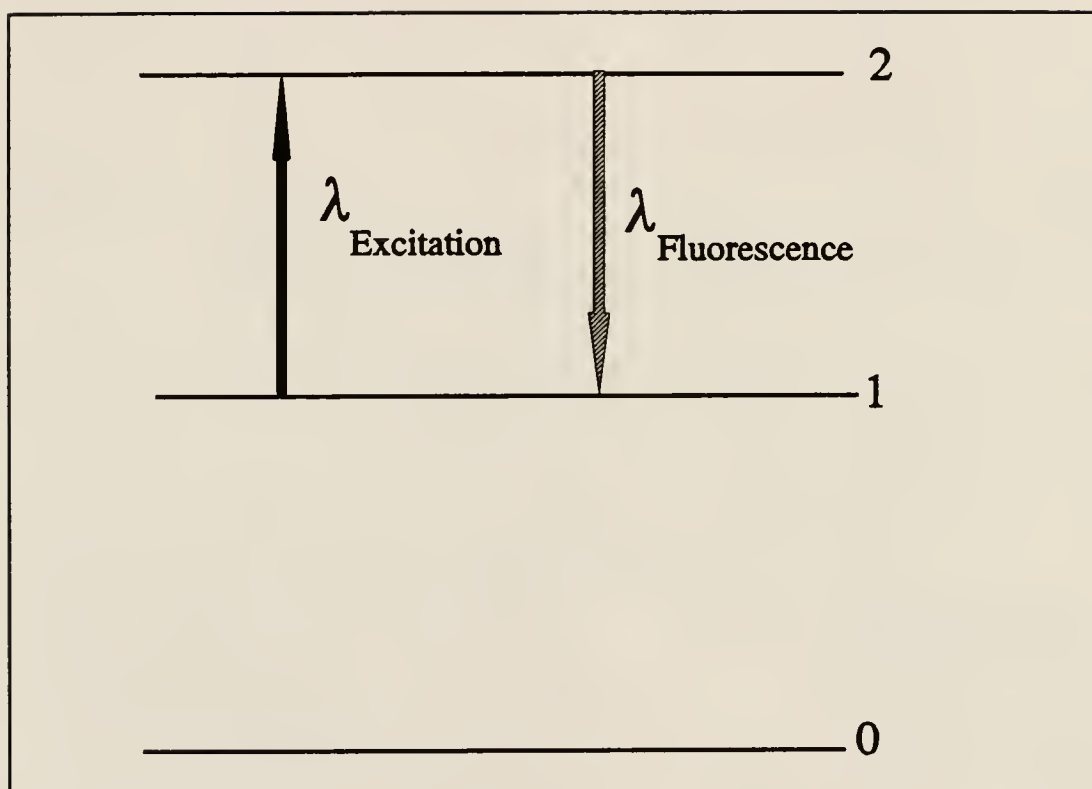


Figure 2-3 : Stokes direct line fluorescence

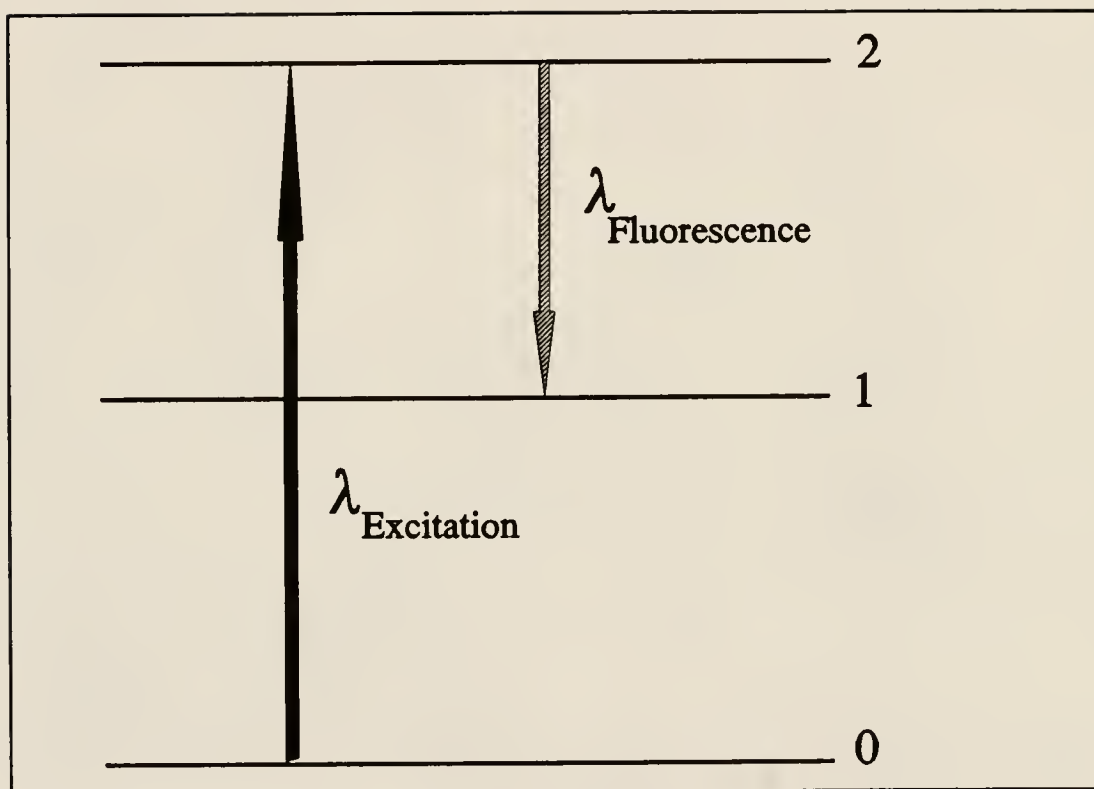


Figure 2-4 : Anti-Stokes direct line fluorescence

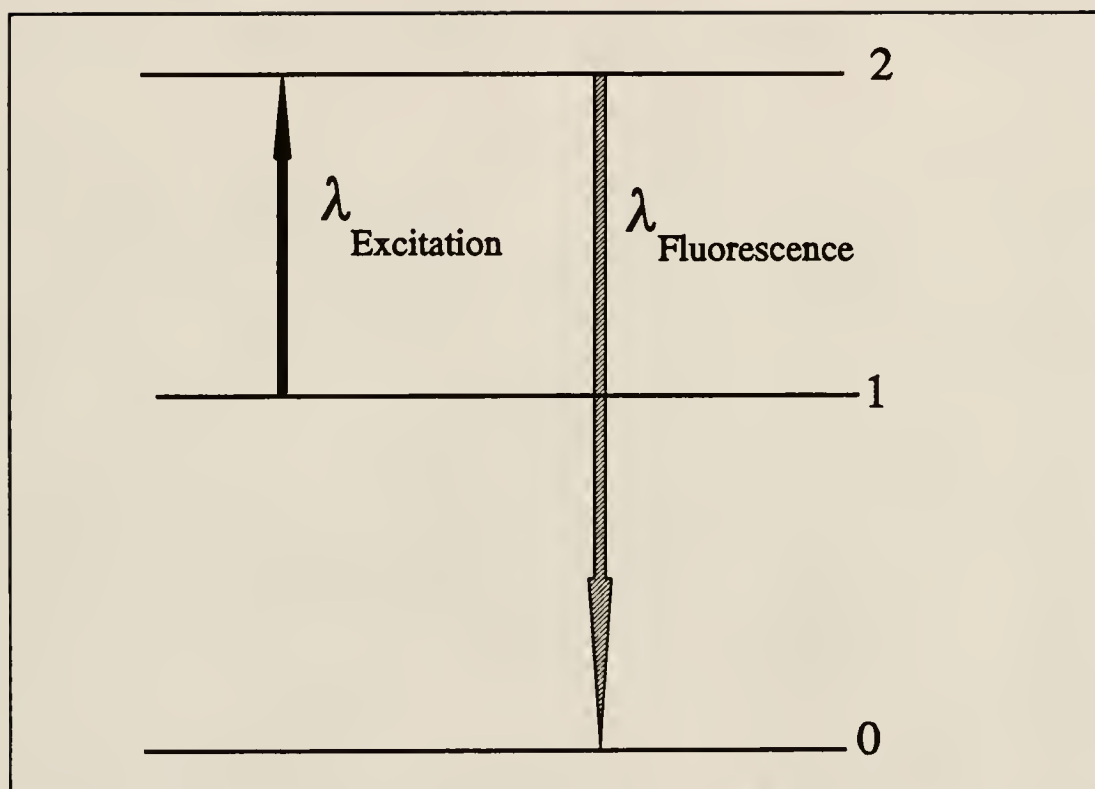


Figure 2-5 : Excited state Stokes direct line fluorescence

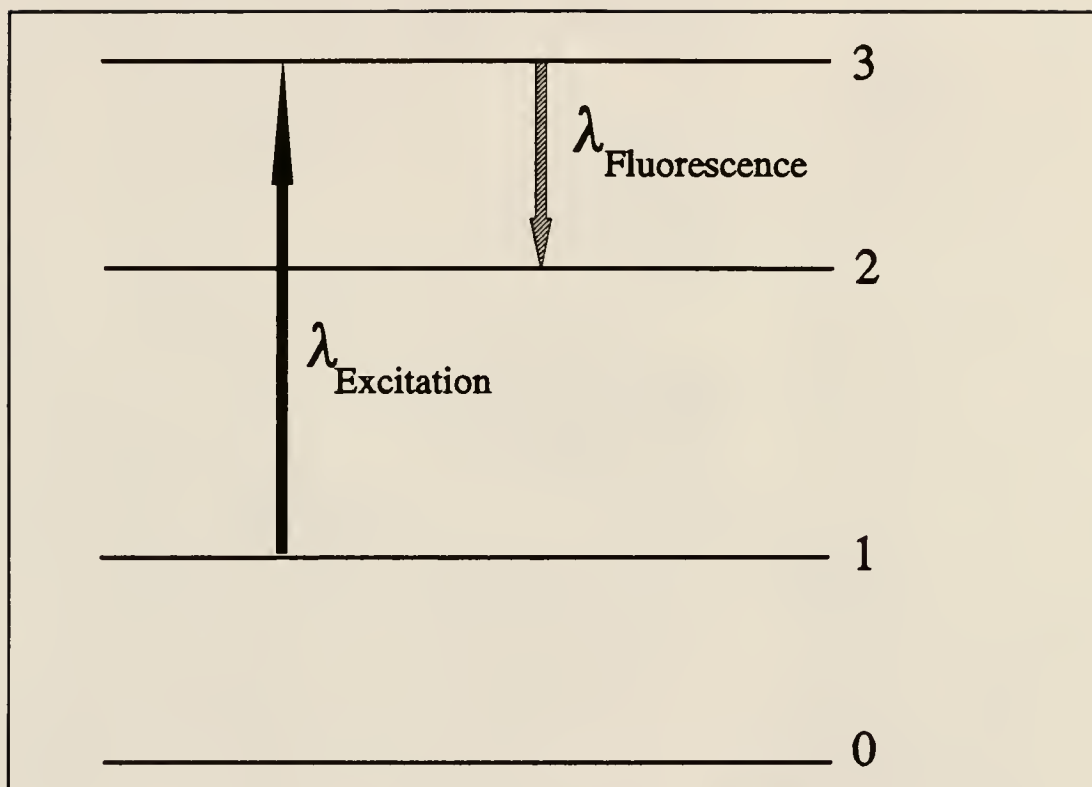


Figure 2-6 : Excited state anti-Stokes direct line fluorescence

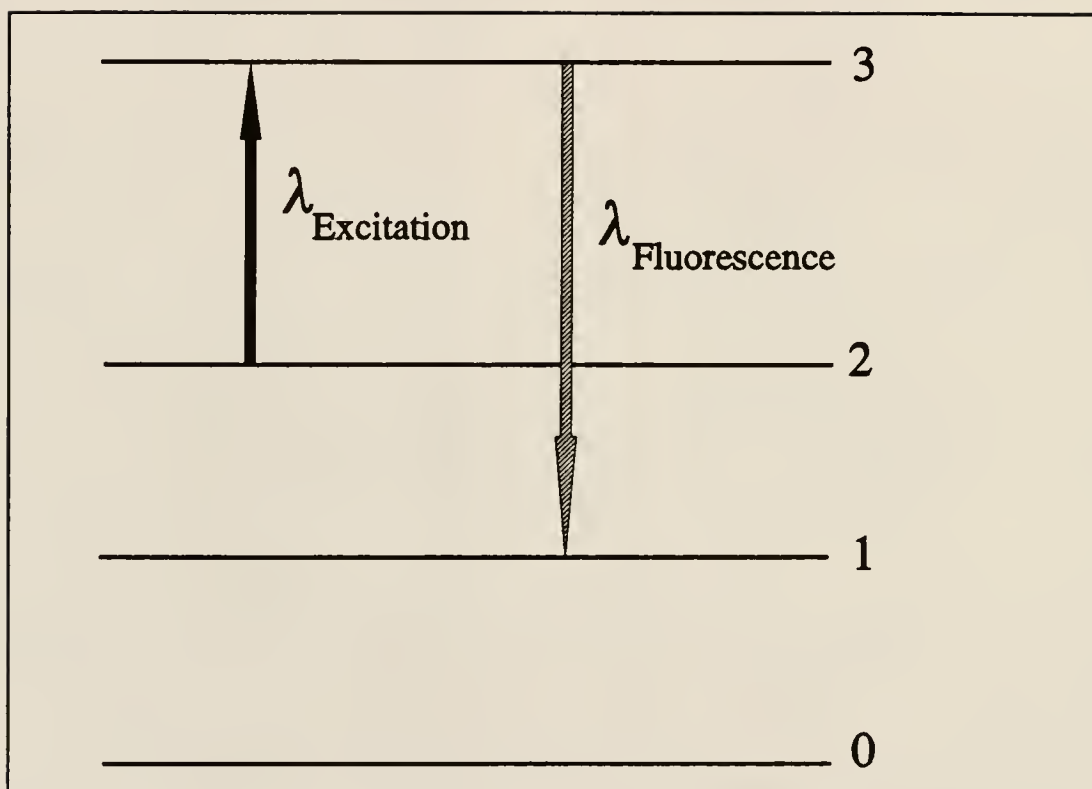


Figure 2-7 : Stokes stepwise line fluorescence

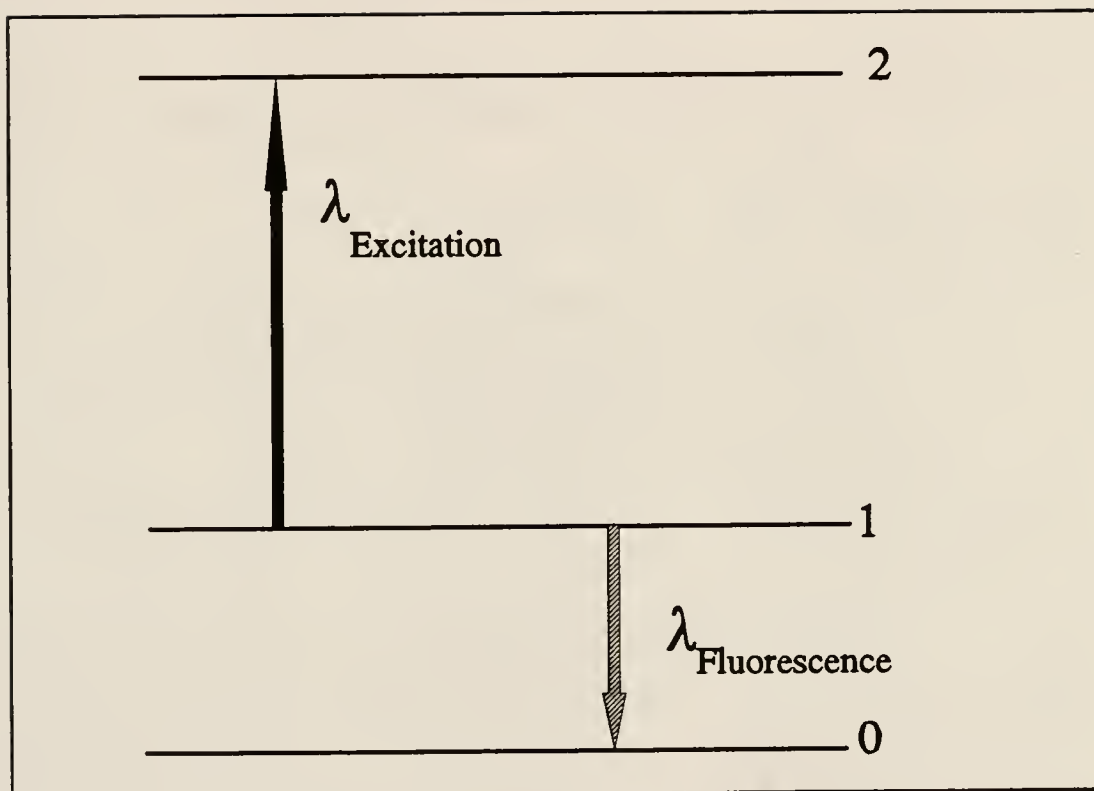


Figure 2-8 : Excited state Stokes stepwise line fluorescence

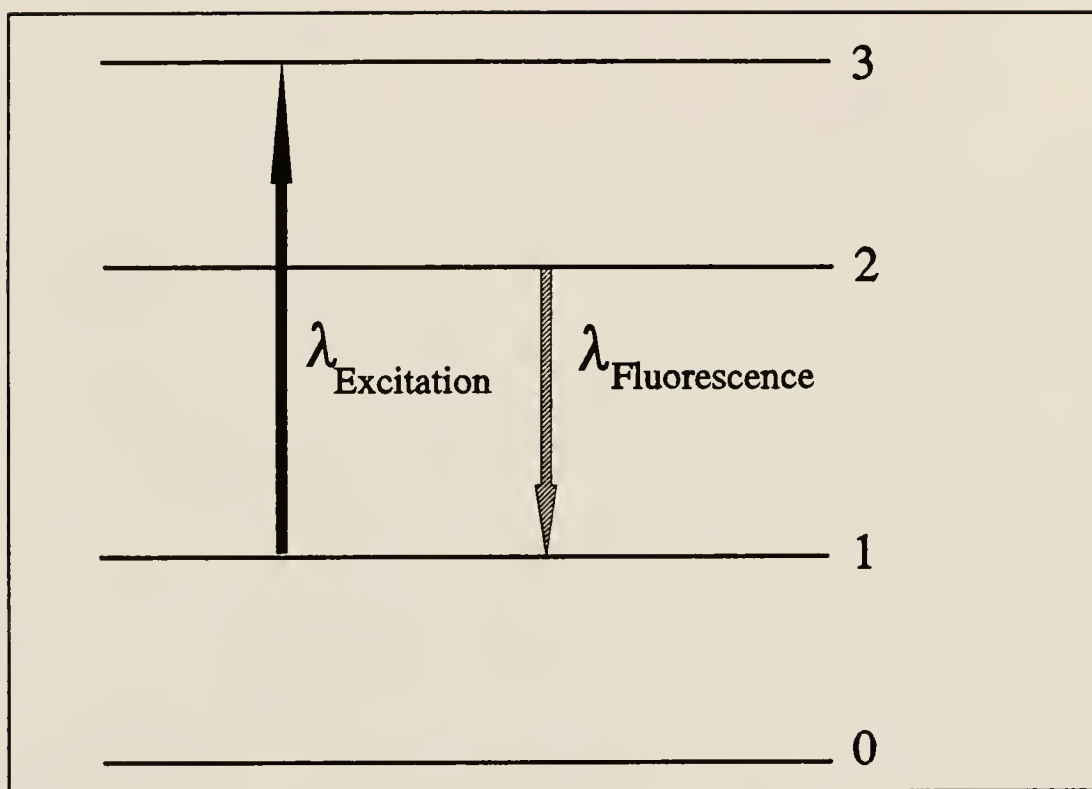


Figure 2-9 : Anti-Stokes stepwise line fluorescence

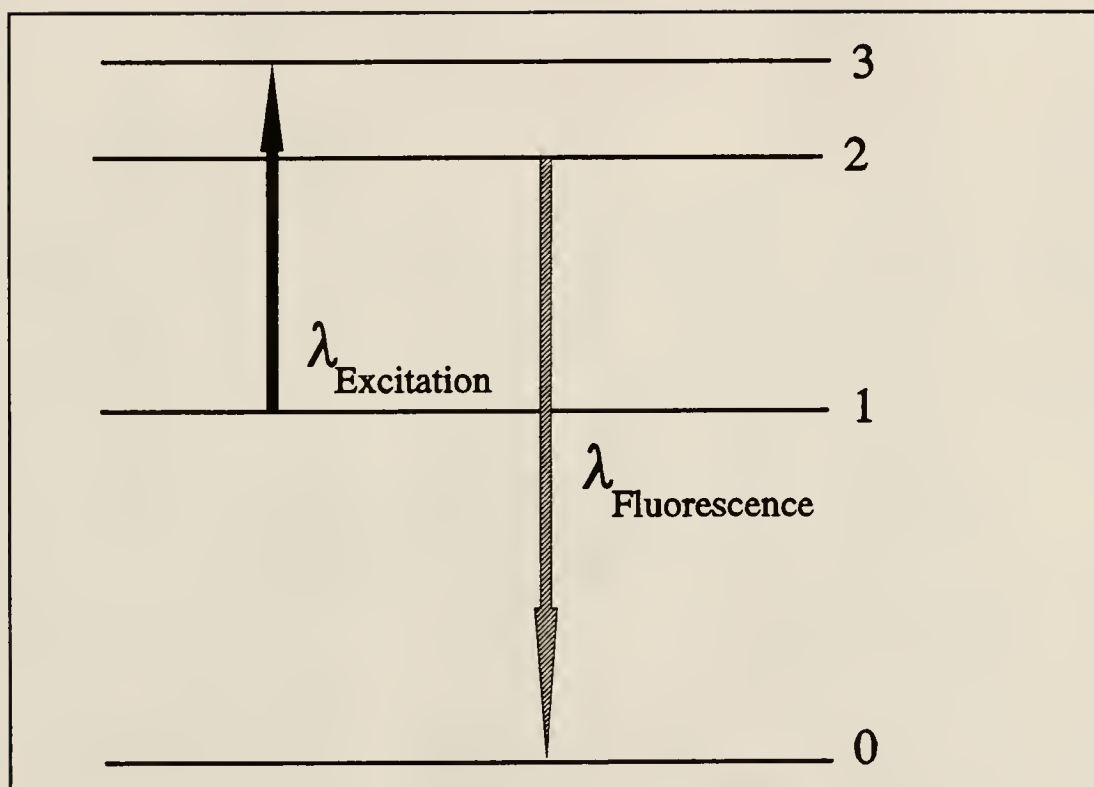


Figure 2-10 : Excited state anti-Stokes stepwise line fluorescence

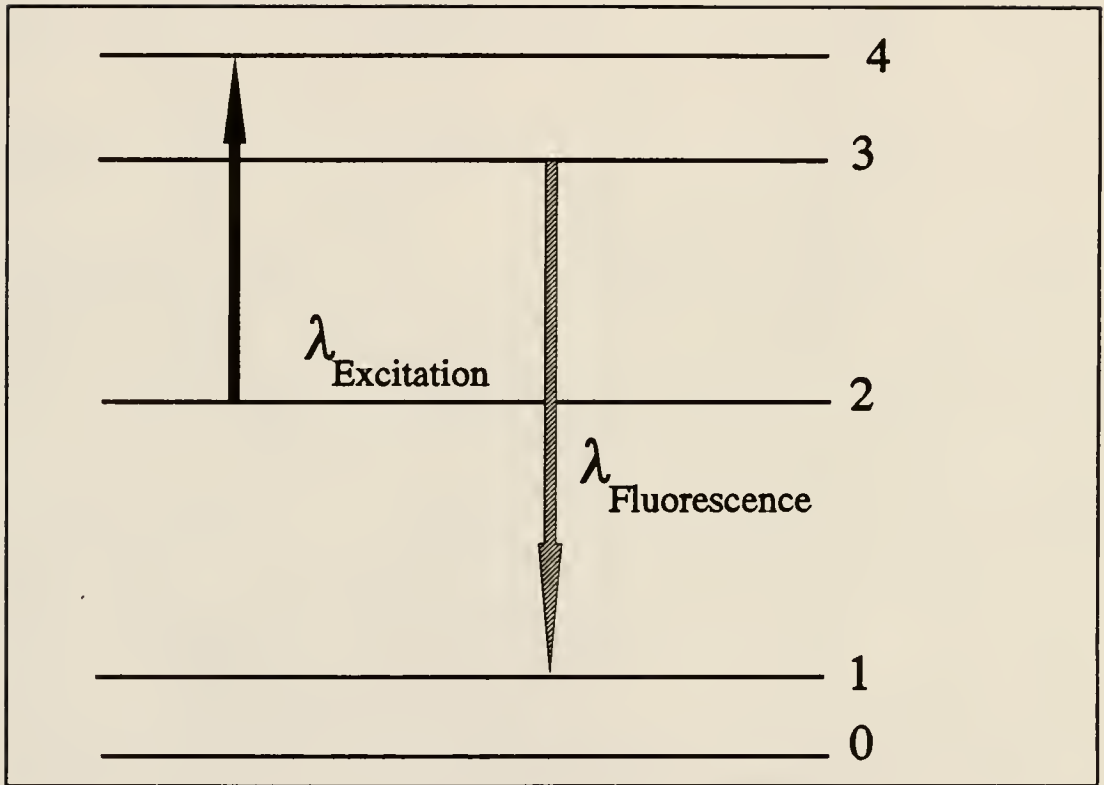


Figure 2-11 : Thermally assisted Stokes or anti-Stokes fluorescence
(Depending upon whether the fluorescence occurs at a longer or
shorter wavelength, respectively, than the absorbed radiation)

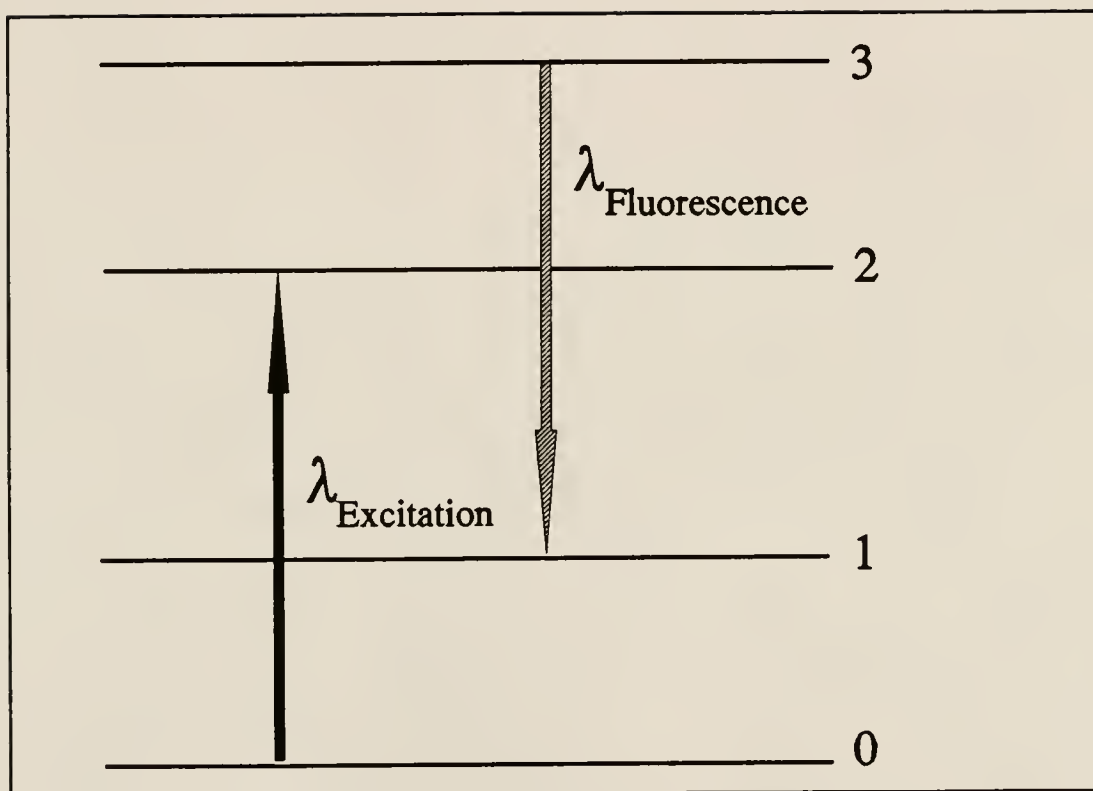


Figure 2-12 : Excited state thermally assisted Stokes or anti-Stokes fluorescence
(Depending upon whether the fluorescence occurs at a longer or
shorter wavelength, respectively, than the absorbed radiation)

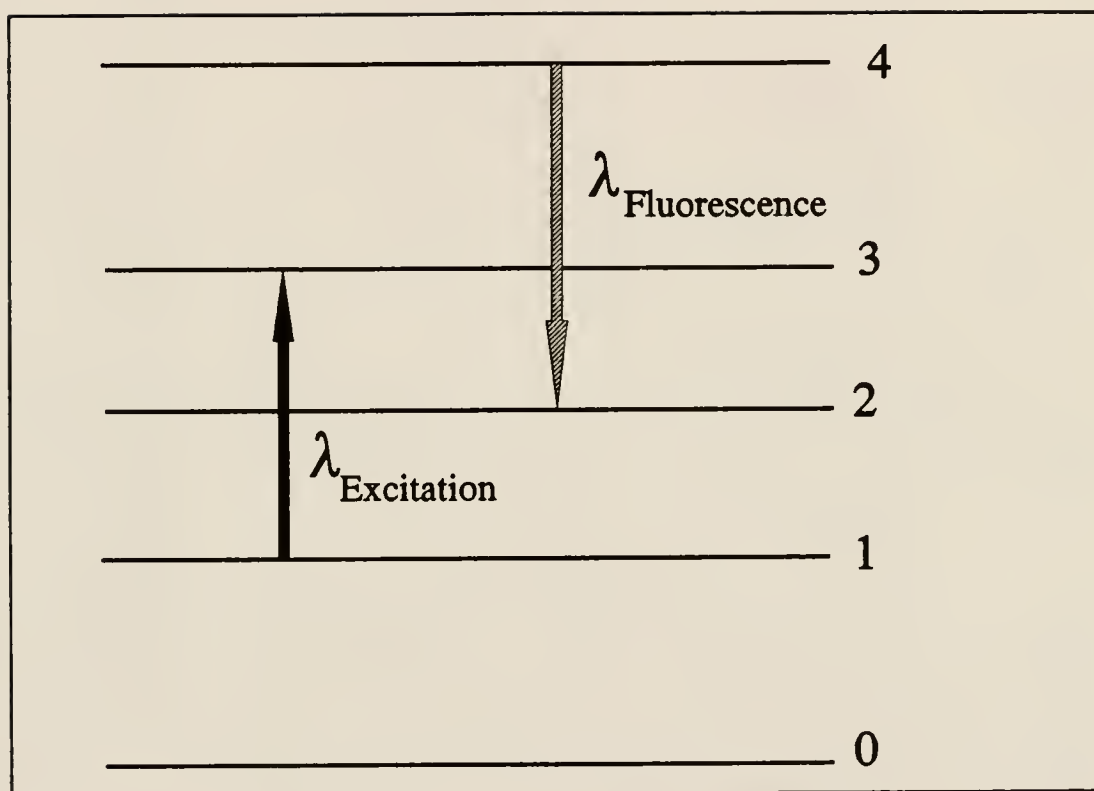


Figure 2-13 : Sensitized fluorescence (D = donor; D^* = excited state donor;
A = acceptor; A^* = excited acceptor; $h\nu_E$ = excitation radiation;
and $h\nu_F$ = fluorescence radiation)



Figure 2-14 : Multi-photon excitation fluorescence

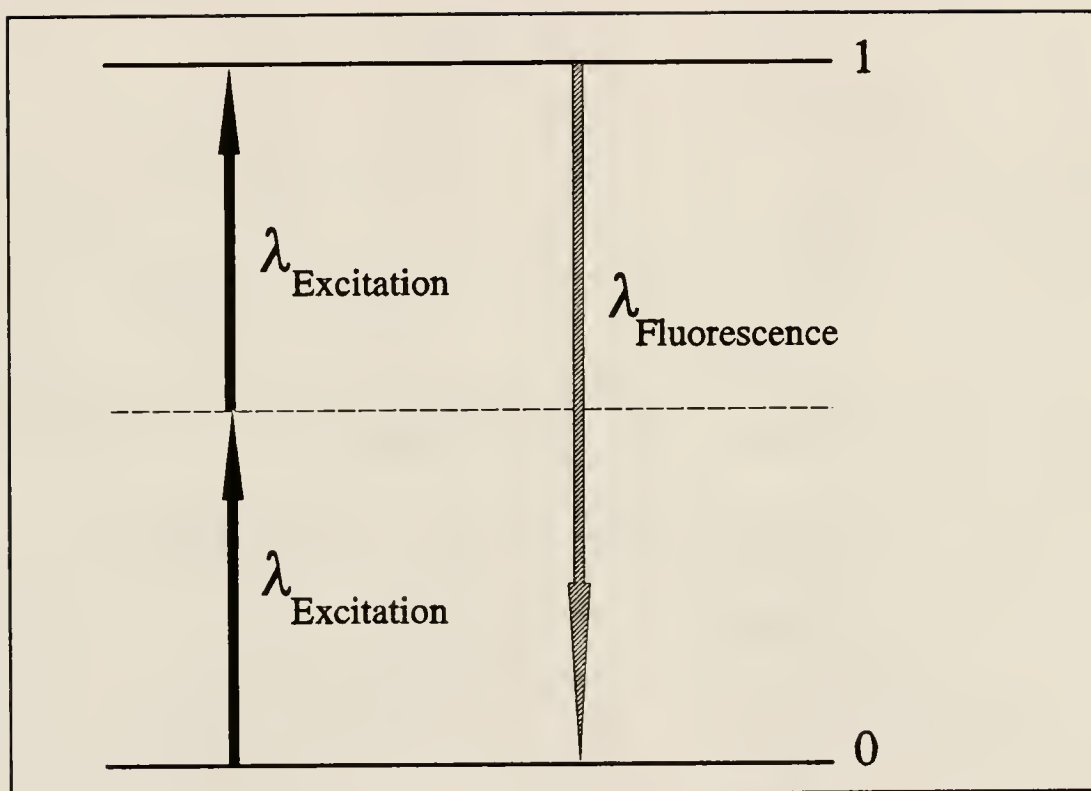
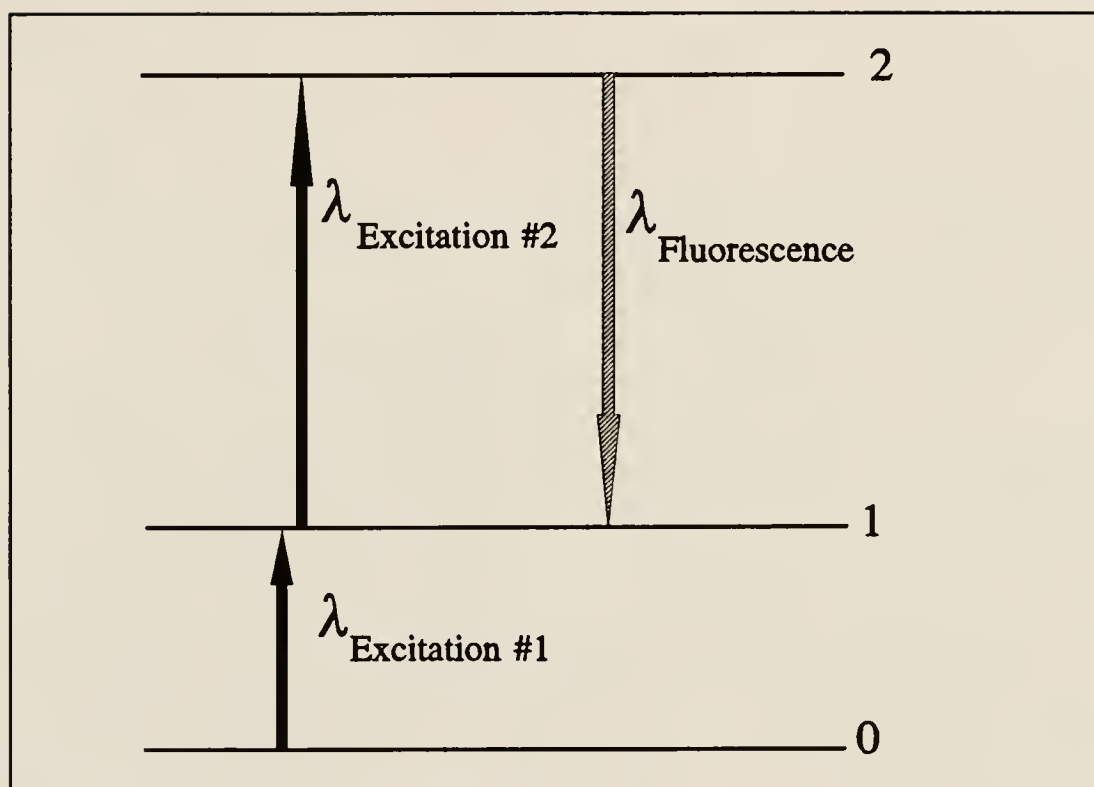


Figure 2-15 : Two-color atomic fluorescence spectroscopy



specifically, two-color excitation techniques where the two photons responsible for excitation of the analyte atom are of different wavelengths corresponding to transitions between real levels (Figure 2-15), resulting in the name two-color excitation fluorescence. These transitions have much greater probabilities and can be any combination of the aforementioned resonance and nonresonance techniques. These techniques were not implemented or recognized for their analytical potential until the application of laser excitation to atomic fluorescence spectroscopy, which will be discussed later.

Theoretical treatment of atomic fluorescence spectroscopy

Winefordner and Vickers⁴ have outlined the theoretical basis for atomic fluorescence as an analytical technique, and their development will be closely followed in this discussion.

The intensity of a resonance fluorescence signal per unit time is proportional to the intensity of the absorbed excitation radiation per unit time through the expression

$$P_F = \phi P_{abs} \quad (2-1)$$

where P_F is the fluorescence power, P_{abs} represents the amount of incident radiation absorbed, and ϕ is a proportionality constant representing the number of atoms undergoing the fluorescence process per unit time divided by the number of atoms leaving the ground state as a result of the incident radiation, involved in this absorption process.

The relationship between the incident radiation and quantity of this power that is absorbed by the sample is

$$P_{abs} = P_v^0 (1 - e^{-k_0 L}) \Delta \nu \quad (2-2)$$

where P_v^0 is the spectral intensity of the incident radiation (W/sec), k_0 is the atomic absorption of center of the absorption line (cm^{-1}), L is the average absorption path length (cm), and $\Delta \nu$ is the half-width of the absorption profile (sec^{-1}). This absorption profile is approximated, in this case, as a triangle, which is a good estimate since the absorption line is said to follow a Gaussian distribution in flame spectroscopy. With this approximation, this half-width can be expressed as

$$\Delta \nu = \frac{\pi^{1/2}}{2 (\ln 2)^{1/2}} \Delta \nu_G \quad (2-3)$$

where $\Delta \nu_G$ is the half intensity spectral linewidth of the Gaussian curve (sec^{-1}). The constant k_0 is defined as

$$k_0 = \frac{(\ln 2)^{1/2} \lambda^2 g_1}{4 \pi^{3/2} \Delta \nu_D g_2} n_0 A_{\epsilon} \delta \quad (2-4)$$

where $\Delta \nu_D$ is the Doppler half-width of the absorption line (sec^{-1}), g_0 and g_1 represent the statistical weights of the lower and higher states, respectively, involved in the transition being studied, n_0 is the the ground state population density (cm^{-3}) of the analyte atom species, λ is the wavelength of the center of the absorbtion line (cm), A_{ϵ} is the Einstein coefficient of spontaneous emission from level 1 to level 0 (sec^{-1}), and δ is defined as $(\ln 2)^{1/2}$ times the ratio of the sum of the Lorentz, Holtsmark, and natural half-widths to the Doppler half-width (sec^{-1})¹².

Combining equations (2-1) and (2-2), and adding a self-absorption factor, $e^{-(k_0 L)/2} \cosh(k_0 L/2)$, determined by Kolb and Streed,³⁴ the following expression approximates the energy emitted per unit time as fluorescent radiation:

$$P_F = \Phi P^0 \Delta \nu (1 - e^{-k_0 L/2}) e^{-k_0 L/2} \cosh(k_0 L/2) \quad (2-5)$$

This equation can be rewritten in terms of fluorescence intensity, I_F ($\text{W}/\text{cm}^2 \cdot \text{steradian}$), by dividing P_F by the area, A_F , of the fluorescent cell from which the fluorescence energy is emitted, and by 4π steradians resulting in

$$I_F = \frac{\Phi P^0 \Delta \nu}{4 \pi A_F} (1 - e^{-k_0 L}) e^{-k_0 L/2} \cosh(k_0 L/2) \quad (2-6)$$

As mentioned at the beginning of this theoretical treatment, resonance fluorescence is assumed, and for this case equation 2-6 is an exact expression upon which expansion is required in order to compensate for other types of fluorescence, or a case where several absorption lines are responsible for the fluorescence intensity.

The intensity of the fluorescence is proportional to N , the number of atoms absorbing energy. As n increases, $(1 - e^{-(k_0 L)})$ approaches unity. Therefore, I_F goes through a maximum as n increases. For small values of n , i.e. low concentrations, the fluorescence intensity can be expressed as

$$I_F = \frac{\Phi P^0 \Delta \nu k_0 L}{4 \pi A_F} \quad (2-7)$$

Substituting for k_0 , defined earlier, the following expression is obtained:

$$I_F = \left(\frac{(\ln 2)^{1/2} \phi \Delta \nu L \lambda^2 g_1 A_t \delta}{16 \pi^{5/2} A_F \Delta \nu_D g_2} \right) P^0 N_0 \quad (2-8)$$

This equation for fluorescence intensity is an exact expression for any experimental arrangement and any spectral line. This relationship then can be simplified to

$$I_F = C P^0 N_0 \text{ (W/cm}^2 \cdot \text{ster)} \quad (2-9)$$

which indicates that a linear relationship exists between the intensity of the fluorescence signal and a proportionality constant, C, of the analyte species, providing the theoretical basis for atomic fluorescence spectroscopy.

Applications of Conventional Source AFS

During the introduction of atomic fluorescence spectroscopy and its early growth, there was very little use for this technique for the analysis of "real" samples. There were already other established methods involving either atomic emission or atomic absorption spectroscopy that could be used, and the technique of atomic fluorescence spectroscopy was confined to mainly fundamental research. The sensitivity and selectivity of this method, however, quickly demonstrated its usefulness, and AFS began to be applied to samples previously only studied by other spectroscopic techniques.

Atomic fluorescence spectroscopy has been applied to biological samples such as blood^{35,36,37} and urine^{38,39} for the determination of mercury, gold, zinc, cadmium, and other metallic elements of biological interest detectable in quantities as low as 5 ng/ml. The main topics of discussion surrounding these applications of AFS were in respect to obtaining the sample preparation technique and instrumental conditions that

would result in the lowest limit of detection. This was the same point of interest discussed pertaining to the early analytical applications of AFS to metallurgy,^{40,41} petroleum products and fuels,^{42,43} and environmental analyses^{44,45} for trace determination of metals.

Advantages and Disadvantages

Conventional source atomic fluorescence spectroscopy has been demonstrated to achieve lower detection limits and larger linear dynamic ranges than conventional atomic absorption or atomic emission techniques for the same atom species. Since these are the main goals to be achieved in an analytical technique, it would seem beneficial, then, to examine why atomic fluorescence spectroscopy instrumentation has not achieved appreciable commercial attention.

It is true that atomic fluorescence techniques enjoy unprecedented sensitivity and selectivity along with a linear dynamic range of usually four to seven orders of magnitude. Add to these advantages that the relationship between the incident radiation intensity and the fluorescence signal is a linear one at low concentrations, which is not the case in atomic absorption spectroscopy, and AFS would appear to be a powerful tool, especially for trace analysis. Atomic fluorescence spectroscopy has the potential for simultaneous multielement analysis, suffers from minimal chemical interferences because of the excellent selectivity of the technique, and the instrumentation involved is rather simple and relatively inexpensive. Despite all of these benefits of atomic fluorescence spectroscopy, even today it has found little use in commercial instrumentation.⁴⁶

This is mainly due to the many disadvantages of conventional source AFS techniques including self-absorption at higher concentrations resulting in a non-linear response between incident intensity and fluorescence intensity. These methods also have high background signals due to scatter of the excitation radiation that is difficult to correct for, decreasing the sensitivity of the measurements. Matrix problems have prevented the application of AFS to real samples, and sample preparation can result in blank matrix matching problems. The quantum efficiency of the fluorescence signal, as well as other physical parameters, is dependent upon several atomization source variables which must be monitored closely to maintain reproducible results.

One of the main reasons that AFS instrumentation is not manufactured commercially is that optical emission and mass spectrometric techniques result in comparable detection limits are a multi-element techniques virtually free from matrix effects. These instruments are much more costly than a commercial AFS instrument, but, nonetheless, chemists are using either mass spectrometry or established atomic absorption or atomic emission methods for their trace analysis. This does not take away from the need for information supplied through diagnostic applications of AFS.

Laser Excited Atomic Fluorescence Spectroscopy (LEAFS)

One major area of research in the field of AFS has been the study of a variety of radiation sources meeting the criteria for an ideal excitation source including stability, long life, low cost, high versatility, and, most importantly, high intensity since the fluorescence signal increases linearly with increased incident radiation intensity. These

studies have resulted in the use of excitation sources such as the high-intensity hollow-cathode lamp, demountable hollow-cathode lamps, and spectral vapor discharge lamps.⁴⁷ While these sources did fulfill most of the aforementioned criteria, they lacked versatility in that only a limited number of elements could be studied using them. Continuum sources including high-pressure xenon arcs, overcame this disadvantage, but added the disadvantage of increased background noise and lack of intensity, especially in the ultraviolet region. It became obvious that in order for the vast potential of atomic fluorescence spectroscopy techniques to be realized, some excitation source had to be found which satisfied most of the above criteria.

History of Flame LEAFS

In 1971, Denton and Malmstadt⁴⁸ and Fraser and Winefordner⁴⁹ independently reported using a tunable dye laser as an excitation source for the analytical study of atomic species in a flame. These are the first documented analytical applications of lasers to the field of atomic fluorescence spectroscopy, and in these studies the potential for the use of dye lasers in AFS was demonstrated. Denton and Malmstadt⁴⁸ used a frequency-doubled ruby laser to pump a dye laser and observed fairly sensitive detection of barium atoms in a flame. They also observed a linear response over three orders of magnitude once the high scatter signal resulting from the laser radiation being reflected off of water droplets present in the flame was compensated for.

Fraser and Winefordner⁴⁹ used a nitrogen pumped dye laser system continuously tunable from 360 nm to 650 nm through the use of various dyes. Even though the power

output of the laser system used in this study would be considered low by today's standards for laser systems, the authors were able to show that if a stable, high powered, pulsed light source with a narrow spectral bandwidth and small duty cycle was used, the signal to noise ratio could be greatly improved over conventional source AFS. The limiting noises in AFS were usually random noises including flame background and dark current, and any reduction in the "on time" of the detector would reduce the contribution of these noises to the total noise considerably. Therefore, the short pulses afforded by a dye laser system made them a nearly ideal source for AFS. Through their studies, the authors observed a decrease in the flame background noise coupled with an increase in total noise due to laser scatter from the atom source. This had also been a problem for Denton and Malmstadt⁴⁸ simply because increasing the intensity of the excitation source through the implementation of a dye laser resulted in an increase in scatter as a result of that source. The sensitivities reported in this study for their determination of aluminum, calcium, chromium, iron, gallium, indium, manganese, strontium, and titanium in either a hydrogen/air or an acetylene/air flame compared favorably to those obtained through the use of conventional source AFS, but were not superior. Also in this article, the authors discussed the limitations of this technique based on the wavelength range not encompassing transitions below 360 nm, the range where many ground state, resonance transitions are found. It was suggested at this time that this limitation could be overcome through the use of doubling crystals resulting in laser radiation in the ultraviolet region.

In the early 1970's, Kuhl, Marowsky, and Torge^{50,51} reported the use of a flashlamp pumped dye laser system being utilized as the excitation source for AFS of

sodium in an absorption cell. This report was significant because it represented the first mention of the use of a dye laser whose output was narrowed to a linewidth, reported at 5×10^{-4} nm, that was comparable to true elemental line source linewidths resulting in an absolute detection limit of 2 ng. According to the authors, the main advantage of using a dye laser as the excitation source was its tunability which allowed background interferences to be corrected for through small detunings of the laser wavelength.

Almost from the beginning of the applications of lasers as excitation sources in AFS it was observed that, at high intensities of laser radiation, there was a nonlinear relationship between the laser power and the resulting fluorescence signal. In 1972, Piepmeier discussed the advantages that this phenomenon, known as saturation fluorescence, could have in the field of AFS.⁵² As mentioned earlier, one of the main advantages of conventional source AFS over atomic absorption spectroscopy (AAS) was the linear relationship between the source intensity and the monitored fluorescence signal resulting in AFS demonstrating improved sensitivity over AAS. With pulsed laser excitation, the peak source power was now enough to saturate the absorption step resulting in a now nonlinear relationship between source intensity and fluorescence signal observed. According to Piepmeier, laser excitation resulted in an optically saturated dilute population in a flame causing fluorescence several orders of magnitude more intense than a population excited by a conventional source at lower power. This saturated population demonstrated a much lower dependence on source variations than an unsaturated population. The author used the rate equations approach to approximate

the saturated atomic population, which assumed steady state conditions during the laser pulse.

The main conclusions of his⁵² theoretical treatment were that for excitation spectral irradiances beyond the irradiance required to reach saturation conditions, the atom population responsible for the fluorescence signal was only weakly dependent upon factors that had a much greater effect when saturation was not achieved, such as pulse to pulse variations and quenching within the atomization medium. The result of this was a fluorescence signal which reached a maximum at high laser irradiances and suffered little fluctuation with variations in the source. While the fluorescence signal remained constant for laser irradiances greater than the saturation irradiance, laser scatter in the atom cell continued to increase linearly with increasing laser power resulting in a decreased fluorescence to scatter ratio at high laser powers. It was suggested that there was an optimum laser power resulting in saturation conditions while minimizing the signal due to scatter. This theoretical treatment will be discussed in more detail in another section of this dissertation.

Also in 1972, Fraser and Winefordner⁵³ reported results for laser excited atomic fluorescence spectroscopy (LEAFS) in a flame atom cell. These results included detection limits for thirteen elements and some general conclusions based on the results of their experimentation. For resonance fluorescence measurements, the signal to noise ratio was high due to the laser scatter in the atom source as well as the shot noise of the detector and the pulse variations. This noise was scatter limited at low analyte concentrations, as was suggested by Piepmeier,⁵² and a decrease in detection limits

required a decrease in this scatter noise. This brought the authors to suggest and implement the first nonresonance laser excited atomic fluorescence scheme. The result was a reduced scatter background since the wavelength of the laser radiation and the wavelength being monitored were different, and detection limits as low as $2 \times 10^{-3} \mu\text{g/ml}$ were reported. This publication also reported the first use of multiphoton excited AFS for the detection of cadmium and zinc. As mentioned earlier, two photon excitation techniques are only possible for analytical applications through the implementation of lasers as excitation sources.

In 1973, Omenetto *et al.*^{54,55} reported the analysis of several transition elements using LEAFS in a nitrous oxide/acetylene flame. The significance of these studies was the fact that these elements had never before been analyzed using AFS because of the lack of suitability or availability of line sources. This again demonstrated the usefulness of the application of dye lasers to the field of AFS. Also in these studies, nonresonance fluorescence was monitored again demonstrating the decrease in scatter noise and subsequent improved detection limits.

Also in 1973, Omenetto *et al.*⁵⁶ published a paper similar to the theoretical paper by Piepmeier⁵² on saturated AFS with the difference between the theoretical treatments being the assumption of a line (monochromatic) source by Piepmeier and a quasi-continuum source by Omenetto. At the time of this publication, the quasi-continuum source assumption was a better one for the application to dye lasers with bandwidths on the order of 0.1 to 1 nm, which is much greater than most atomic linewidths.

The authors also presented experimental results that demonstrated the effects of optical saturation as a result of laser excitation on the observed AFS signals. This data caused them to conclude that, as expected, for low excitation source irradiances, the fluorescence signal enjoyed a linear relationship with the source intensity, but that at high source irradiances, this fluorescence signal would become increasingly independent upon the source intensity and eventually reach a maximum value. This maximum fluorescence signal was shown to be a property of the atom system itself and was described using the theoretical treatment presented in this paper.

Also in the article by Omenetto *et al.*,⁵⁶ the authors derived an expression describing the relationship between the source flux for a continuum source and the resulting fluorescence radiance, assuming a two level system at steady state conditions. This relationship is valid at both high and low source intensities. The authors discussed the possibility of mapping the population of the atom source using saturated LEAFS since such measurements would be independent of the quantum efficiency (i.e. independent of collision processes). This would be important analytically because of the high quenching environment in most flame reservoirs.

This paper confirmed the conclusions of Pipemeier⁵² that saturated fluorescence signals are independent of source fluctuations. It also confirmed that at laser irradiances greater than the saturation irradiance, the fluorescence signal would eventually reach a maximum signal while the scatter noise would continue to increase. The authors suggested the best way to circumvent this disadvantage was to optimize the fluorescence

signal to noise ratio rather than optimizing conditions resulting in simply the greatest signal.

In 1978, in an article by Boutilier *et al.*,⁵⁷ steady state atomic fluorescence radiance expressions were given for two and three level atomic systems excited by a continuum source for both saturation and non-saturation conditions. Two types of three level atomic systems were considered in their treatment for the fluorescence radiance expressions that were derived. The first case was for alkali-like atoms (i.e. sodium, potassium, etc.) where the two excited state levels were assumed to be very close in energy, with radiative processes between these two levels being forbidden. The second case considered elements where all three levels were assumed to be well-separated in energy, with radiative transitions being allowed between all levels except the two lowest levels (i.e. the intermediate level is a metastable level). This theoretical treatment included derivations of all possible radiative and nonradiative transition combinations resulting in several conclusions to be made by the authors about the fluorescence radiance expressions. First, for dilute atom vapors (low optical densities), the fluorescence radiance is linearly related to the total atom population for all source intensities. For two level atomic systems, the fluorescence signal resulting from excitation from a source under saturation conditions is independent of collisional deactivation processes. For any atom not accurately depicted as a two level system, however, some knowledge of these nonradiational processes would be required to gain information about the relationship between the fluorescence radiance and the atom population.

Also in 1978, Weeks, Haraguchi, and Winefordner⁵⁸ published the results of a comprehensive study of 24 elements using flame LEAFS. For comparison purposes, several of the elements were investigated, implementing both resonance as well as nonresonance excitation and fluorescence schemes. The authors determined that resonance fluorescence was limited by laser scatter noise under otherwise ideal conditions, while nonresonance fluorescence schemes and the freedom from laser scatter interferences enjoyed by these techniques were limited by either noises due to the dark current, the amplifier, the flame background emission, molecular background fluorescence, or any combination of these noise sources.

This study resulted in detection limits demonstrating improvement over previous studies by up to two orders of magnitude, yet the authors still felt that there was much room for improvement of flame LEAFS as an analytical technique. Many of these suggested improvements revolved around the need for a higher output power dye laser since the laser used in this study was sometimes close to, but not always reaching, the saturation spectral energy density for many of the ultraviolet transitions. This limitation prevented the authors from being able to take full advantage of saturated conditions in these schemes. The use of an alternative atomizer was also suggested to reduce noise and improve the sensitivity of this method.

History of Furnace LEAFS

While flame LEAFS was enjoying some success, the search was still on for alternative atomization sources to which LEAFS could be applied to improve upon the

results obtained in a flame cell. As atomizers, flames suffer from many problems preventing the analytical application of LEAFS from achieving its full potential in terms of sensitivity and selectivity. Flames are susceptible to chemical and ionization interferences as well as low quantum efficiencies of fluorescence in most flame gas mixtures. As a result of these limitations, the field of LEAFS was redirected to applications in graphite furnaces, ICPs, and other atomization reservoirs.

The first mention of LEAFS employing a graphite furnace as an atom source was back in 1974 when Neumann and Kriese⁵⁹ reported the use of a flashlamp pumped dye laser system employed in the analysis of lead. A comparison of the laser to other excitation sources, such as the hollow cathode lamp and the electrodeless discharge lamp, was made at this time. The graphite furnace was proven superior to flame atomizers for several reasons. The furnace has an exceptionally high atom density during the atomization cycle and the analysis is performed in an inert environment helping to reduce interferences. The authors reported that LEAFS in a graphite furnace provided superior detection limits as well as a greater linear range of response than any previously mentioned conventional source AFS technique.

Since this first report of graphite furnace LEAFS, this technique has been used to determine many elements at very low levels. In fact, the use of graphite furnace LEAFS has resulted in the lowest detection limits of any spectrochemical analytical technique to date.^{53,60,61,62} Graphite furnace LEAFS has been demonstrated to be a technique with selectivity and sensitivity coupled with the ability to handle small samples as well as samples with complex matrices. The future of this technique is very

promising, and could lead to an eventual achievement of the intrinsic limit of detection.⁶³

While this technique would seem ideal for continued application to the field of LEAFS, it is not without its limitations. These include the limited number of elements that can be analyzed through this technique as well as the difficulty with interferences despite the inert atmosphere in which the measurements are taken. Successful application of this technique to real samples would require vacuum atomization which entails a considerable increase in experimental complexity.

History of ICP-LEAFS

The ICP was first implemented as an atomizer for AFS by Montaser and Fassel⁶⁴ in 1976. The excitation was provided by EDLs and Osram lamps which the authors considered the best existing excitation source since they were the most intense sources for transitions in the ultraviolet range. Detection limits were reported for cadmium, zinc, and mercury comparable to previously reported detection limits for atomic emission ICP studies. In addition to the good detection limits, this method demonstrated excellent selectivity with no adverse effects on detection limits for complex mixtures of up to 17 concomitant elements. Since this initial ICP-AFS study, conventional source AFS has also been performed very successfully using hollow cathode lamp (HCL) excitation.⁶⁵ HCL excitation is effective for those elements that provide sufficient radiant intensity of a resonance transition in a hollow cathode discharge. Because of this limitation, there are many elements that cannot be evaluated with HCLs as excitation sources.

The first report of ICP-LEAFS appeared when Pollard *et al.*⁶⁶ discussed the first application of dye laser excitation to fluorescence excitation in the ICP. Although the results were not very favorable using a continuous wave (CW) laser, the authors reported excellent linearity and suggested that pulsed laser excitation could result in improved limits of detection of this method. This technique was also proposed as a useful method to perform diagnostic studies in the ICP.

Quickly following this study in 1980 was a report by Epstein *et al.*⁶⁷ using both a flashlamp pumped dye laser and a nitrogen pumped dye laser as excitation sources for ICP-LEAFS. The detection limits of this method were not an improvement over ICP emission techniques or ICP-AAS. Nonetheless, the authors were optimistic about the future of this technique stating that these were simply preliminary studies, and that there was much room for improvement. It was again mentioned at this time that ICP-LEAFS could be a very powerful tool in the field of plasma diagnostics.

In 1984, Omenetto *et al.*⁶⁸ published an article discussing the analytical potential of ICP-LEAFS beginning with the admission that the results presented to that point were disappointing as compared to emission ICP methods. In their study, they were unable to reproduce the poor and erratic detection limits previously reported, and, in fact, their experimentation resulted in LODs superior to other fluorescence results and, in most cases, to emission methods as well. Both resonance and nonresonance schemes were investigated resulting in better signal to noise due to decreased scatter in the nonresonance cases, as expected. The authors also discussed the ease with which saturation conditions were achieved since there are fewer collisional loss mechanisms in

this atom cell as compared to a flame. The forward power was also mentioned to be about 1kW to increase the atomic population available for probing by the laser radiation.

In 1985, Huang, Lanauze, and Winefordner⁶⁹ utilized ICP-LEAFS to study some precious metals and refractory elements resulting in detection limits in the range of 1.3 to 58 ng/ml and linear ranges of over four orders of magnitude in most cases. These limits of detection were found to be superior or comparable to those obtained through the use of flame AAS and similar to those obtained by ICP emission. Also investigated in this study was the effect of rf power on the fluorescence signal with the intensity of the atomic line monotonically decreasing with increased rf power. The lower the rf power, the greater signal, with the plasma becoming unstable at powers less than 600 W.

History of LEAFS in Other Atomization Reservoirs

While the majority of previous LEAFS studies have been performed in a flame cell and the most recently, and probably future studies, have been carried out in an ICP, other atomization reservoirs have been implemented in the field of laser excited atomic fluorescence spectroscopy. These include the glow discharge, an atom source primarily utilized in emission studies for trace element analysis in metal samples. This technique has the advantage of solid sampling with little sample preparation required.⁷⁰ The full analytical potential of GD-LEAFS has not been recognized, but the studies that have been performed^{70,71} reported detection limits on the order of 10 ng in aqueous solution and 8 $\mu\text{g/g}$ in a solid for indium and 20 pg in aqueous solution and 0.1 $\mu\text{g/g}$ in a solid for lead.

In 1983, Kosinski, Uchida, and Winefordner⁷² reported the use of a modified ICP torch for ICP-LEAFS resulting in detection limits for 12 elements comparable to those obtained with HCL excitation. The comparison of this method with ICP-OES, however, showed the LEAFS technique lacking in sensitivity.

History of Two Photon LEAFS

As mentioned earlier, two-photon excitation fluorescence spectroscopy was carried out in a flame atom cell for the analysis of cadmium and zinc.⁵³ This study entailed the absorption of two photons from the laser excitation radiation at the same wavelength corresponding to an energy of half that of the resonance wavelength through a virtual level. As was also previously mentioned, this technique has no analytical usefulness with any other excitation source other than a laser, because of the low probabilities of the transitions involving the virtual level. Even with laser excitation, it is not always possible to obtain saturation conditions in these cases.

In 1978, two-photon excitation was implemented in a study of the excited states of sodium⁷³ to investigate the collisional coupling between higher excited levels. The authors were able to attain these higher states through the absorption by the sodium atom of two excitation photons of equal wavelength through a virtual level. The wavelengths were chosen based on the desired scheme to be studied, either $3S \rightarrow 3D$, $3S \rightarrow 4D$, or $3S \rightarrow 5S$. Using a flashlamp pumped dye laser, the authors reported achieving saturation conditions providing an estimate of the value of the saturation parameter which can then be used to determine the collisional and radiative rate constants.

Miziolek and Willis⁷⁴ then used two photon excitation for the analytical analysis of lead using two different wavelengths and exciting through a real excited state level to populate the higher lying excited state. The authors called this process double-resonance emission spectroscopy, and utilized this method to reduce scatter noise by monitoring the fluorescence signal at a wavelength originating from the uppermost excited level at a different wavelength than either of the excitation steps.

Another study employing two-color excitation for analytical determination was reported by Rogers *et al.*⁷⁵ for the determination of mercury with graphite furnace atomization. The authors reported detection limits on the order of 10^3 atoms/cm³.

In 1988, Leong *et al.*⁷⁶ used what they called double resonance spectroscopy for the analytical determination of lead in a graphite furnace. The fluorescence signal was monitored as the result of excitation at both 283.306 nm and 600.193 nm from a Nd-YAG dual dye laser system from both of the excited state levels taking part in the excitation steps. With the direct line fluorescence signal as a result of two step excitation being monitored, the authors reported detection limits in the picogram range and direct line fluorescence as the result of one step excitation resulted in an LOD of 3 fg.

In addition to analytical applications, two-photon excitation fluorescence spectroscopy has proven to be a very useful diagnostic tool. These types of techniques have been used to a great extent in the evaluation of combustion species in flames such as oxygen,⁷⁷ atomic nitrogen,⁷⁸ and hydrogen.^{79,80,81,82}

History of Two-Color Excitation Fluorescence

Two photon excitation schemes involving a real level as an intermediate excited state would facilitate saturation conditions as a result of greater transition probabilities involved in the two excitation steps, but would then require two different wavelengths of laser radiation for the two respective excitation steps. This is typically carried out utilizing a dual dye laser system with both lasers pumped by the same laser providing the advantage of tunability as well as intensity in order to study the transitions involving the high lying excited states.

There are many possible variations on the theme of two-color excitation spectroscopy including monitoring the fluorescence from the intermediate excited state level instead of the highest excited state. These experiments usually entail the monitoring of a fluorescence signal as the result of one step excitation and the subsequent addition of a second excitation step tuned to a transition allowing it to directly perturb the population of the monitored level. In most cases, the fluorescence signal from the intermediate level will decrease upon introduction of the second excitation step responsible for depleting the population of the monitored level. This technique has taken on many names in the literature, but the methodology of all of the techniques is essentially the same.

These types of techniques are based on the monitoring of an excited level as the population of that level is being depleted through the introduction of a second excitation step. Intuitively, the fluorescence signal will decrease upon introduction of this depleting

excitation radiation and this decrease in signal has caused these techniques to more generally be termed fluorescence dip spectroscopy.

Omenetto *et al.*⁸³ used fluorescence dip spectroscopy for the determination of calcium, barium, strontium, and magnesium. The authors reported this to be a very sensitive technique demonstrating unprecedented selectivity. In all excitation and fluorescence schemes, the signal was monitored at a wavelength different than that of either excitation wavelengths thereby eliminating scatter noise. Also in this article, the authors outlined a theoretical approach for modeling such excitation and fluorescence schemes based on the rate equations approach. A similar model will be presented later in this dissertation.

Advantages and Disadvantages of LEAFS

While laser excited atomic flame spectroscopy has been shown to be a technique with excellent sensitivity, superior to atomic emission or atomic absorption methods, and, with saturated two step capabilities, unprecedented selectivity perhaps approaching elemental specificity, it is not without its limitations. The main disadvantage of these systems is the cost involved in the instrumentation. In order to take advantage of the tunability of a dye laser, there needs to be some means of pumping this laser, and while that was earlier performed using a flashlamp, it is now almost exclusively performed by another laser. Add to that the two color excitaton schemes improving the sensitivity and selectivity, and another laser is required. With all other optics and atomization sources tossed in, this system could easily cost \$200,000. This is more than the average

industrial lab can afford to spend on a fluorescence system, which is why there are many ES and AAS instruments yet only a handful of fluorescence instruments commercially available, and the ones that exist do employ HCL excitation, even though laser excitation has many advantages over HCL excitation, simply because of the cost involved.

With the exception of this large disadvantage, LEAFS has many advantages over OES, AAS, and conventional source AFS techniques, which have been outlined throughout the previous discussion. For most routine analysis, however, the existing, less expensive methods are sufficient, and LEAFS has not made it to the forefront in industry. This does not detract from the need for fundamental physical information about atom systems as well as temperature profiling and other physical information about the atomization reservoirs that are used in conjunction with these other detection methods everyday. The best way to carry out the studies resulting in this type of information is through the use of LEAFS.

CHAPTER 3 DIAGNOSTIC APPLICATIONS OF LEAFS

Diagnostic Characterization of Atom Sources

It is difficult to distinguish between the diagnostic and analytical applications of LEAFS since they complement each other so well. It is undisputed that a knowledge of the underlying physical principles of analytical as well as physical information about the analyte species are necessary to improve upon existing analytical techniques. Initial studies regarding the state of atom sources typically involved the insertion of some sort of probe into the flame, plasma, or other atom reservoir, and sampling the condition of this probe over a small volume.⁸⁴ The many disadvantages involved with such measurements include the effect that the probe itself has on the atom cell and the resulting effect this would have on the measurement being taken. It was therefore necessary to find a method to determine physical information about these atom sources, as well as the species being investigated in them, without disturbing the source. Spectroscopic methods provide the best means for obtaining spatially and temporally resolved measurements of several physical parameters of these atom cells without perturbing the processes occurring in them.

First, emission spectroscopic techniques were used to investigate the horizontal^{85,86} and vertical^{87,88} spatial distribution of excited atoms. Also explored

were the determination of various kinds of temperature,^{89,90} and electron number densities.^{91,92} Atomic absorption spectroscopy was implemented in the investigation of number densities of analyte atoms using hollow cathode lamps⁹³ as well as other excitation sources. Argon number densities were also examined using AAS in a microwave induced argon plasma.⁹⁴ These spectroscopic methods provide "line-of-sight" measurements, however, not allowing for temporal or spatial resolution. In order to gain spatial information, the desired quantity must be derived by somewhat elaborate procedures, usually the Abel inversion method.⁹⁵

Omenetto, Benetti, and Rossi⁸⁴ reported using atomic fluorescence spectroscopy for the measurement of flame temperatures. The authors proposed four different fluorescence schemes and compared the resulting temperature measurements to each other as well as with those determined using the other spectroscopic methods mentioned above. They found that the ability to investigate a smaller volume than with other spectroscopic methods allowed for more reliable temperature profiling resulting in more consistent values.

Subsequent applications of AFS to atom source diagnostics have resulted in physical information about these sources such as flow velocities,⁹⁶ electron and ion densities,^{97,98} temperatures within the atom cell,⁵⁴ and collisional cross sections of flame or plasma species.^{99,100} AFS has been applied to measurement of some constants of atomic studies including damping constants of atoms in flames,¹⁰¹ lifetime of excited atoms,¹⁰² atomic cross sections,³ and diffusion studies.

AFS found many uses as a diagnostic tool in a variety of atomization reservoirs with the eventual application of lasers as excitation sources to these techniques. Laser excitation combines the advantage of small volume probing with increased intensity over conventional sources thereby maximizing the fluorescence signal. In addition, lasers more often cause saturation conditions to occur simplifying the investigations of atom species in these atom cells.

In 1968, Measures⁸⁴ introduced what he called selective excitation spectroscopy which was, basically, atomic fluorescence using a pulsed laser as excitation. This method was proposed and utilized as a means for determining the local values of electron temperature and electron density in low-temperature plasmas. The author commented that because a pulsed laser was implemented, both spatial and temporal resolution in these measurements were possible, demonstrating the versatility of this technique.

While it would seem that only so much information can be gained through such studies, resulting in the stagnation of this field, these properties are very dependent upon atomizer conditions. These conditions of the atom cells used in AFS are ever changing to meet the needs of the proposed study, resulting in discrepancies between values for the same type of atomizer. Even if the same conditions are reported from laboratory to laboratory, there are inconsistencies in reported information.⁵

Investigation of Atomic Parameters Using LEAFS

While it is not necessary to use laser excitation AFS for the determination of physical atomic parameters, it is beneficial to do so because of the relative ease of

theoretical modeling for calculation of this information under saturation conditions. The most commonly used theory to model atomic transitions follows the rate equations approach, and this approximation will be discussed in detail in a later chapter.

Through the implementation of LEAFS and the just mentioned theory, several physical parameters have been evaluated including transition lifetimes,^{103,104,105} transition probabilities,¹⁰⁶ and transition oscillator strengths.¹⁰⁷ With temperature information and the knowledge of one or more physical parameters, it is sometimes possible to utilize the rate equations theoretical modeling to calculate other atomic parameters such as quantum efficiencies.⁵⁴

LEAFS was employed in a reduced pressure plasma¹⁰⁸ as a diagnostic tool in this atom source to gain a better understanding of the ICP as sampled by a mass spectrometer. The sodium D lines were observed because of their high fluorescence quantum efficiencies, and the resulting information was used to profile the temperature of the expanded plasma. A similar study was carried out for a reduced pressure flame atomizer,¹⁰⁹ again as a diagnostic tool to investigate the temperature profile in this flame expansion.

Investigation of Atomic Parameters Using Two-Color LEAFS

While the need for fundamental atomic information for transitions involving the ground state is not yet completely met, the immediate need in this field is information about transitions involving two atomic excited levels. Two-color excitation spectroscopy

is a fast growing field, and yet the fundamental information about these transitions being utilized in these investigations is practically nonexistent.¹¹

Two-color excitation fluorescence spectroscopy has proven to be a very useful diagnostic tool. These types of techniques have been used to a great extent in the evaluation of combustion species in flames such as oxygen,¹¹⁰ atomic nitrogen,¹¹¹ and hydrogen.^{112,113,114,115}

There are many possible variations on the technique of two-color excitation spectroscopy including monitoring the fluorescence from the intermediate excited state level instead of the highest excited state. These experiments usually entail the monitoring of a fluorescence signal as the result of one step excitation and the subsequent addition of a second excitation step tuned to a transition allowing it to directly perturb the population of the monitored level. In most cases, the fluorescence signal from the intermediate level will decrease upon introduction of the second excitation step responsible for depleting the population of the monitored level. This technique has taken on many names in the literature, but the methodology of all of the techniques is essentially the same.

This type of excitation and fluorescence scheme was implemented in 1983 for the determination of the energies of the Rydberg levels of nitric oxide in a supersonic jet.¹¹⁶ Further work by this same research group^{117,118} in this same area showed that it was possible to determine absorption cross sections for excited state transitions involved in the excitation and fluorescence scheme.

Extinction spectroscopy was discussed by Pedrotti¹¹⁹ for the study of lithium in determination of radiative lifetimes and autoionization rates. The author used "high-powered narrowband dye laser radiation to extinguish the emission of VUV radiation from lines emitted by a hot plasma." This was accomplished through the introduction of the radiation from this dye laser tuned to a transition connecting the upper level of a strongly emitting VUV line to another excited state. The author suggested that this technique was useful because it allowed the observation of levels not seen in emission spectroscopy due to rapid upper level radiation and also not seen in absorption spectroscopy because these transitions often times do not involve the ground state.

Another variation on this theme is photionization controlled-loss spectroscopy used by Salmon and Laurendeau^{120,121} for the investigation of atomic hydrogen in a premixed hydrogen/oxygen/nitrogen flame. The main obstacle in the prior studies for this purpose was that quenching was dominant as a loss mechanism difficult to control or monitor. In the case of photoionization controlled-loss spectroscopy, however, the addition of a second excitation step selectively ionized atoms initially excited through a first excitation step making this selective ionization the primary loss mechanism. This was a process that could be controlled and compensated for with the fluorescence signal from the originally excited level being monitored and decreasing upon introduction of the second excitation step due to this second laser's depletion of the population of this monitored level. Using this technique, the authors were able to profile the number density of atomic hydrogen in several different gas mix ratios demonstrating the diagnostic potential of this and similar techniques.

Fluorescence reduction spectroscopy was used by Bonin *et al.*¹²² for the determination of the absolute photoionization cross section of the cesium $^7D_{3/2}$ level. They used two dye lasers to first excite an atom to an excited state through the absorption of two photons of the same wavelength via a virtual level and then subsequent photoionization as a result of the introduction of another dye laser while monitoring direct line fluorescence from the initially populated level. This study also demonstrated the utility of these methods as diagnostic tools in providing much needed physical atomic information.

These types of techniques are based on the monitoring of an excited level as the population of that level is being depleted through the introduction of a second excitation step. Intuitively, the fluorescence signal will decrease upon introduction of this depleting excitation radiation and this decrease in signal has caused these techniques to more generally be termed fluorescence dip spectroscopy.

Pago and Gudeman¹²³ used fluorescence dip spectroscopy to study transition-metal atoms produced in a rf glow-discharge sputtering machine. Rydberg spectra of titanium, vanadium, iron, cobalt, and nickel were analyzed to obtain ionization potentials agreeing with other reported results to 1 cm^{-1} . Also obtained were quantum defects for *nd* and *ns* series not showing detectable s-d mixing which would lead to asymmetric line shapes characteristic of autoionization.

Axner, Norberg, and Rubinsztein-Dunlop¹²⁴ then investigated the physical properties of laser enhanced ionization (LEI) and LIF (laser induced fluorescence) signals in a flame. The experimental results were shown to be in good agreement with those

obtained theoretically through a rate equations approximation. The authors also studied the effect of laser intensity on the resulting fluorescence signal as well as the fluorescence dip reinforcing what Peipmeier⁵² discussed about the importance of saturation conditions. Another study presented was the relationship between LEI enhancement and the LIF dip. As was expected, the closer to the ionization continuum the atom was promoted, the greater the resulting LEI signal due to thermal ionization from the excited level. This phenomenon was studied while varying both first and second step intensities, and the results were presented and fully explained through theory. It was suggested in this article that fluorescence dip spectroscopy had tremendous potential as a diagnostic tool.

In 1992, Xu *et al.*¹²⁵ used fluorescence dip spectroscopy to investigate the barium atom and, specifically, the $6s6p^1P_1$ to $6s5d^1D_2$ transition. The authors reported that the nonspontaneous radiative (amplified spontaneous emission or superradiation) relaxation of barium $6s6p^1P_1$ to $6s5d^1D_2$ from the laser excited upper level was enhanced by laser light that was resonant with the $6s5d^1D_2$ to the $5d6p^1F_3$ transition to deplete the population of the lower level.

Simeonsson, Ng, and Winefordner¹²⁶ used fluorescence dip spectroscopy to measure the quantum efficiencies of fluorescence for excited state transitions of silver, copper, iridium, and lead in an ICP environment. The results were shown to be in good agreement with theory, again based on a rate equations approach assuming a three level system. The authors commented that in most cases a three level model was an oversimplification and that some modifications needed to be made to compensate for the effects of collisions on the steady state populations.

Taking into consideration the fact that, as mentioned, a three level approximation was not a valid one in most cases, Simeonsson *et al.*¹²⁷ discussed a rate equations approach for an approximated five level atom system and the possibility of a negative fluorescence dip. In other words, the authors predicted that there was the possibility of an increase in the fluorescence signal upon introduction of a second excitation step in a fairly low collision atomization medium. More on this possibility and actual experimental data to support it will be discussed later.

Advantages and Disadvantages of LEAFS as a Diagnostic Tool

In the previous discussion, it has been demonstrated that LEAFS is an invaluable tool to better understand atom reservoirs in which analytical chemists perform investigations as well as the atom systems they perform these investigations on. This has been shown to be one of the primary needs in the field of analytical chemistry. Unfortunately, while LEAFS is the best method through which to obtain this information, it carries with it the limitation of the expense and complexity of the required system. This has been discussed earlier and is the greatest disadvantage as applied to LEAFS.

In the case of analytical studies, this disadvantage was overcome through the implementation of conventional excitation sources for AFS or the use of OES or AAS as alternative techniques. The application of these methods for diagnostic studies as alternative techniques will not yield the desired information. This is most easily performed through the use of lasers since the theoretical treatment applied requires

saturation conditions which only the use of an excitation source with the power of a laser can attain.

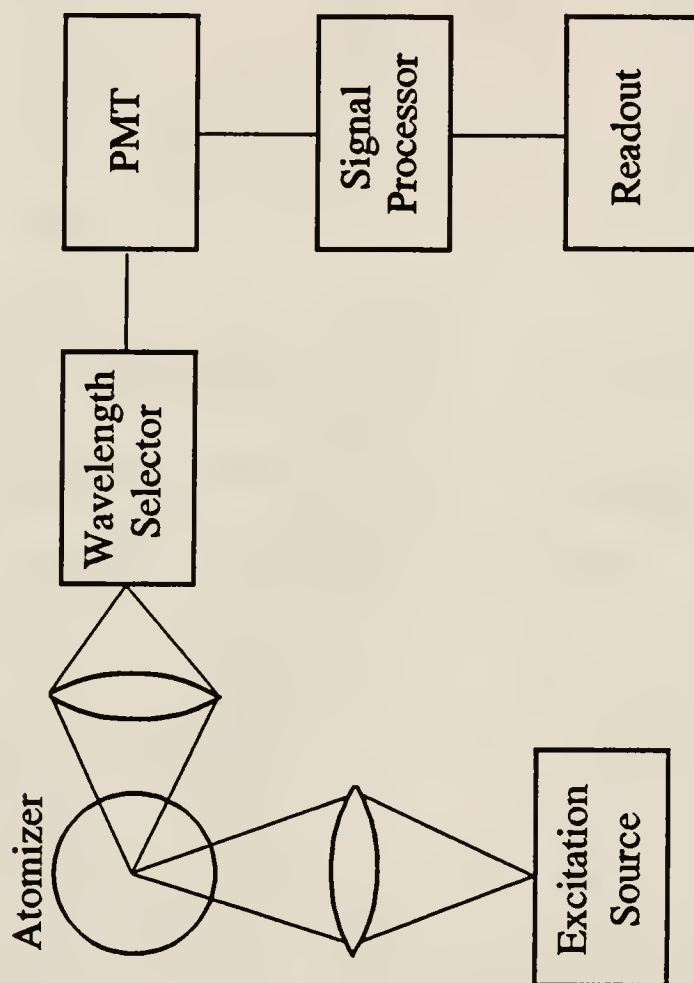
CHAPTER 4 INSTRUMENTATION USED IN LEAFS

The instrumental requirements for LEAFS are similar to those for emission spectroscopy with the exception of the need for an external excitation source, in this case, a laser. A block diagram of instrumentation required to perform a LEAFS experiment is shown in Figure 4-1. The experimental setup consists of an excitation source, an atomizer in which the analyte is investigated, a wavelength selection device, a photodetector, and an electronic amplifier/readout system. The excitation source is positioned perpendicular to the collection axis to minimize the detection of radiation from the excitation source.

Excitation Sources

The ideal source for AFS experiments would be stable and emit radiation at the desired wavelength at a very high radiance. Lasers make excellent sources for AFS with radiant power emitted from them being several orders of magnitude greater than that for conventional excitation sources. Both continuous wave (CW) and pulsed dye lasers have been used to provide tunable radiation as the excitation source, but pulsed dye lasers have seen the most use in LEAFS. The very high peak irradiances achieved through the use of pulsed dye lasers easily result in saturation conditions for the transition of interest. This high irradiance also allows nonresonance transitions to be explored, thereby

Figure 4-1 : Block diagram of LEAFS instrumentation



reducing the noise contribution of the laser scatter in the atom cell. While the use of laser excitation is the closest to an ideal source for AFS, the high cost involved in obtaining appropriate instrumentation has kept the full potential of this technique from being realized.

While dye laser excitation is typically used as the means for excitation in LEAFS, dye lasers require excitation themselves in order for a lasing action to occur. Flashlamp pumping has been used, but the resulting pulse from the dye laser has a low average power because of the long pulse duration, which in many cases will not result in saturation conditions. Laser pumping results in shorter pulses from the dye laser with total per pulse power sometimes lower than that for flashlamp pumped, but with peak intensities that are much greater usually effecting saturation conditions.

Principles of Lasers

The laser consists of three components : 1) an active medium which amplifies an incident electromagnetic wave, 2) an energy source which selectively pumps energy into the active medium resulting in the population of selected levels and eventually resulting in a population inversion, and 3) an optical resonator, composed of two mirrors, which stores part of the emission and allows some to escape as the lasing.¹²⁸ A population inversion occurs when the upper level population can be made to exceed that of the lower level, and when this occurs, the system behaves as an amplifier. When this occurs, the atomic or molecular system is said to be an active medium.¹²⁹ Such an amplifier is called a laser which stands for *light amplification by stimulated emission of radiation*.

The optical resonator (Figure 4-2) causes selective feedback of the radiation emitted from the active medium.¹²⁸ This active medium is located between two mirrors in the resonator, one of the mirrors being partially transparent. Defining the resonator cavity length as d' , the optical pathlength as d , and the length of the active medium as b , d is given as

$$d = \eta b + \eta' (d' - b) \quad (4-1)$$

where η is the refractive index of the active medium and η' is the refractive index of the atmosphere in the rest of the resonator. The electromagnetic field is directed back and forth through this resonator cavity and is amplified with each pass through the active medium. Lasing is produced when some of this amplified radiation is allowed to pass through the partially transparent mirror. This laser amplifier can be converted into an oscillator above a certain pump threshold. Oscillation begins when the gain of the active medium becomes equal to the losses in the system.¹²⁹

There are many ways through which a population inversion can be attained. It is not possible to reach a population inversion in a two level system since the absorption and emission processes must be equal and the maximum population that the upper level can attain would be one half of the total population. Therefore, systems resulting in lasing action must consist of three or more levels (Figure 4-3). The required excitation process, called pumping, can be achieved through a number of methods including electrical methods employing an electrical discharge, by chemical reactions, or by rapid adiabatic expansion.¹²⁹ The output energy will always be less than the pump energy,

Figure 4-2 : The optical resonator.

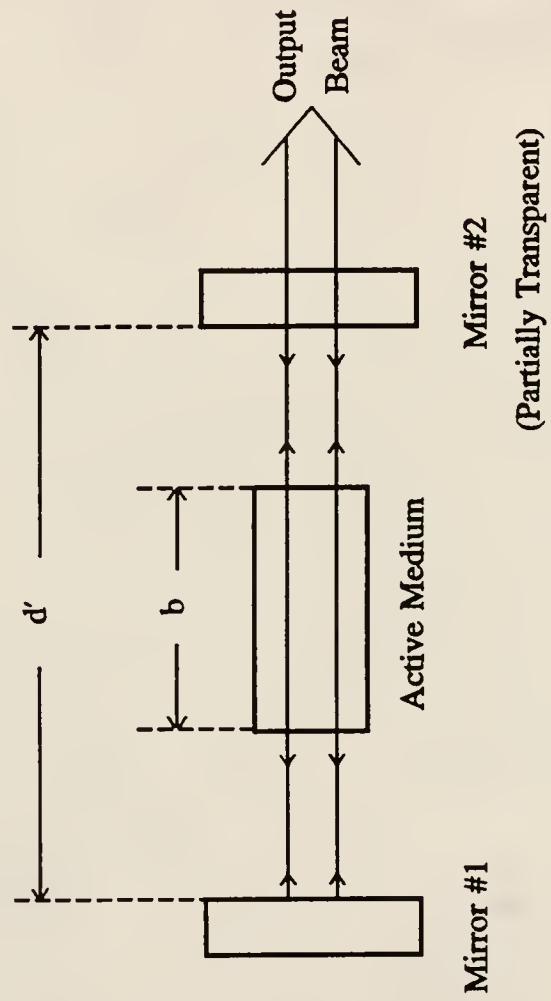
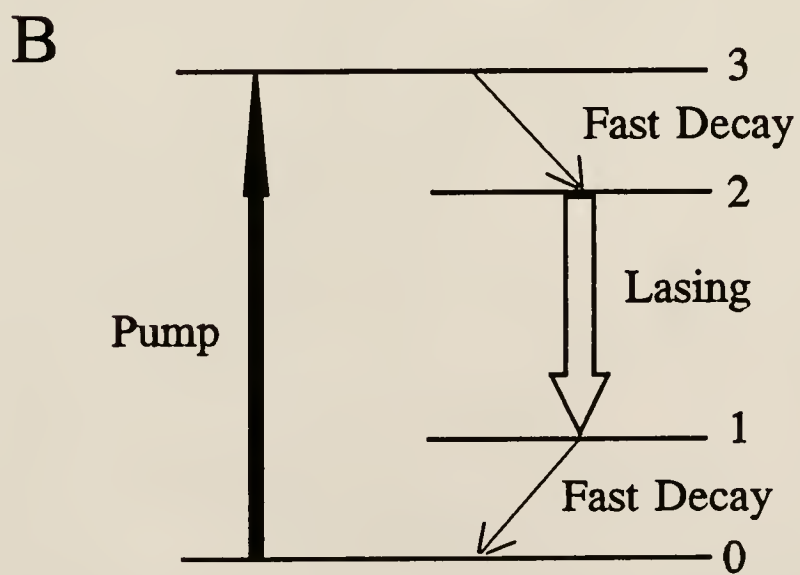
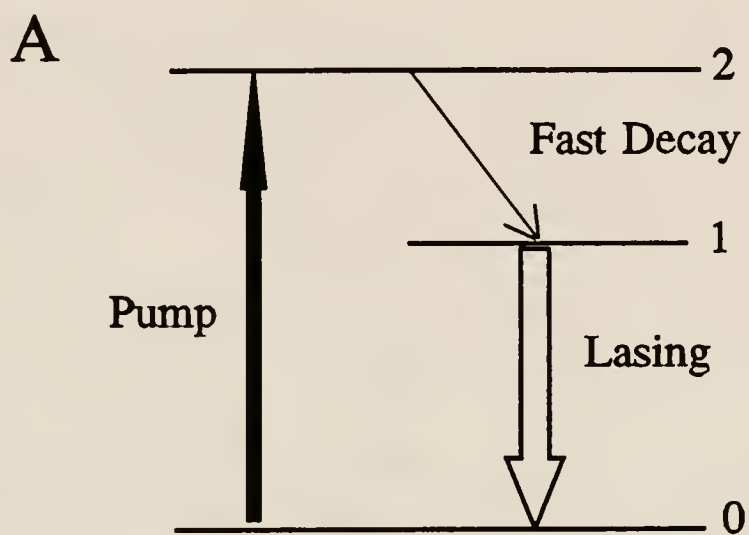


Figure 4-3 : Lasing schemes. (A) In the three level scheme, atoms are pumped to level 2 and this population undergoes rapid relaxation to level 1. If the lifetime of level 1 is significantly greater than that of level 2, the population of level 2 will grow and eventually become greater than the population of the ground state. (B) In the four level scheme, pumping occurs from level 1 to level 3 resulting in a population inversion between levels 2 and 1. It is easier to attain a population inversion in the four level case.



sometimes with efficiencies of 20% or lower, but the resulting radiation has properties unique to lasers alone and, specifically, different than conventional excitation sources.

Types of Lasers

One laser that has been used as a pump for a dye laser in LEAFS experiments is the Nd:YAG. This laser consists of Nd^{+3} in a yttrium-aluminum-garnet host. The active medium in the case of this laser is a rod which is optically pumped to result in either CW or pulsed radiation. The pulsed Nd:YAG has laser pulse durations on the order of nanoseconds and enjoys very high output powers. The Nd:YAG laser emission occurs at $1.06\text{ }\mu\text{m}$, and this wavelength is frequency doubled into the visible range for use as a pump source for a dye laser.

The most common, and numerous, of all lasers are gas lasers. All of the noble gases have been made to lase, and these lasers, along with the helium-neon laser, are some of the most reliable lasers. Unfortunately, they are not really appropriate choices as pump sources for dye lasers. One gas laser commonly used as a pump laser for a dye laser is the nitrogen laser which uses a vibronic transition of the nitrogen molecule at 337.1 nm .¹²⁹ The nitrogen laser emits a short pulse with peak powers up to 100 kW.

Excimer lasers are among the newest of the gas lasers and are used to a large extent as pump lasers for LEAFS experiments today. In this type of laser, a gaseous mixture (e.g. Xe, HCl, and Ne) is subjected to an electrical discharge resulting in the formation of an excimer (e.g. XeCl), hence the name excimer. Excimers are molecules which are bound in the excited state but are unstable in their ground states.

Figure 4-4 : Schematic potential diagram of an excimer molecule.

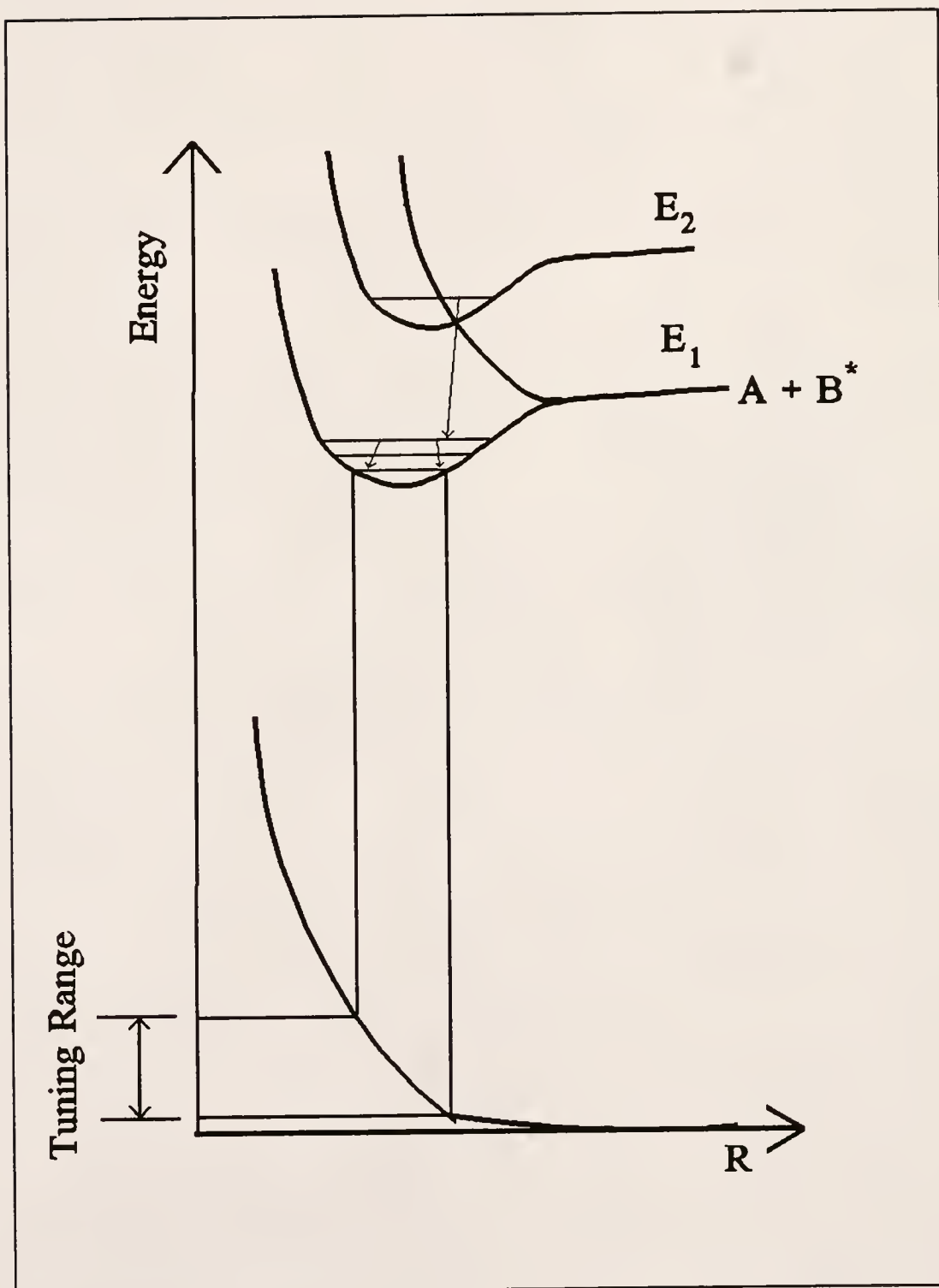


(Figure 4-4).¹²⁸ The excimers of different gas species are ideal candidates for the active medium of lasers since a population inversion is constantly maintained. A variety of ultraviolet wavelengths are available with different gas mixtures (Table 4-1). These lasers are tunable over a small wavelength range dependent upon "the slope of the repulsive potential and on the internuclear positions r_1 and r_2 of the turning points in the excited vibrational levels" (354).¹²⁸ (Figure 4-4). Because of the relatively long wavelength (308 nm) and long lifetime of the gas mixture, the XeCl excimer laser has proven to be the most useful of the excimer lasers for pumping dye lasers.

The dye laser is the main source of excitation for LEAFS experiments, but, as mentioned earlier, it requires pumping from another excitation source. The lasers just discussed as well as a flashlamp and CW laser not included in this discussion have been used for this purpose, and the results of these studies are shown in Table 4-2. The dye laser cavity (Figure 4-5) consists of a dispersive device allowing for wavelength selection and optics directing the excitation radiation through a dye cell. This cell is filled with a solution of dye which absorbs the incident radiation resulting in oscillations within the dye cell and subsequent lasing emitted from the cell.

Atomization Reservoirs used in LEAFS

Several atomization cells have been evaluated for implementation with LEAFS. Most LEAFS work has been performed in flames, but more recently other atomizers are being routinely used in LEAFS including plasmas, glow discharge devices, and electrothermal atomizers. As is the case for other atomic spectrometric methods, the

Table 4-1

Typical Excimer Laser Characteristics¹²⁹

Laser Medium	Wavelength (nm)	Pulse Energy (J)	Average Power (W)
ArF	193	0.2 - 0.3	10
KrCl	222	0.03	1
KrF	248	0.3 - 0.4	18
XeFl	308	0.08 - 0.2	8
XeF	351	0.08 - 0.15	7

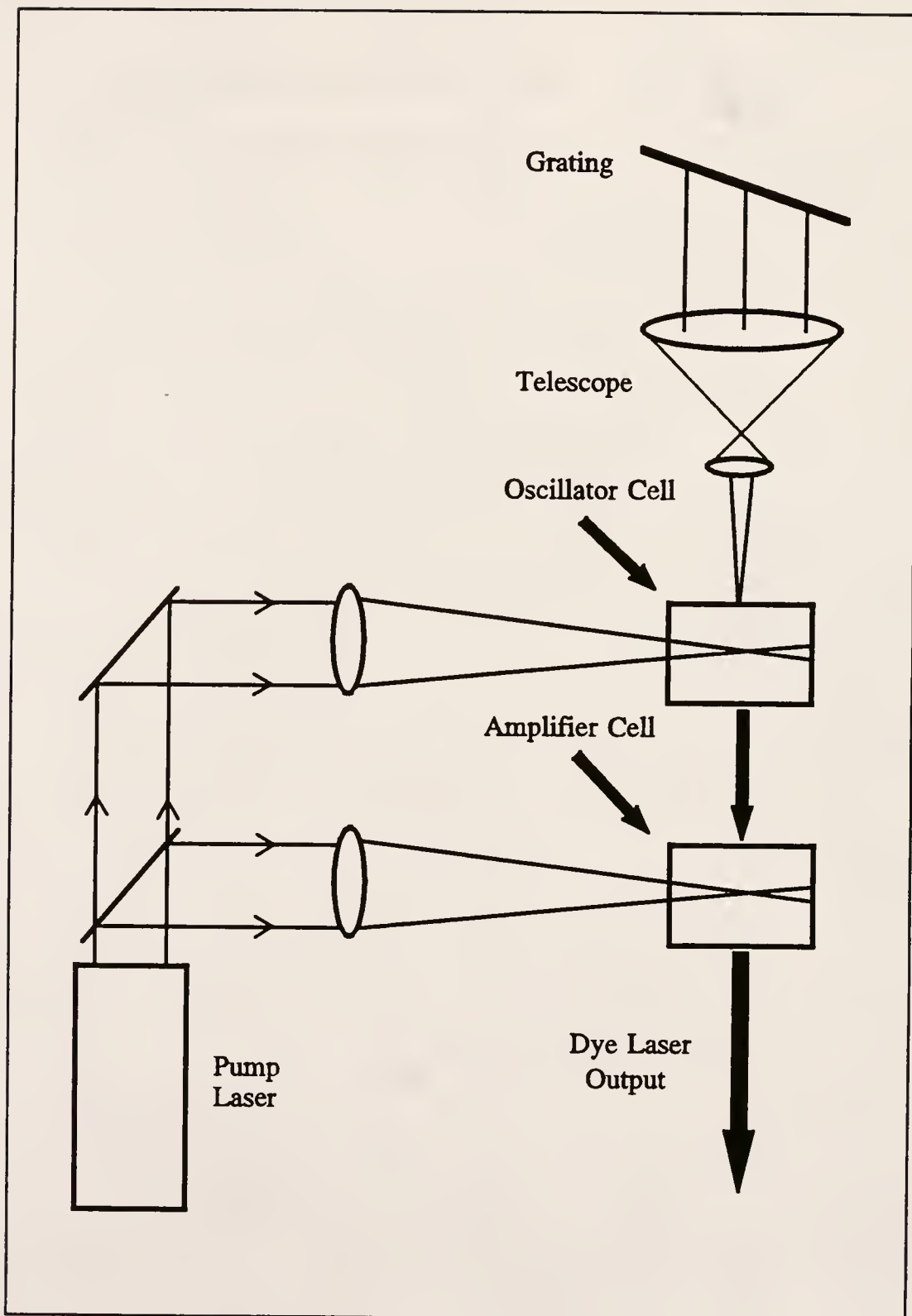
Table 4-2

Typical Pulsed Dye Laser Characteristics¹²⁹

Pump Source	Tunability Range (nm)	Peak Power (kW)	Pulse Duration (ns)	Repetition Rate (Hz)
Flashlamp	220 - 960	100 - 500	250 - 750	1 - 10
N ₂	400 - 970	1 - 100	1 - 8	1 - 100
Nd:YAG	195 - 500	100 - 10,000	5 - 10	1 - 30
Excimer	217 - 970	100 - 1000	10 - 20	1 - 500
CW*	400 - 1000	0.1 - 5	0.015	10 ³ - 4x10 ³

* Synchronously pumped, mode-locked, cavity dumped.

Figure 4-5 : Dye laser.



ideal atomizer would have a large and stable nebulization-atomization efficiency. That is, it is desirable to maximize the percentage of nebulized analyte that is actually atomized and present for analysis in the atom cell.

In particular, for AFS methods, the atomizer should have a high enough temperature and long enough residence time to insure complete vaporization of solution particles, thereby reducing the scatter noise which, in some cases, is the limiting noise in a fluorescence measurement. If an excited state fluorescence scheme is being studied, or if thermal excitation is necessary from the excited level to the level from which the fluorescence is being monitored, these processes should easily take place in the chosen atomizer.

Flames

The flames used in spectroscopic analyses are hot, chemical flames resulting from reaction between a fuel and an oxidant. Chemical flames have characteristic structures based on the fuel/oxidant combination used. Flame types can be separated into the categories of turbulent flames and laminar flames.

Turbulent flames were the first flame type applied to LEAFS because total consumption burners result in a higher concentration of atomic vapor in this atom cell available for excitation. Total consumption burners are unpremixed burners which, as the name implies, introduce the entire aspirated sample into the flame cell. This, combined with the fact that these burners are operated at lower temperatures than laminar flow burners, results in many droplets not being vaporized and atomized. This in turn

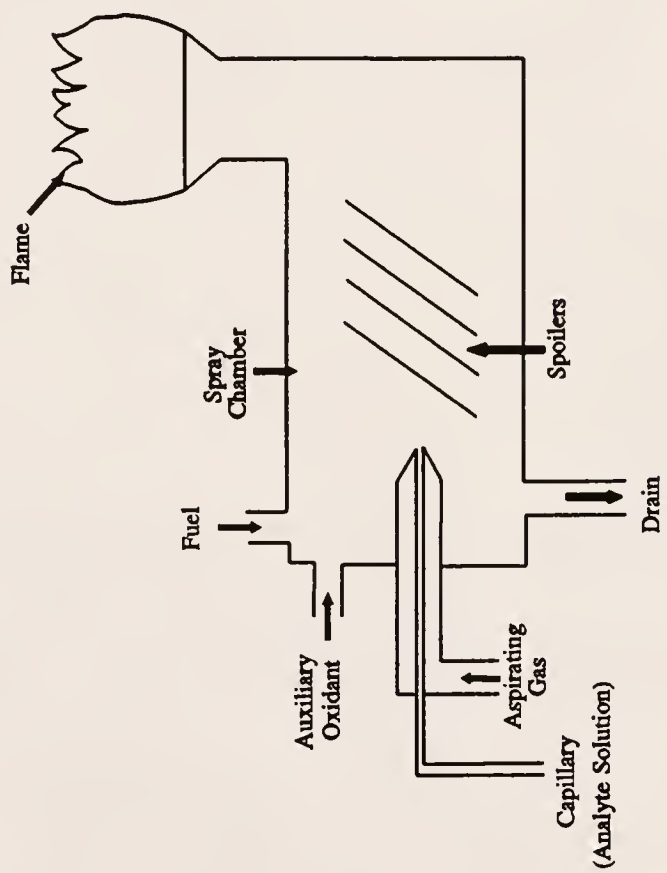
causes scatter noise from the laser radiation reflecting off of these droplets. Because of this large disadvantage, turbulent flow burners have enjoyed limited use in LEAFS.¹³⁰

The implementation of laminar, premixed flames in LEAFS results in reduced droplet size and, therefore, a decrease in the laser scatter noise, but at the same time introduces the disadvantage of the consequent lower atom concentrations available for analysis. In addition to this reduction in noise, premixed flames are sometimes surrounded by a sheath of inert gas (i.e. argon or nitrogen) to minimize the interaction of flame gases with air.¹³¹ These flames have less flicker noise problems than the turbulent flow burners simply because of the smooth, steady flow produced by this type of burner. Most laminar flames use a pneumatic, concentric nebulizer and spray chamber (Figure 4-6). In most cases, capillary burner heads are used to make it possible to change the shape and pathlength of the flame.¹²⁹

The type of flame to be used is typically selected on the basis of compromises among atomization efficiency, background emission, and quenching characteristics¹²⁹. Qualitatively, quenching properties increase in the order $\text{Ar} < \text{H}_2 < \text{H}_2\text{O} < \text{N}_2 < \text{CO} < \text{O}_2 < \text{CO}_2$.³³ Early on, hydrogen-based flames were employed because of the low background noise and low quenching. A mixture of oxygen and argon provides improved detection limits over those obtained in hydrogen based flames, but these mixtures result in lower temperature flames which do not efficiently vaporize all of the introduced sample.

Most LEAFS experiments have been carried out in air/acetylene or a nitrous oxide/acetylene flame because of their high atomization efficiency coupled with minimal

Figure 4-6 : Premixed spray chamber nebulizer/burner.



interferences and scattering. There is a higher quenching efficiency in such sources, but many times this limitation can be offset through the use of lasers as the source of excitation.

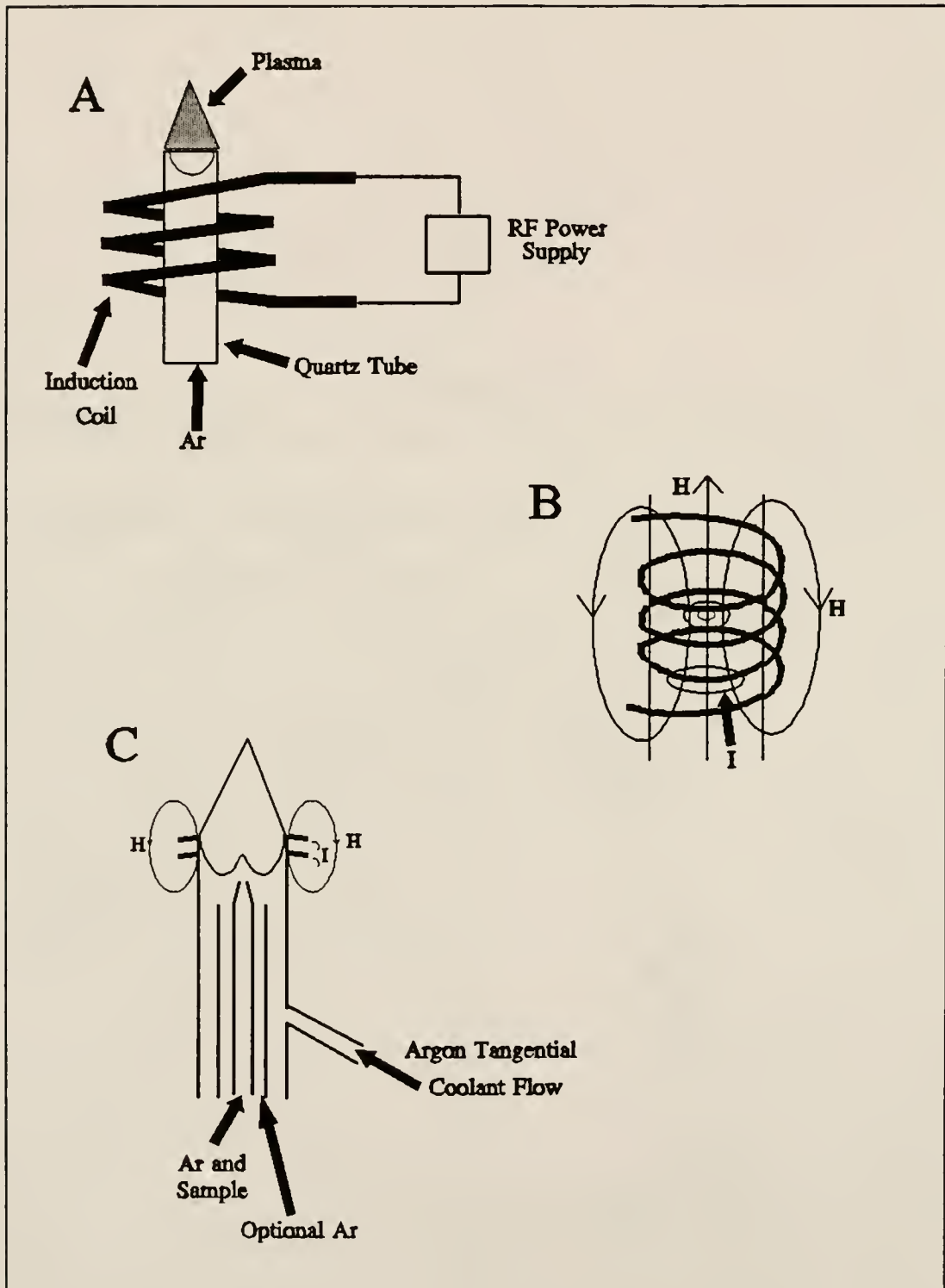
Plasmas

A plasma is a hot, ionized gas. Electrically generated plasmas have been used as an atom source for optical emission spectroscopy, AAS, and, more recently, AFS. These flame-like plasmas operate at significantly higher temperatures than flame atomizers and are chemically inert environments compared to flames. The sample is introduced into the plasma through the use of a pneumatic nebulizer where it is readily vaporized and atomized in this high temperature atom cell.

The most commonly used plasma in the field of AFS is the inductively coupled plasma (ICP). The plasma is typically formed in a quartz tube surrounded by an induction coil which is connected to a high frequency generator operating at frequencies from 5 to 50 MHz (Figure 4-7). The resulting output powers are typically between 1 to 5 kW. An inert gas, usually argon, acts as the support gas for the plasma as well as a the coolant gas for the quartz tube.¹²⁹ The plasma is formed when a Tesla coil produces "seed" electrons and ions in this quartz tube. A plasma will form, provided the magnetic field strength is strong enough and the gas streams follow a particular, rotationally symmetrical pattern.¹³²

For the implementation of LEAFS in an ICP, the forward power must be kept as low as possible while still maintaining a stable plasma in order to maximize the atom

Figure 4-7 : Operation of the ICP. (A) An induction coil connected to an RF generator surrounds a quartz tube through which Ar is flowing. A plasma then forms when the Ar becomes conductive. (B) The magnetic fields (H) and eddy currents (I). The high frequency alternating currents in the coil generate magnetic fields. The ions and electrons are accelerated in an eddy current. (C) Complete ICP torch.



population present. The high temperatures in the ICP (7000 to 8000 K) result in an appreciable amount of the analyte being present in an ionized form. It is also advisable to view high in the plasma where the temperature is usually in the range of 3000 to 3500 K to probe the most concentrated atomic population.

Very little work has been done using a direct current plasma (DCP) as an atom cell for LEAFS. In a DCP, a flow of partially ionized gas is forced out of a small orifice at a high velocity.¹²⁹ The plasma is produced by a dc discharge, similar to a dc arc, struck between two or more electrodes. A comparison of detection limits obtained with the ICP and the DCP shows no difference in the atom cells,¹³³ but there has really not been enough work done in the DCP to make a valid comparison. Most DCP-LEAFS work is confined to its use as a diagnostic tool for studying effects within the plasma. One study involved the measurement of the enhancement effects of emission signals in matrices composed of easily ionized elements.¹³⁴ This measurement is a difficult one in emission spectroscopy because the signal cannot be resolved over the observation axis because of the DCP's lack of symmetry, and, as a result, cannot be evaluated mathematically. This is not the case with LEAFS, however, which has the capability to probe a nonsymmetrical source to study the atom population with spatial resolution.

There has been even less attention paid to microwave induced plasmas (MIPs) as an atom source for LEAFS than to DCPs. Like the ICP, the MIP is formed from "seed" electrons and ions created through the spark of a Tesla coil. These electrons oscillate in a microwave field (usually at 2450 MHz) and gain kinetic energy resulting in the formation of the plasma.¹²⁹ Because of the lower temperatures present in these types of

plasmas, they are really only useful in the study of alkali and alkaline earth metals. One study performed on sodium using MIP-LEAFS¹³⁵ resulted in a detection limit on the order of pg/cm³.

Electrothermal Atomizers

Several electrothermal atomizers (ETAs) have been used as atom cells for LEAFS including open atomization devices (graphite cup and rod ETAs), and enclosed atomization reservoirs (graphite tube ETAs).¹³⁶ When using ETAs for analysis, a small sample is deposited and the atomizer is electrically heated producing atomic vapor. This vapor is then probed and the resulting fluorescence signal collected. With graphite furnaces, the atomization takes place in a cylindrical tube or a hollow cup. When the process takes place in the cup, the atom vapor above the cup is probed and the subsequent fluorescence is collected, but in a tube, the atoms to be probed remain in the tube for up to one second where the excitation takes place and the fluorescence signal is collected at a 90° angle from this excitation radiation. The graphite rod is the simplest of the ETAs to use, but the cup offers great improvement over the rod because it is at least partially contained and separated somewhat from the atmosphere. By far the most desirable ETA for LEAFS is the graphite tube which contains the atoms in a hot environment separated from the atmosphere during the laser excitation and fluorescence steps.

The linear dynamic range for ETA-LEAFS is 4 to 7 orders of magnitude with LODs in the range of pg. ETA excitation methods provide the advantages of direct solid

sampling with little or no pretreatment along with the disadvantage of matrix interferences. In cases where sensitivity is the goal to be achieved, the graphite furnace is the method of choice yielding superior LODs over both plasma and flame LEAFS. These devices are not, however, used routinely for LEAFS experiments in lieu of atomizers with continuous sampling capabilities making the total analysis time in ETAs much longer in comparison.

Other Atomization Reservoirs used in LEAFS

Other forms of sample introduction and atomization have been used in conjunction with LEAFS, but none of these other methods has really caught on yet with respect to routine analysis. As was mentioned earlier, an extended sleeve torch was implemented in an ICP-LEAFS study in an attempt to reduce interferences while viewing in the low temperature region of the plasma.⁷²

The glow discharge has not been used to a great extent as an atom source for LEAFS, but has been studied as a possibility for just such a use. The glow discharge is a gas discharge generated between two planar electrodes in a cylindrical glass tube at a reduced pressure.¹²⁹ A dc voltage source and a current-controlling series resistance are connected to the electrodes. Using metallic electrodes in the tube produces the spectrum of the metals present. Although conducting materials are the most easy to analyze in this atom source, non-conductors can also be investigated if mixed with a conducting material, such as copper powder, and pressed into a pellet. Direct vaporization from a solid sample is desirable because this technique involves little sample pretreatment and

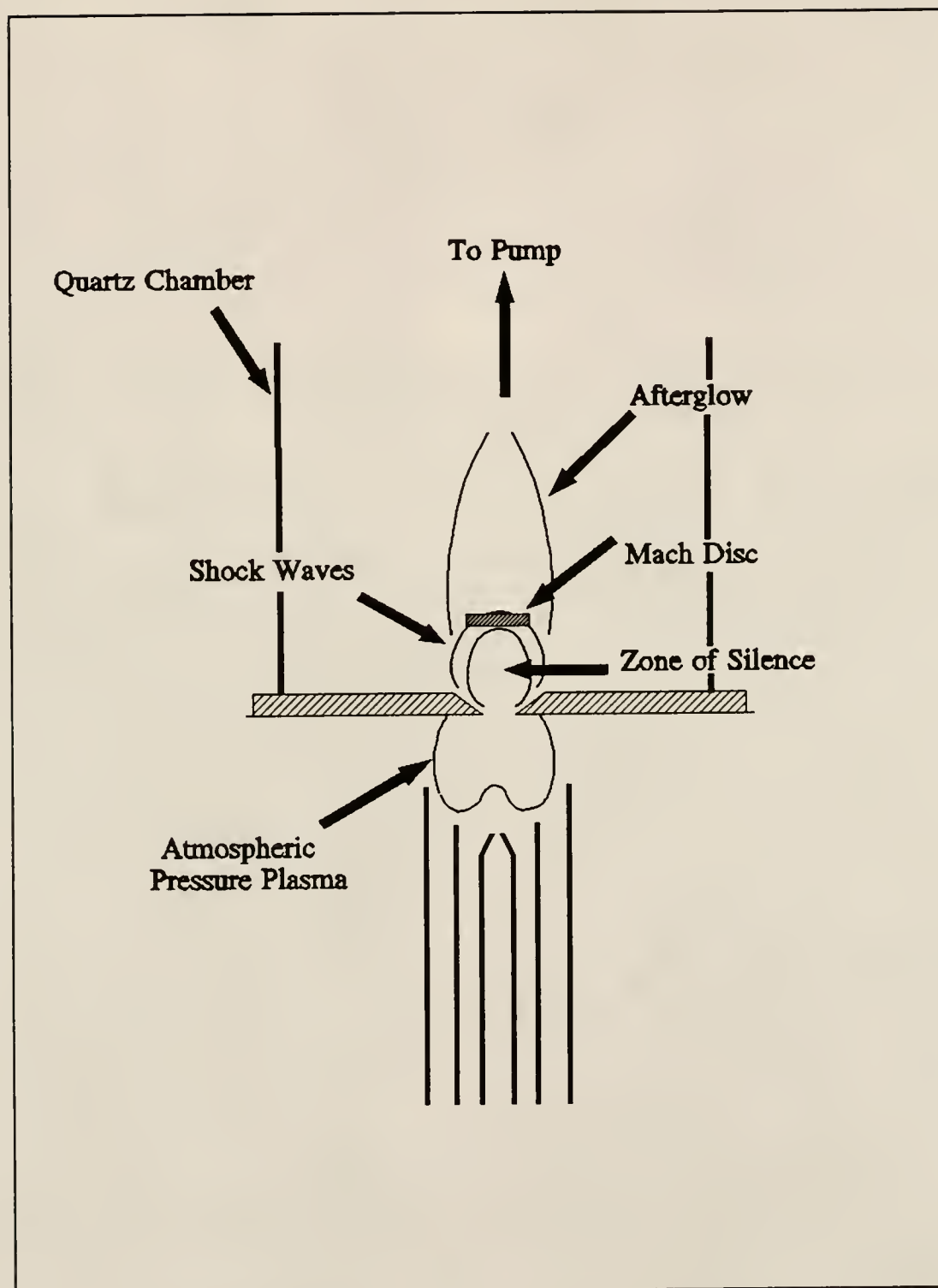
preparation. Since this is not always possible, solution deposition and subsequent drying of an analyte solution onto this electrode result in atomization of the sample on the surface, with this population then probed by laser excitation. For atomic fluorescence, the glow discharge can be operated in either the dc mode or a pulsed mode. In the pulsed mode, the fluorescence can be observed while the discharge is off resulting in a decrease in background emission by a factor of 10 to 100.

Reduced pressure flames and plasmas have also been employed in LEAFS studies.^{108,109} In the low pressure plasma application¹⁰⁸ an expansion chamber (Figure 4-8) was positioned over the ICP with a sampling orifice similar to that used in ICP-mass spectrometric instrumentation. This chamber consisted of a quartz cylinder with a fairly large diameter to minimize the refraction effects on the entering laser beam being used to probe the atomic population in the reduced pressure plasma.

Wavelength Selection Devices

For AFS studies, the requirements for a wavelength selection device depend upon the source being used for excitation. Line sources or laser excitation, provide a distinct advantage in this selection process due to the "self-monochromating" nature of atomic fluorescence.¹²⁹ When using laser radiation as an excitation source, there are very few chances for optical interferences unless concomitant atoms are excited and fluoresce within the bandpass of the selected monochrometer. Another source of interference is any laser scatter collected and focussed onto the entrance slit of the monochrometer, but

Figure 4-8 : ICP torch low pressure sampling apparatus.



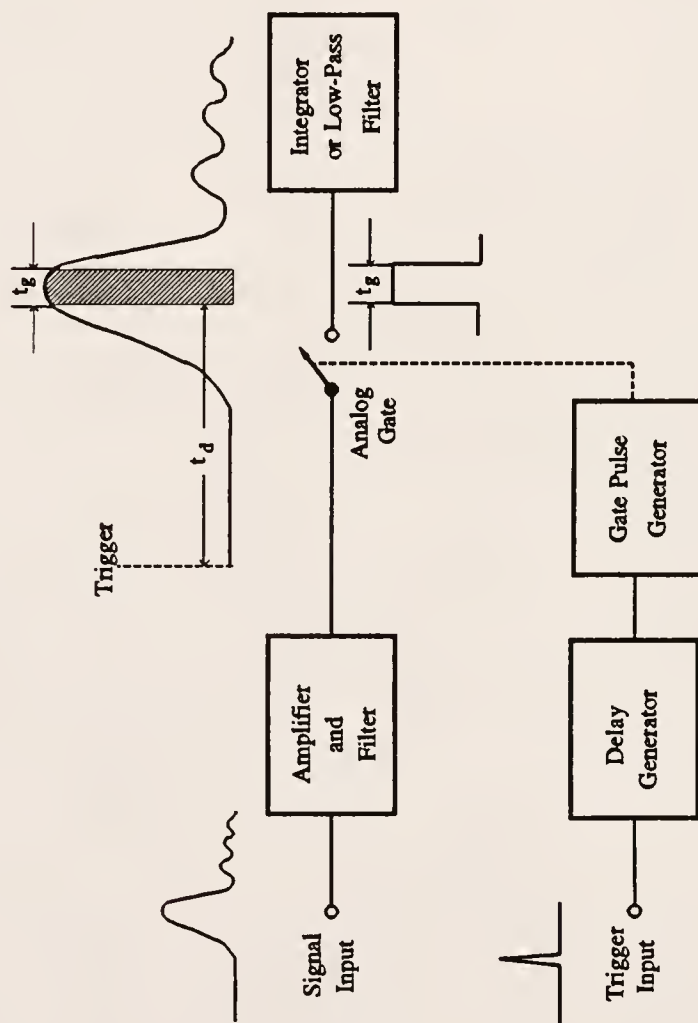
this can be minimized by either changing atomization conditions or monitoring fluorescence from a nonresonance line.

Detection Methods used in LEAFS

Detection systems for laser excited fluorescence consist of photomultiplier tubes coupled with either an oscilloscope or a boxcar averager. The photomultiplier tube (PMT) must be wired for fast response as a result of using pulsed laser excitation. A boxcar is analogous to a sampling oscilloscope with the added benefit of signal processing¹³⁷ and is used for the measurement of repetitive signals, particularly those with short pulse durations and low duty cycles.¹²⁹ The boxcar can be operated in either a scanned mode or as a pulsed measurement. The gate width is typically set anywhere from 5 ns to 50 ns, depending upon the signal collection and processing desired (Figure 4-9).

To understand the function of a boxcar integrator, a typical example will be given and discussed. Take, for example, the fluorescence signal produced as a result of pulsed laser excitation. The laser pulse is monitored by a photodiode providing the trigger signal. The fluorescence signal is measured by the photomultiplier tube (PMT) and, after current-to-voltage conversion, this signal is sent to the boxcar input. Signal output as the result of many pulses is averaged at this time greatly reducing the signal to noise. The entire signal peak can be averaged, or, alternatively, a small time slice correlating to the maximum fluorescence signal can be selected. This gated detection method also allows

Figure 4-9 : Boxcar integrator. The signal input is amplified and connected to an integrator for a gate time t_g . This gate pulse occurs at a time delay, t_d , set relative to the trigger signal.



time resolved studies to be performed as the result of scanning a narrow gate over the fluorescence peak.

CHAPTER 5 RATE EQUATIONS THEORETICAL TREATMENT OF LEAFS

Two Level Atomic System

In most cases, a rate equations approach is a valid way in which to address LEAFS theory. The theoretical treatment presented in this dissertation has been outlined in the literature^{138,139} and the approach presented here is based on these discussions. This treatment begins by approximating the populations of a two level atomic system (Figure 5-1) with the lower level (level 1) representing the ground state, and the upper level (level 2) being an excited state of this proposed atom system. The population densities, n_1 and n_2 , for these two levels can be described in terms of the radiative and nonradiative rates of excitation and de-excitation processes either adding to or depleting the population of the desired level. Some assumptions made in this implementation of the rate equations model include that the atom population is a dilute species in a gaseous phase at atmospheric pressure. In the absence of any externally applied fields, the atom distribution in the energy levels follows the Boltzmann distribution

$$\frac{n_2}{n_1} = \frac{g_2}{g_1} \exp\left(-\frac{h\nu}{kT}\right) \quad (5-1)$$

where h is Planck's constant ($J \cdot s$), ν is the frequency of the transition between levels 1 and 2 (Hz), k is Boltzmann's constant (J/K), g_1 and g_2 are the statistical weights of levels

1 and 2, respectively, n_1 and n_2 are the population densities of levels 1 and 2 (atoms/cm³), respectively, and T is the temperature of the system (K). The rate equation depicting the rate of decay of atoms from level 2, neglecting collisional contributions, is given as

$$\frac{dn_2}{dt} = -n_2 A_{21} \quad (5-2)$$

where A_{21} is the Einstein coefficient of spontaneous emission from level 2 to level 1 (s⁻¹).

When a laser is introduced into the system to probe the existing atom population distribution, the population densities respond according to the radiative power of the laser excitation (Figure 5-2). The rates of excitation, R_{12} (s⁻¹cm⁻³), and de-excitation, R_{21} (s⁻¹cm⁻³), between the levels in this case are

$$R_{12} = (B_{12} \rho_\nu(\nu_{12}) + k_{12}) n_1 \quad (5-3)$$

$$R_{21} = (B_{21} \rho_\nu(\nu_{12}) + k_{21} + A_{21}) n_2 \quad (5-4)$$

where B_{12} and B_{21} are the Einstein coefficients of induced absorption and emission, respectively (J/cm³Hz), A_{21} is the Einstein coefficient of spontaneous emission (s⁻¹), $\rho_\nu(\nu_{12})$ is the spectral energy density (J/cm³Hz) of the laser beam probing the atom population, and k_{12} and k_{21} are the collisional rates of excitation and de-excitation (s⁻¹), respectively. The time dependent relationship depicting the changes in the population density of the excited level is written as the sum of the forward and reverse rate equations.

Figure 5-1 : Diagram of processes in a two level atom.

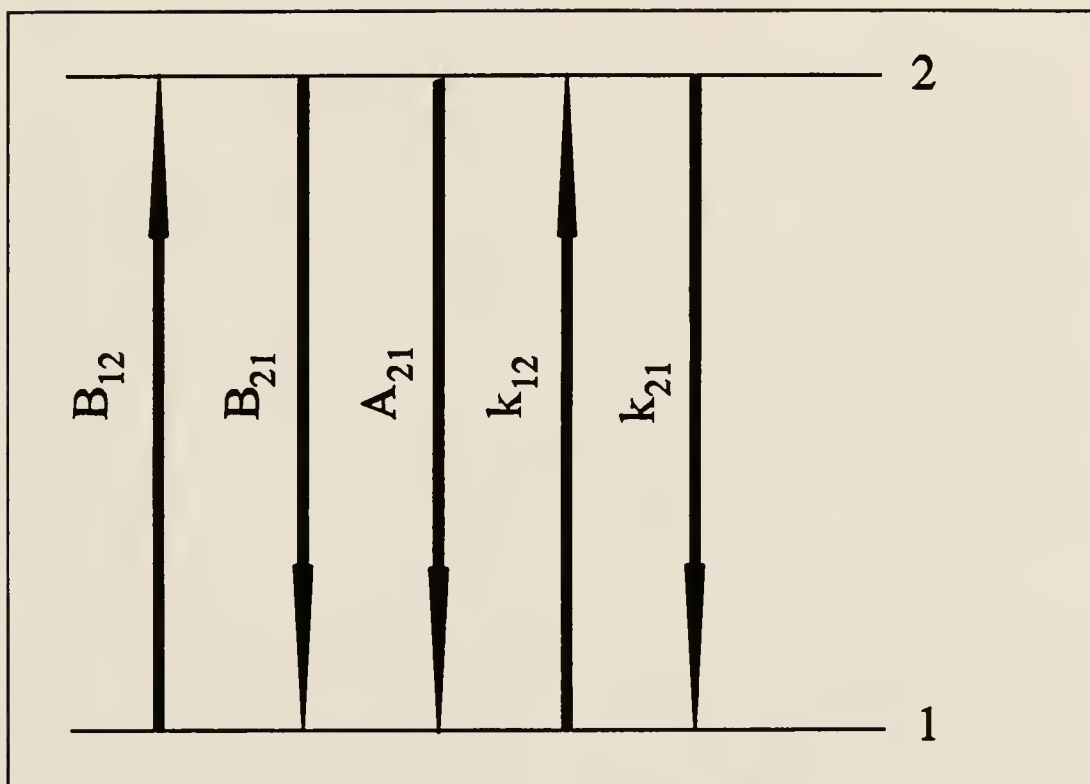
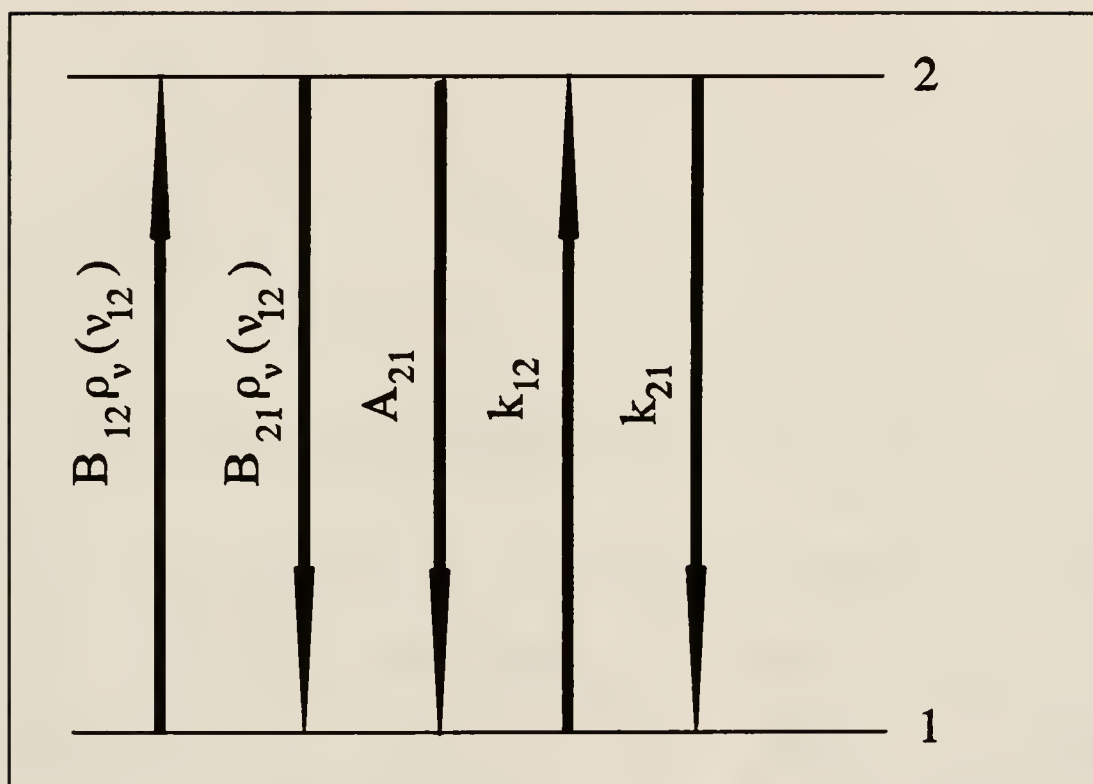


Figure 5-2 : Diagram of the processes of a two level atom experiencing laser excitation at $\lambda_{1 \rightarrow 2}$.



$$\frac{dn_2(t)}{dt} = (B_{12}\rho_v(\nu_{12})) n_1(t) - (B_{21}\rho_v(\nu_{12}) + k_{21} + A_{21}) n_2(t) \quad (5-5)$$

This differential equation can be solved and simplified utilizing the following mathematical relationships¹²⁹ :

$$g_1 B_{12} = g_2 B_{21} \quad (5-6)$$

$$A_{21} = \left(\frac{8\pi h\nu_{12}^3}{c^3} \right) B_{21} = DB_{21} \quad (5-7)$$

and for $g_1 = g_2$

$$B_{12} = B_{21} = B \quad (5-8)$$

$$k_{21} = k_{12} \exp(h\nu/kT) \quad (5-9)$$

The resulting solution represents the population density of level 2 in terms of the total atom population density, n_T (atoms/cm³), assuming that the statistical weights of the two levels are equal

$$n_2(t) = n_T B \rho_v(\nu_{12}) t_r (1 - \exp(-t/t_r)) \quad (5-10)$$

where t_r , the response time (or pumping time, (s)) of the atom population to the induced absorption and emission process, is given by

$$t_r = (2B\rho_v(\nu_{12}) + k_{21} + A_{21})^{-1} \quad (5-11)$$

It can be seen from the above expressions that if $B_{12}\rho_v(\nu_{12})$ is sufficiently large (i.e. the transition is saturated), the population density is given by

$$n_2 (\max) = \frac{n_T}{2} \quad (5-12)$$

If the statistical weights of the levels are not equal, which is often the case, a weighing factor must be added to equation (5-12) to compensate for this inequality of quantum states in the two levels, and then the population density of level 2 can then be expressed as

$$n_2 (\max) = n_T \left(\frac{g_2}{g_1 + g_2} \right) \quad (5-13)$$

The saturation spectral energy density ($\text{J}/\text{cm}^3\text{Hz}^{-1}$) (i.e. the spectral energy density required of the laser excitation to attain saturation conditions over the area of the beam) is defined as

$$\rho_v^s(v_{12}) = \frac{A_{21} + k_{21}}{2B} \quad (5-14)$$

assuming equality of the statistical weights, g_1 and g_2 , of the 2 levels connected by the laser excitation. Using this value for the spectral energy density in equation (5-10), it is found that this saturation spectral energy density produces a population for level 2 that is equal to one half of the maximum population density achieved for saturated, steady state conditions. At this point, the role that collisions play in LEAFS measurements becomes apparent. Examining equation (5-11), it can be seen that the response time is inversely proportional to the rate of collisional deactivation of level 2, k_{21} . It stands to reason that the spectral energy density required to achieve the maximum steady state population will increase as k_{21} increases. As the total rate of depopulation of level 2,

both radiative and nonradiative, increases, the energy required to compensate for these losses must increase in return.

Another physical parameter of interest in atomic studies is the quantum efficiency of fluorescence, Y_{21} , defined as the Einstein coefficient of spontaneous emission divided by the total probability of deactivation of level 2, or

$$Y_{21} = \frac{A_{21}}{A_{21} + K_{21}} \quad (5-15)$$

This parameter directly represents the relative rate of radiative de-excitation to total deactivation for a given level population.

This expression assumes atom excitation from level 1 to level 2 is a result of photon absorption. It also assumes that losses from level 2 can occur through a variety of pathways including collisions from level 2 to any level above or below level 2, or by radiative relaxation (fluorescence) from level 2 to any level below level 2. The quantum efficiency, Y_{21} , is an indication of the probability that an excited state atom present in level 2 will release a photon as it returns to its ground state, level 1 (i.e. fluoresces) rather than through some nonradiational process. It is intuitive that the higher the rate of collisional deactivation from level 2 to level 1, or the greater the number of pathways for collisional de-excitation, the lower the probability that the atom will produce fluorescence emission from level 2 to level 1.

The quantum efficiency can also be expressed in terms of the lifetime of the excited level in both the presence and absence of collisions. In the absence of collisions

resulting in losses from level 2, the spontaneous (radiative) lifetime of the level, τ_{sp} , is given by

$$\tau_{sp} = \frac{1}{A_{21}} \quad (5-16)$$

In the presence of collisions, A_{21} , the Einstein coefficient for spontaneous emission, is no longer the only mechanism through which the population of level 2 can suffer losses, and the lifetime of the level will decrease according to any collisional de-excitation. That is, the effective, or observed, lifetime of the level in the presence of collisions is

$$\tau_{eff} = \frac{1}{A_{21} + k_{21}} \quad (5-17)$$

with τ_{eff} always being less than τ_{sp} . As mentioned earlier, the quantum efficiency, Y_{21} , can be expressed in terms of these lifetimes as

$$Y_{21} = \frac{\tau_{eff}}{\tau_{sp}} \quad (5-18)$$

The saturation spectral energy density, $\rho^s(\nu_{12})$ is also dependent upon the rate of collisional de-excitation, and can be defined in terms of the quantum efficiency or τ_{eff} , assuming $g_1 = g_2$, as

$$\rho^s_v(\nu_{12}) = \frac{A_{21} + k_{21}}{2B} = \frac{A_{21}}{2BY_{21}} = \frac{1}{2B\tau_{eff}} \quad (5-19)$$

Through examination of these equations, it is apparent that as the collisional deactivation rate constant, k_{21} , increases, the quantum efficiency related to the transition between the two levels, Y_{21} , will decrease, and the saturation spectral energy density, $\rho^s(\nu_{12})$, will

increase. For example, if $k_{21} = A_{21}$, then the quantum efficiency would be reduced by a factor of 2, and the spectral energy required to attain saturation conditions in this case would increase by a factor of 2.

These relationships make sense as the definition of the quantum efficiency is the probability that the absorbed photon will result in a fluorescence photon being emitted. With an increase in k_{21} , a loss mechanism of level 2 other than fluorescence, intuitively, the result will be a lower probability of fluorescence (i.e. a decrease in Y_{21}). In following this argument, it is also intuitive that the energy required to saturate the transition, $\rho^s(\nu_{12})$, would have to increase with increased collisional deactivation in order to compensate for this loss in the population of level 2. Collisions, therefore, play a large role in the determination of several factors related to saturation conditions of absorption and fluorescence schemes.

Three Level Atomic System

When discussing the analysis of atom systems using two-color excitation schemes, it becomes necessary to expand the previous theoretical discussion to an approximated three level atomic system (Figure 5-3). When this atom system is probed with laser excitation at wavelengths $\lambda_{1 \rightarrow 2}$ and $\lambda_{2 \rightarrow 3}$, the populations of the levels respond to the excitation radiation (Figure 5-4). The resulting rate equations describing the population of the atomic levels are

$$R_{12} = B_{12} \rho_{\nu}(\nu_{12}) \quad (5-20)$$

$$R_{23} = B_{23} \rho_v (v_{23}) \quad (5-21)$$

$$R_{13} = 0 \quad (5-22)$$

$$R_{21} = A_{21} + k_{21} + B_{21} \rho_v (v_{12}) \quad (5-23)$$

$$R_{32} = A_{32} + k_{32} + B_{32} \rho_v (v_{23}) \quad (5-24)$$

$$R_{31} = k_{31} \quad (5-25)$$

It is apparent through examination of these expressions that several assumptions have been made. All collisional activation from a lower level to a more excited level has been neglected as these processes are negligible as compares to the laser excitation. Also neglected were losses either as a result of ionization or the presence of a metastable level.

These equations result in the time dependent population expressions below, written as the sum of the forward and reverse rate equations.

$$\frac{dn_1(t)}{dt} = R_{21}n_2(t) + R_{31}n_3(t) - R_{12}n_1(t) \quad (5-26)$$

$$\frac{dn_2(t)}{dt} = R_{12}n_1(t) + R_{32}n_3(t) - (R_{21} + R_{23})n_2(t) \quad (5-27)$$

$$\frac{dn_3(t)}{dt} = R_{23}n_2(t) - (R_{32} + R_{31})n_3(t) \quad (5-28)$$

From these expressions, the steady state population of the uppermost excited level, n_3 , is derived as

Figure 5-3 : Diagram of the processes of a three level atom.

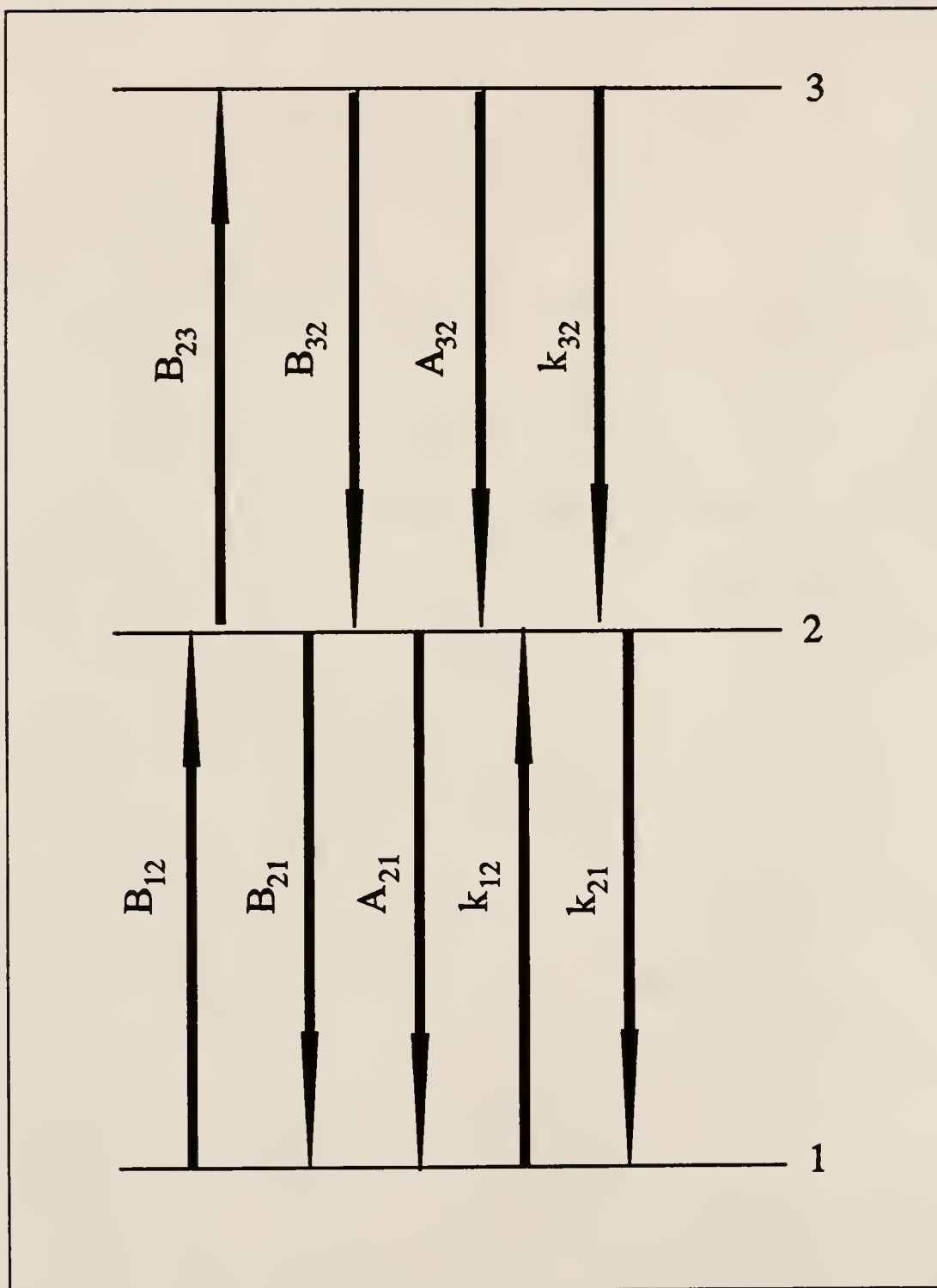
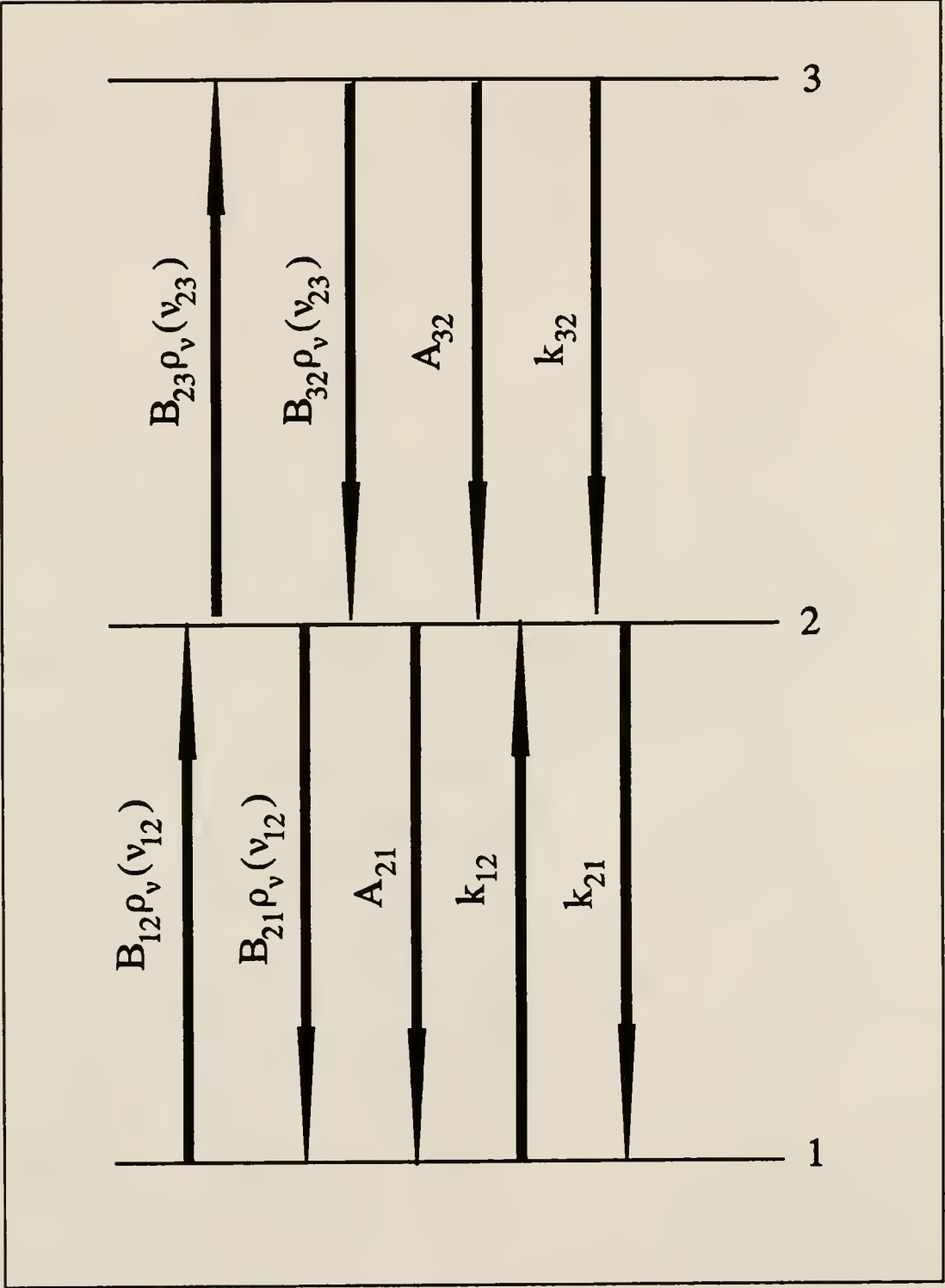


Figure 5-4 : Diagram of the processes of a three level atom experiencing laser excitation at $\lambda_{1 \rightarrow 2}$ and $\lambda_{2 \rightarrow 3}$



$$n_3 = \frac{B_{12}\rho_v(\nu_{12}) B_{23}\rho_v(\nu_{23}) n_T}{B_{12}\rho_v(\nu_{12}) B_{23}\rho_v(\nu_{23}) \left(\frac{g_1 + g_2 + g_3}{g_3} \right) + (A_{32} + k_{21} + k_{31})} \times \quad (5-29)$$

$$\frac{1}{\left[(A_{21} + k_{21} + B_{21}\rho_v(\nu_{12}) \left(1 + \frac{g_1}{g_2} \right) \right] + \left[B_{32}\rho_v(\nu_{23}) \left(A_{21} + k_{21} + k_{23} \left(\frac{g_3}{g_2} \right) \right) \right]} \quad (5-30)$$

Assuming $B_{12}\rho_v(\nu_{12})$ and $B_{23}\rho_v(\nu_{23})$ to be sufficiently large (i.e. the spectral energy densities, $\rho_v(\nu_{12})$ and $\rho_v(\nu_{23})$, are large enough to effect saturation conditions for both transitions), the above equation reduces to the following simple expression :

$$n_3(\max) = \left(\frac{g_3}{g_1 + g_2 + g_3} \right) n_T \quad (5-31)$$

Fluorescence Dip Spectroscopy

Three Level Atom System

In order to fully understand the information that can be gained through a fluorescence dip measurement, it is necessary to know what factors determine the magnitude of the fluorescence dip. A theoretical model based on the rate equations approach for time independent and time dependent fluorescence dips that can predict the behavior of a single atom, ion, or molecule has been proposed.¹⁴⁰ This section will include some simple mathematical relationships between the observed fluorescence dip and fundamental atomic physical information based on this discussion.

This treatment will assume a three level model, where the only processes considered are those included in Figure 5-4. At initial conditions, the total population, n_T , will be assumed to be present in the ground state, that is, the system is assumed to be at rest. When this population experiences excitation from a laser tuned to a wavelength corresponding to the first transition with intensity sufficient to overcome all radiative and non-radiative de-excitation (i.e. the transition is saturated), expressions for the relative population densities can be written assuming steady state conditions. As was demonstrated in the previous discussion, the relative population densities are directly proportional to the statistical weights of the levels (Equation 5-13). Each level shares a portion of the total population density according to the ratio of its statistical weight to the sum of the statistical weights of the levels involved in the excitation/de-excitation process. Under steady state, saturation conditions, the maximum population density of level 2, $n_2(\text{max})$, is equal to the total population, n_T , multiplied by the ratio $g_2/(g_1+g_2)$ where g_1 and g_2 are the statistical weights of levels 1 and 2, respectively.

When this same atom population experiences excitation from two lasers at different wavelengths corresponding to the two transitions connecting the three levels, $\lambda_{1\rightarrow 2}$ and $\lambda_{2\rightarrow 3}$, and both of these transitions are assumed to be under saturated, steady state conditions as a result of this laser excitation, the population densities again are proportional to the respective statistical weights of the levels. In this case of two step excitation, the maximum population density of level 2, $n_2(\text{max})$, is equal to the total atom population multiplied by the ratio $g_2/(g_1+g_2+g_3)$, where g_1 , g_2 , and g_3 are the statistical weights of the levels involved in the excitation scheme.

In the case of fluorescence dip spectroscopy, the value desired is that of the difference in the above quantities. That is, the fluorescence dip measurement involves both one and two step excitation while monitoring the fluorescence from the initially populated level (level 2) in both cases and taking the difference between these two values (Figure 5-5). It is intuitive that the fluorescence signal will be less in the two step excitation case due to the depletion of the fluorescent level as a result of the second excitation step.

The maximum fluorescence dip (i.e. assuming steady state, saturation conditions), Δ_{\max} , is defined as the difference in the relative population densities of level 2, n_2/n_T , for one and two step excitation

$$\Delta_{\max} = \left[\frac{(n_2)^{ss}}{n_T} \right]_{(off)} - \left[\frac{(n_2)^{ss}}{n_T} \right]_{(on)} \quad (5-32)$$

where off represents one step laser excitation and on two step laser excitation, or

$$\Delta_{\max} = \frac{g_2}{(g_1 + g_2)} - \frac{g_2}{(g_1 + g_2 + g_3)} \quad (5-33)$$

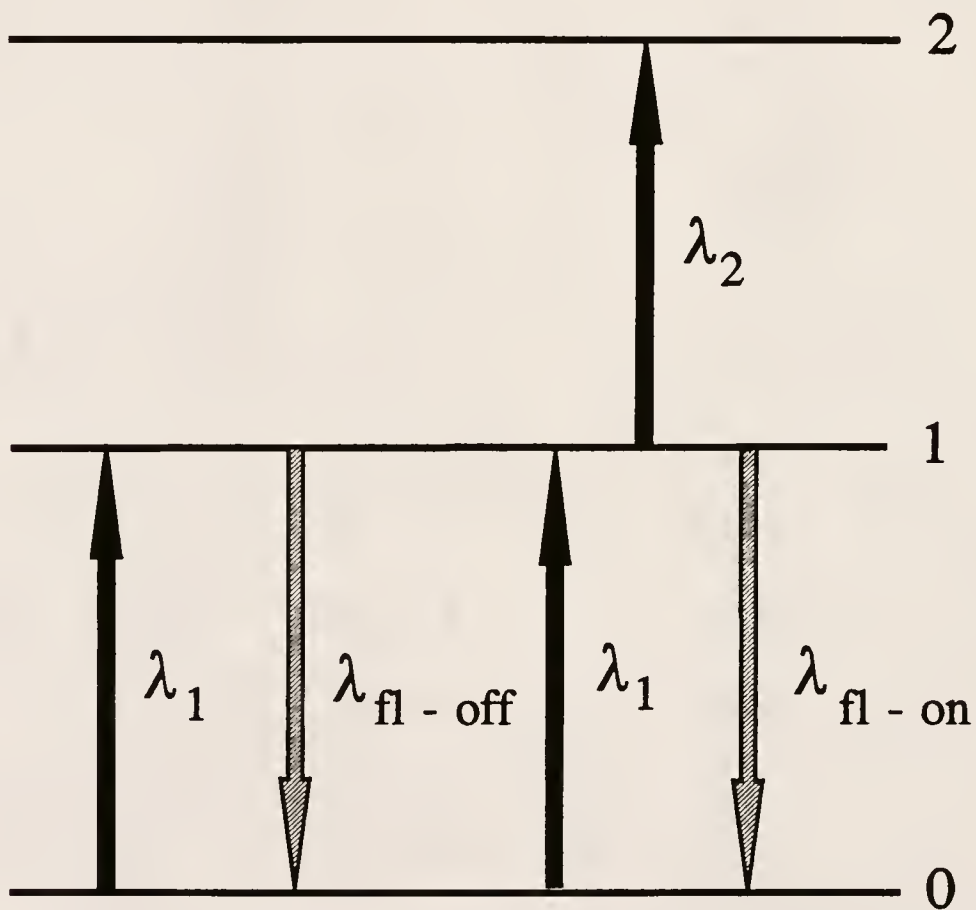
$$= \frac{g_2 g_3}{(g_1 + g_2)(g_1 + g_2 + g_3)} \quad (5-34)$$

Another useful parameter is the relative fluorescence dip, Δ'_{\max} , defined as

$$\Delta'_{\max} = \frac{\Delta_{\max}}{\left[\frac{(n_2)^{ss}}{n_T} \right]_{off}} \quad (5-35)$$

Figure 5-5 : Diagram of the fluorescence dip measurement.

Fluorescence Dip Theory



$$\text{Dip} = (\text{fl - off}) - (\text{fl - on})$$

This parameter indicates relatively how much the two step excitation depletes the population effected through one step excitation for level 2. In the same manner as for Δ_{\max} , this parameter can be expressed solely in terms of the statistical weights involved in the excitation processes as

$$\Delta'_{\max} = \frac{g_3}{(g_1 + g_2 + g_3)} \quad (5-36)$$

The relative fluorescence dip is a valuable parameter because it is independent of the total atom population and is unaffected by pre- or post-filter effects.

The previous expressions, as explained, are for fluorescence dips measured under saturation conditions. If excitation at λ_{2-3} is present at less than the saturation irradiance, the observed dip will be less, and this relationship can be shown to be directly associated to the spectral energy density of excitation for this second step by successively attenuating this second step and plotting the relative dip as a function of $\rho_s(\nu_{23})$, the spectral energy density. A saturation curve for the second excitation step is produced which reveals parameters of this excited state transition including $\rho^s_s(\nu_{23})$, the saturation spectral energy density, defined as the spectral energy density at which the relative fluorescence dip is equal to one half of the maximum relative dip. This saturation spectral energy density can be used to calculate the quantum efficiency, Y_{32} , through the relationship

$$\rho^s_s(\nu_{23}) = \left[\frac{(g_1 + g_2)}{(g_1 + g_2 + g_3)} \right] \left[\frac{8\pi h\nu^3}{c^3} \right] \frac{1}{Y_{32}} \quad (5-37)$$

A plot of the inverse of the experimentally determined relative fluorescence dip against the inverse of the spectral energy density results in a linear relationship, the slope of which can be used to determine the quantum efficiency :

$$\frac{1}{\Delta'} = \left[\frac{8\pi h\nu^3}{c^3} \right] \frac{(g_1 + g_2)}{g_3} \left[\frac{1}{\rho_\nu(\nu_{23}) Y_{32}} \right] + \left[\frac{(g_1 + g_2 + g_3)}{g_3} \right] \quad (5-38)$$

This experimentally determined relative fluorescence dip can also be used to determine the Einstein absorption coefficient, B_{23} , of the transition between the two excited levels through the following expression :

$$\Delta'(\tau) = 1 - \frac{\left[1 - \exp\left(-\left(\frac{g_2}{g_1 + g_2}\right) B_{23} \rho_\nu(\nu_{23}) \Delta \tau\right) \right]}{\left[\left(\frac{g_2}{g_1 + g_2}\right) B_{23} \rho_\nu(\nu_{23}) \Delta \tau \right]} \quad (5-39)$$

Once B_{23} is determined, it can be used to evaluate the absorption oscillator strength for this transition, f_{23} (dimensionless)

$$f_{23} = \frac{4\epsilon_0 m_e h}{e^2} \nu_{23} B_{23} \quad (5-40)$$

where ϵ_0 is the permittivity of free space ($\text{Lmol}^{-1}\text{cm}^{-1}$), m_e is the mass of an electron, and e is the charge of an electron in coulombs. The Einstein coefficient for spontaneous emission, A_{32} , can then be given by

$$A_{32} = \left(\frac{g_2}{g_3} \right) \left(\frac{8\pi h\nu^3}{c^3} \right) B_{23} \quad (5-41)$$

where c is the speed of light (cm/s).

Five Level Atom System

Although for some elements the three level model is a valid approximation, there are some experimental situations where the assumption of a three level atom system is not a good one. The electronic structure of some elements can be such that some of the levels may couple through collisions, to or from the considered levels, greatly altering the resulting fluorescence dip measurement. Other mechanisms resulting in losses from levels considered in the excitation and fluorescence scheme include ionization or relaxation to a metastable level, which would invalidate the steady state approximation for this three level model. Therefore, to more closely approximate a true atomic population, it is necessary to include some of these loss mechanisms in the theoretical treatment.

A more realistic representation is a rate equation model assuming a five level atom system (Figure 5-6). The time dependent rate equations written as the sum of the forward and reverse rate equations are

$$\frac{dn_1(t)}{dt} = R_{31}n_3(t) + R_{21}n_2(t) - R_{13}n_1(t) \quad (5-42)$$

$$\frac{dn_2(t)}{dt} = R_{42}n_4(t) + R_{32}n_3(t) - (R_{23} + R_{21})n_2(t) \quad (5-43)$$

$$\frac{dn_3(t)}{dt} = R_{43}n_4(t) + R_{23}n_2(t) + R_{13}n_1(t) - (R_{34} + R_{32} + R_{31})n_3(t) \quad (5-44)$$

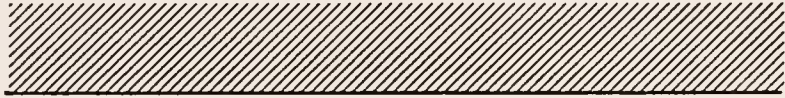
$$\frac{dn_4(t)}{dt} = R_{34}n_3(t) - (R_{41} + R_{43} + R_{42})n_4(t) \quad (5-45)$$

$$\frac{dn_i(t)}{dt} = R_{4i} n_4(t) \quad (5-46)$$

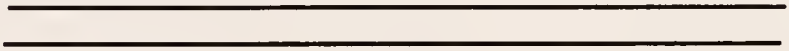
The given five level atom (Figure 5-6) demonstrates an electronic structure similar to that of both silver and copper, the two atom systems involved in the work presented in this dissertation. Included in this model are two intermediate, closely spaced, excited state levels (levels 2 and 3), two uppermost excited state levels which are closely spaced enough to behave as one level through collisional mixing at atmospheric pressure (level 4), and the ionization continuum, although losses through this latter mechanism are considered to be low. If enough is known about this five level system, the rate equations can be solved with a computer program and determined numerically resulting in the time independent populations of the five levels in this system.

The relative populations of the levels involved in the atomic system of interest can be modeled using the rate equations approach to examine the effects of collisions on these populations. While holding all other relationships between the atomic levels constant, assuming equality of all of the statistical weights of the levels, and assuming laser excitation from the ground state to the second excited state (level 3) and from this excited state to another excited state level (level 4), the collisional coupling between levels 2 and 3 was varied and the resulting relative populations were solved for (Figures 5-7 to 5-9). With low collisional mixing between these two, closely spaced, intermediate levels (Figure 5-7) the relative population of level 2, n_2 , increases slowly as a result of collisions from level 3 as well as radiative relaxation from level 4 and does not even begin to approach the relative population of level 3. With moderate and high rates of

Figure 5-6 : Diagram of a five level atom.



i



4



3



2



1

collisional coupling between level 2 and 3 (Figures 5-8 and 5-9), the relative population of level 2, n_2 , approaches and eventually becomes equal to n_3 once the system has reached steady state where the two levels can be considered to behave as one level.

Negative/Inverse Fluorescence Dip

Through the examination of the rate equation describing the behavior of the five levels considered in this approximation, it was noticed that the collisional relationship between the two closely spaced, excited state, intermediate levels (levels 2 and 3) had a profound effect on the fluorescence dip measurement. This collisional relationship can be monitored through the monitoring of the thermally-assisted, nonresonance fluorescence (Figure 5-10). In this example, laser excitation is supplied at $\lambda_{1 \rightarrow 3}$ while the fluorescence as a result of collisions from level 3 to level 2 (i.e. the fluorescence from level 2) is measured. Then a second excitation step is added at $\lambda_{3 \rightarrow 4}$, and again the nonresonance fluorescence from level 2 is monitored. The amount that the monitored fluorescence signal will decrease is dependent upon several relationships that level 2 has with the other levels in the atom. One of these relationships that can affect the population of level 2, and therefore the fluorescence signal and the fluorescence dip measurement, is the collisional relationship between levels 2 and 3. If these levels are substantially coupled (i.e. the collisional relationship is great), this nonresonance dip will be present, but not to the same extent as the dip for the resonance fluorescence. If the collisional relationship between levels 2 and 3 is great enough so as to be able to assume these two

Figure 5-7 : Computer generated plot of relative population densities of atomic levels as the result of laser excitation at λ_{1-3} and λ_{3-4} versus time with low collisional activity between levels 2 and 3.

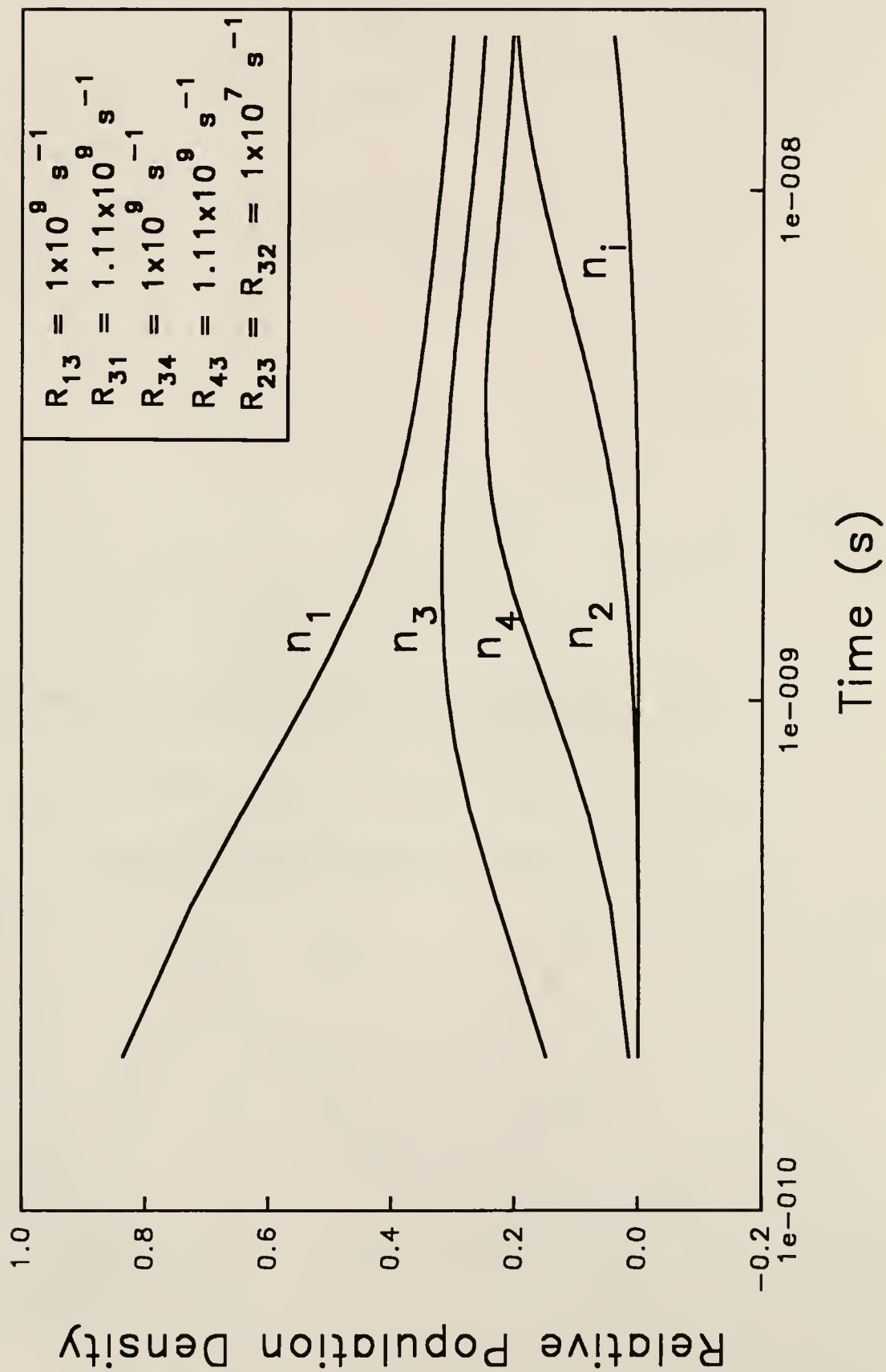


Figure 5-8 : Computer generated plot of relative population densities of atomic levels as the result of laser excitation at λ_{1-3} and λ_{3-4} versus time with moderate collisional activity between levels 2 and 3.

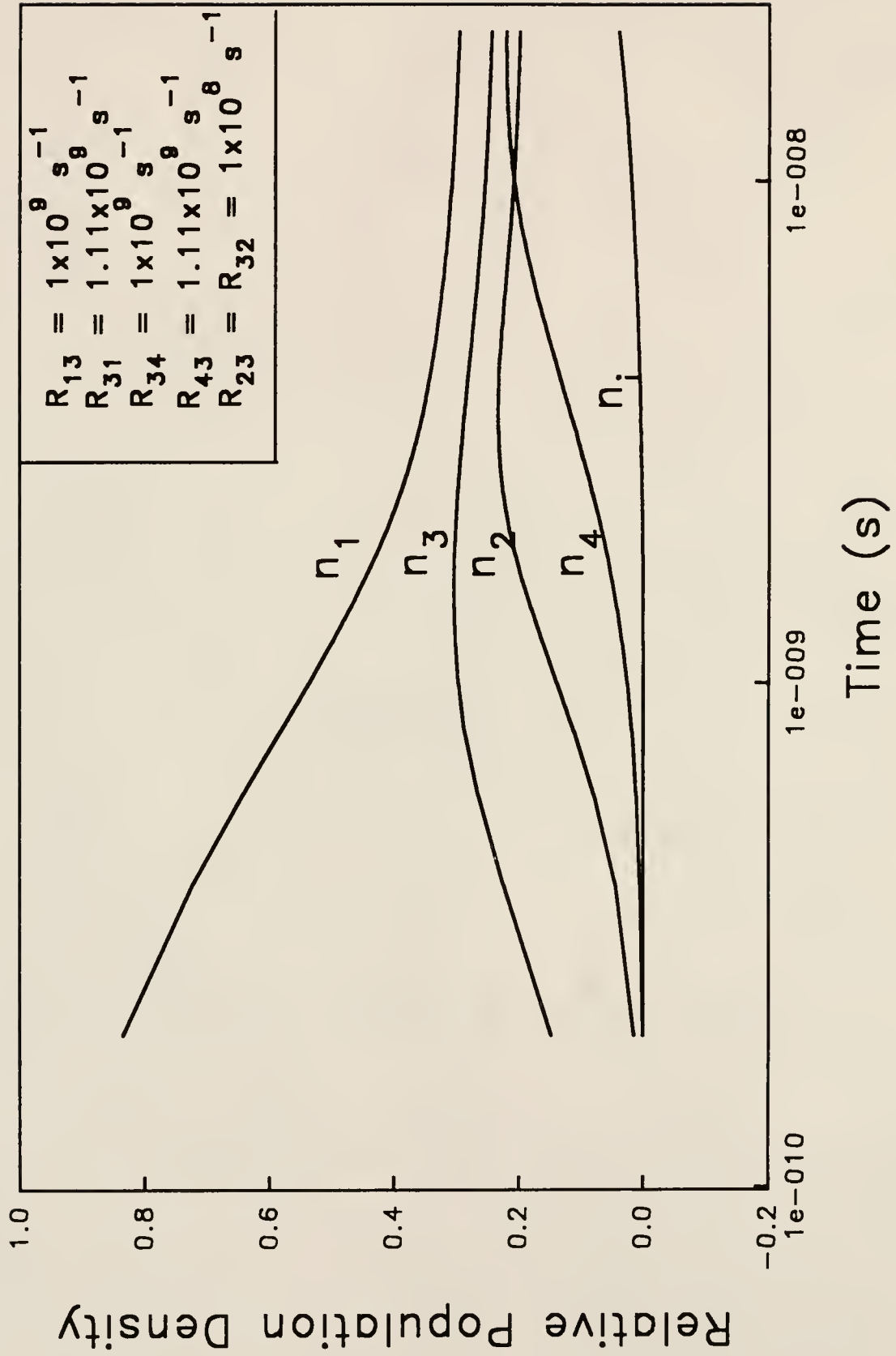


Figure 5-9 : Computer generated plot of relative population densities of atomic levels as the result of laser excitation at λ_{1-3} and λ_{3-4} versus time with high collisional activity between levels 2 and 3.

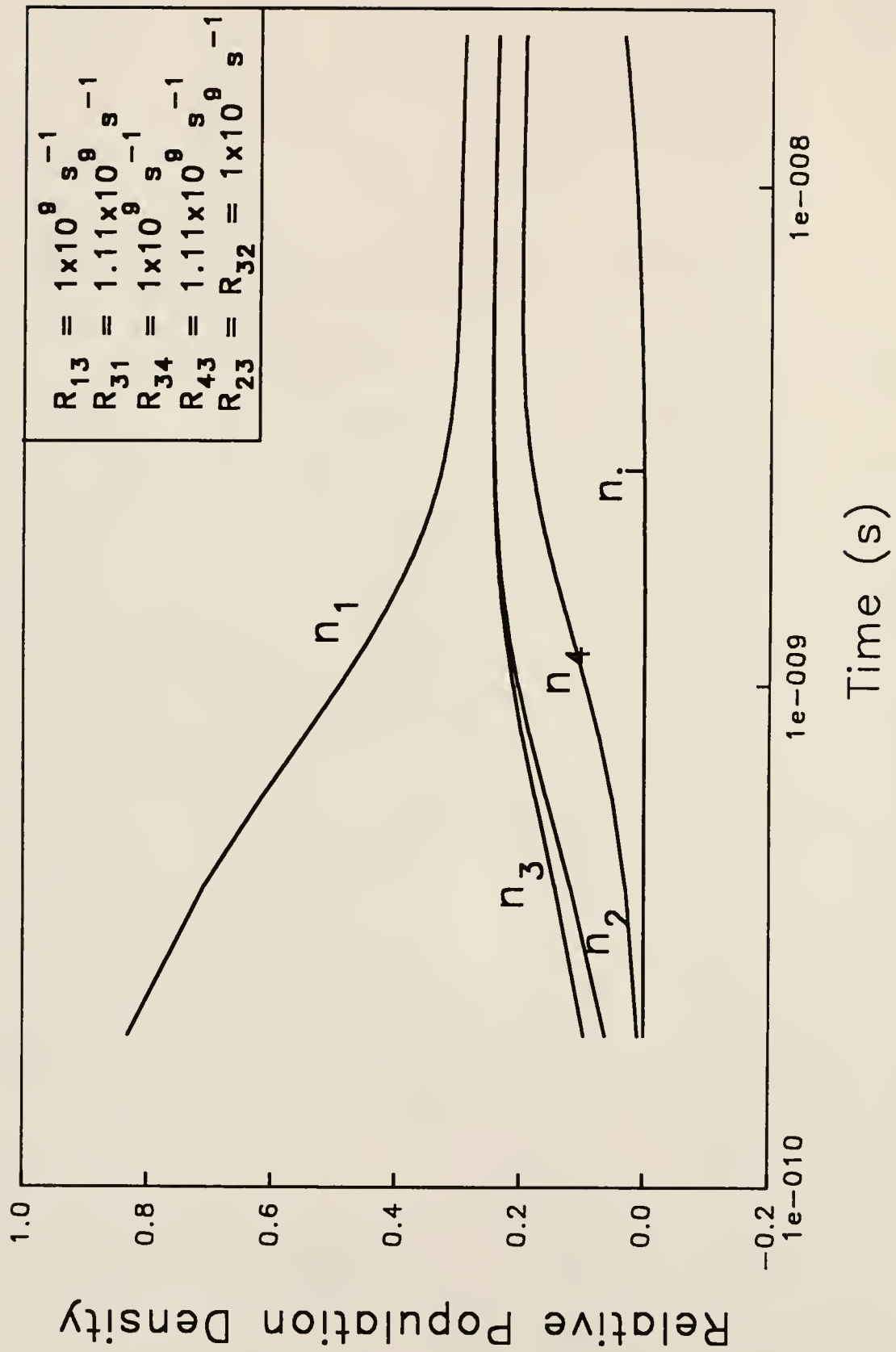
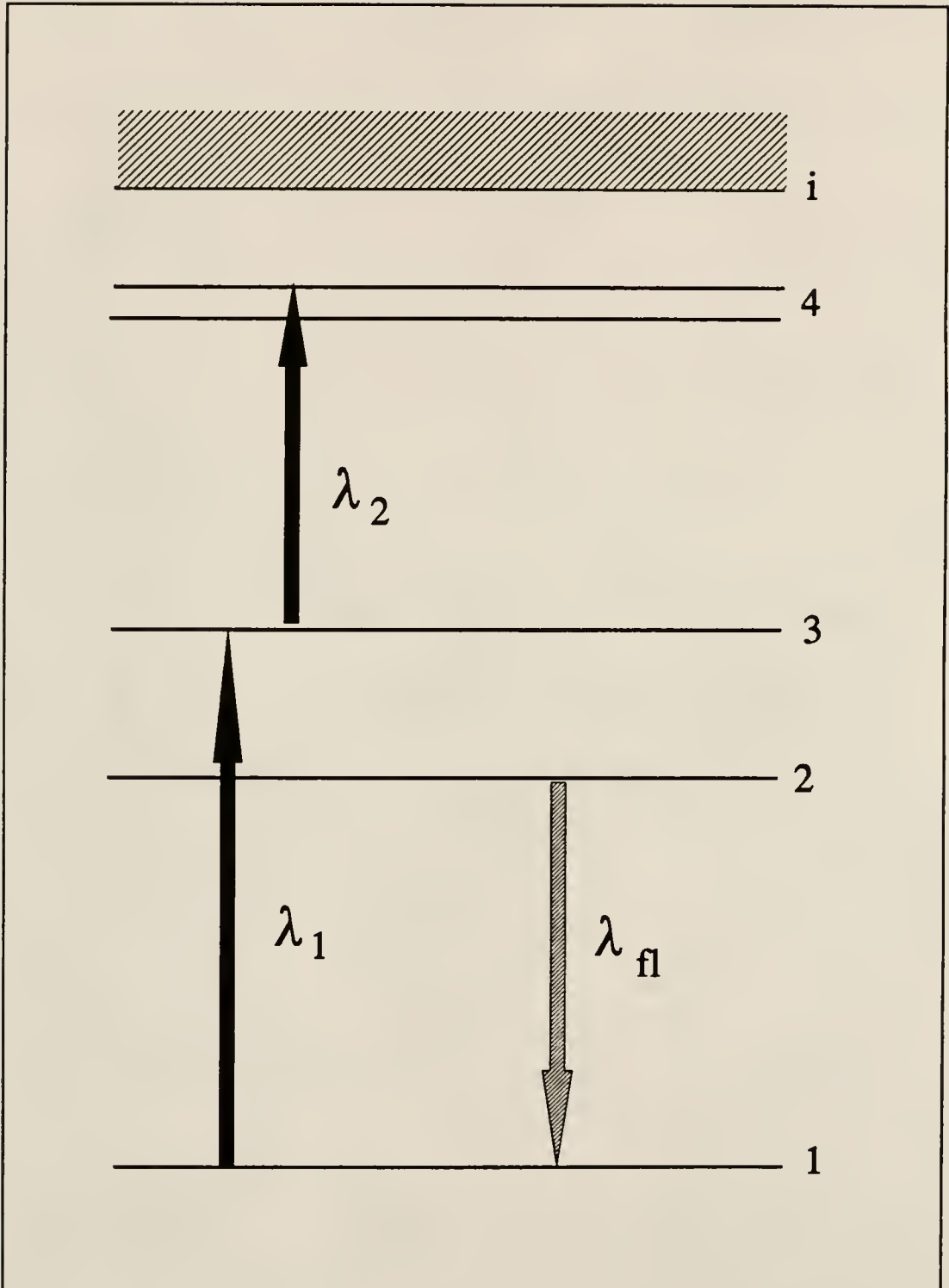


Figure 5-10 : Thermally assisted, nonresonance fluorescence scheme
for a five level atom



intermediate levels share the same population equally, this nonresonance dip will be equal to the resonance dip.

At a very low collisional mixing rate for levels 2 and 3, this thermally assisted, nonresonance fluorescence dip can become inverted, or negative (i.e. the fluorescence signal as a result of two step excitation becomes greater than the fluorescence signal as a result of one step excitation). Examples of excitation and fluorescence schemes that will result in only positive dips (Figure 5-11) and possibly negative dips (Figure 5-12) are given in order to clarify the concept of the inverted fluorescence dip. This interesting phenomenon can be predicted through an analysis of the rate equations describing this system where the relative populations for levels 2 and 3 are given as

$$\left(\frac{n_2}{n_T}\right)_{(off)} = \frac{1}{1 + \left(\frac{g_1 + g_2}{g_3}\right) \left(\frac{k_{23} + A_{21}}{k_{32}}\right)} = \frac{1}{1 + M} \quad (5-47)$$

$$\left(\frac{n_2}{n_T}\right)_{(on)} = \frac{1}{1 + (g_1 + g_3 + g_4) \left(\frac{k_{23} + A_{21}}{g_4 A_{42} + g_3 k_{32}}\right)} = \frac{1}{1 + N} \quad (5-48)$$

$$\left(\frac{n_3}{n_T}\right)_{(off)} = \frac{1}{1 + \left(\frac{g_1 (k_{23} + A_{21}) + g_3 k_{32}}{g_3 (k_{23} + A_{21})}\right)} = \frac{1}{1 + W} \quad (5-49)$$

$$\left(\frac{n_3}{n_T}\right)_{(on)} = \frac{1}{1 + \left(\frac{(g_1 + g_4) (k_{23} + A_{21}) + g_4 A_{42} + g_3 k_{32}}{g_3 (k_{23} + A_{21})}\right)} = \frac{1}{1 + Z} \quad (5-50)$$

Following the relationship given in equation (5-33), the fluorescence dip for level 2 is the difference between equations (5-48) and (5-49), and the fluorescence dip for

Figure 5-11 : Positive fluorescence dip.

Positive Fluorescence Dip

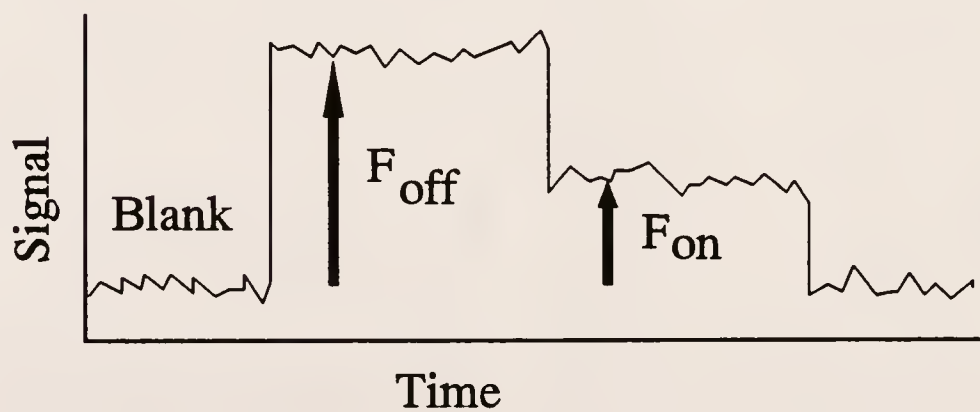
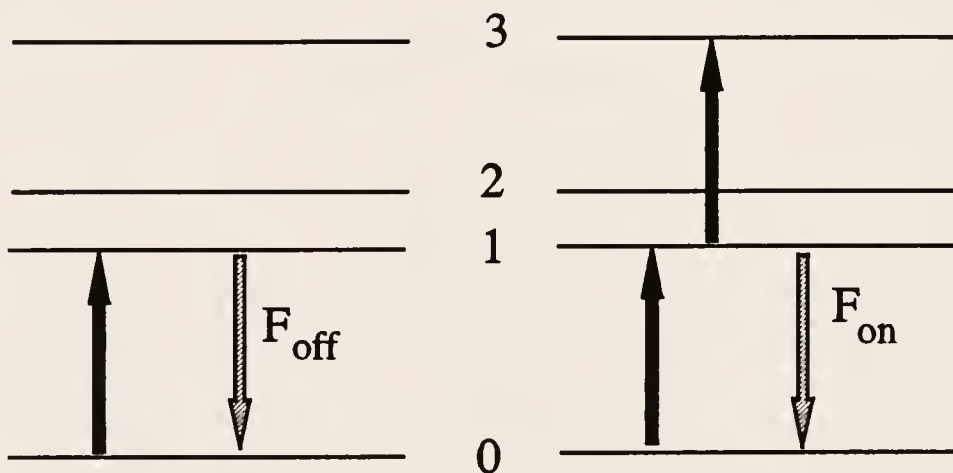
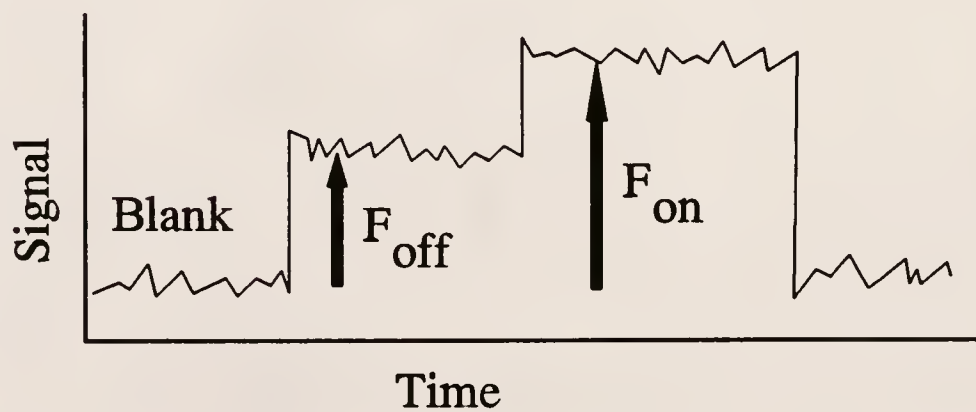
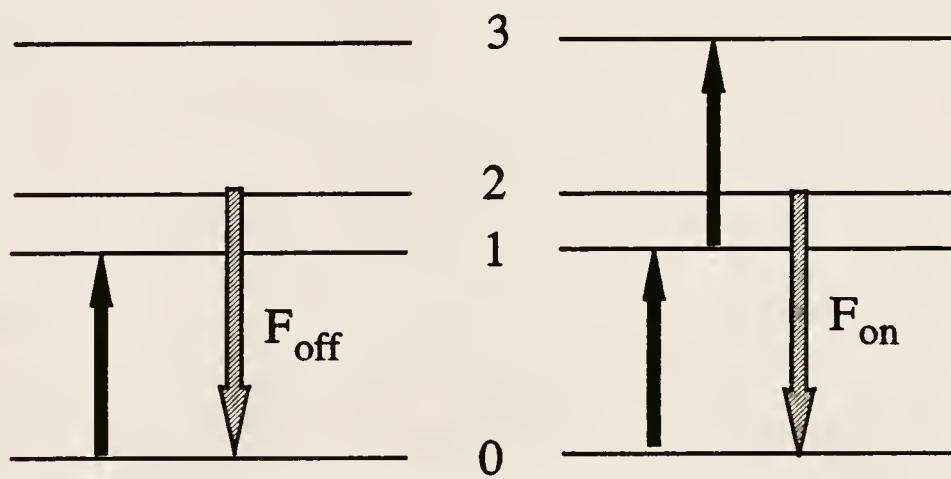


Figure 5-12 : Negative fluorescence dip.

Negative Fluorescence Dip



level 3 is the difference between equations (5-50) and (5-51). For the following discussion, it will be useful to give ratios of the quantities M to N and W to Z.

$$\frac{M}{Z} = \left(\frac{g_1 + g_3}{g_3} \right) \left(\frac{1}{g_1 + g_3 + g_4} \right) \left(\frac{g_4 A_{42} + g_3 k_{32}}{k_{32}} \right) \quad (5-51)$$

$$\frac{W}{Z} = \frac{1}{1 + \left(\frac{g_4 (k_{23} + A_{21}) + g_4 A_{42}}{g_1 (k_{23} + A_{21}) + g_3 k_{32}} \right)} \quad (5-52)$$

In order for a normal, positive dip to occur (i.e. the one step excited fluorescence signal must be greater than the two step excited fluorescence signal) for level 2, M must be less than N and for level 3, W must be less than Z. For an inverted (negative) dip to occur, it is obvious that the opposite (i.e. M greater than N or W greater than Z) must be true.

It can easily be seen through examination of equation (5-52) that for an inverted dip to occur from level 2 (i.e. M greater than N), A_{42} , the radiative relaxation from level 4 to level 2, must be greater than k_{32} , the collisional coupling rate between levels 3 and 2. At low k_{32} , the initial fluorescence signal from level 2, as the result of one step excitation will be weak as the population of the monitored level, dependent upon collisions from level three, will not be large. With introduction of the second excitation step at $\lambda_{3 \rightarrow 4}$, a new mechanism through which level two can become populated has been introduced, which is through radiative relaxation from level 4 to level 2. If this process is a strong one, the population of level 2 will be increased, once the second excitation step has been added resulting in a negative, or inverted, dip.

Careful inspection of equation (5-52) shows that the ratio of W/Z can never be greater than one. The significance of this is that the fluorescence dip for level 3 can only

range from zero (when $W=Z$) to positive values (when $W < Z$). Therefore, negative dips are only possible for some types of thermally assisted, nonresonance fluorescence dip measurement, and never possible for resonance fluorescence dip measurements.

This can also be seen through plots of the relative fluorescence dips with respect to time calculated from the relative populations given in Figures 5-13 to 5-15 while compensating for the inequality of the statistical weights of the levels. At low collisional activity (Figure 5-13), a large inverted fluorescence dip is predicted for level two since A_{42} , the Einstein coefficient of spontaneous emission from level 4 to level 2, is substantially greater than k_{32} , the collisional relationship between levels 2 and 3 resulting in the population of level 2. Under moderate (Figure 5-14) and high (Figure 5-15) collisional conditions, the dip for both levels is positive and the fluorescence dip values for level 2 and 3 approach equality demonstrating the close relationship present between them causing them to behave in the same manner.

Time Dependent Fluorescence Dips

In practice, very few atom systems can be accurately described in terms of steady state systems. Net losses through either ionization or relaxation to a metastable level during the laser interaction can have a significant effect upon the relative populations of the other levels of the atom system. If this is the case, the monitored population (i.e. fluorescence signal) will be affected as will, in turn, the fluorescence dip. The modeling of a non-steady state system is much more complex than that for a steady state system,

Figure 5-13 : Computer generated plot of the relative fluorescence dips of levels 2 and 3 as the result of laser excitation at first $\lambda_{1 \rightarrow 3}$ and then both $\lambda_{1 \rightarrow 3}$ and $\lambda_{3 \rightarrow 4}$ versus time with low collisional activity between levels 2 and 3.

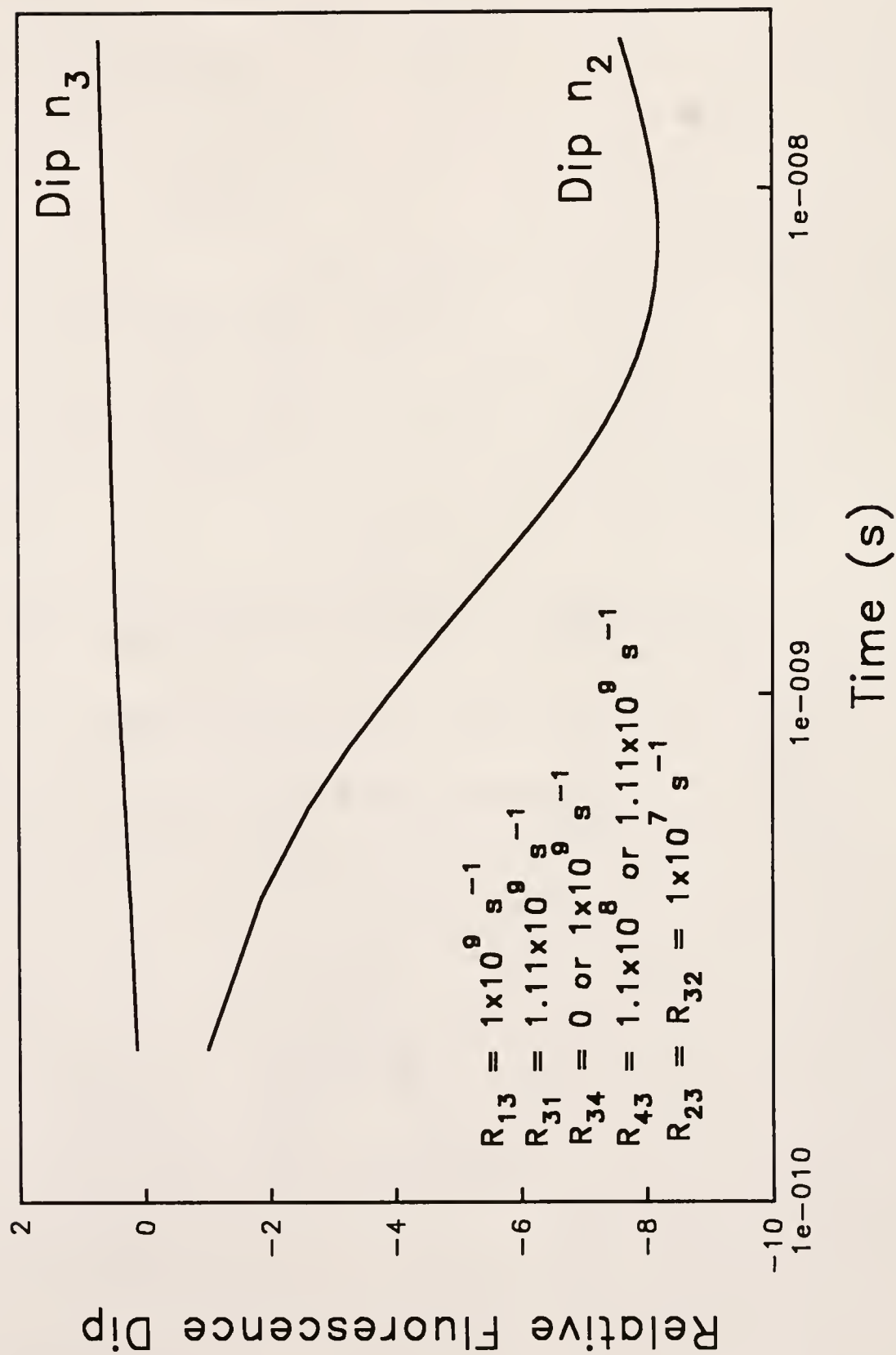


Figure 5-14 : Computed generated plot of the relative fluorescence dips of levels 2 and 3 as the result of laser excitation at first $\lambda_{1 \rightarrow 3}$ and then both $\lambda_{1 \rightarrow 3}$ and $\lambda_{3 \rightarrow 4}$ versus time with moderate collisional activity between levels 2 and 3.

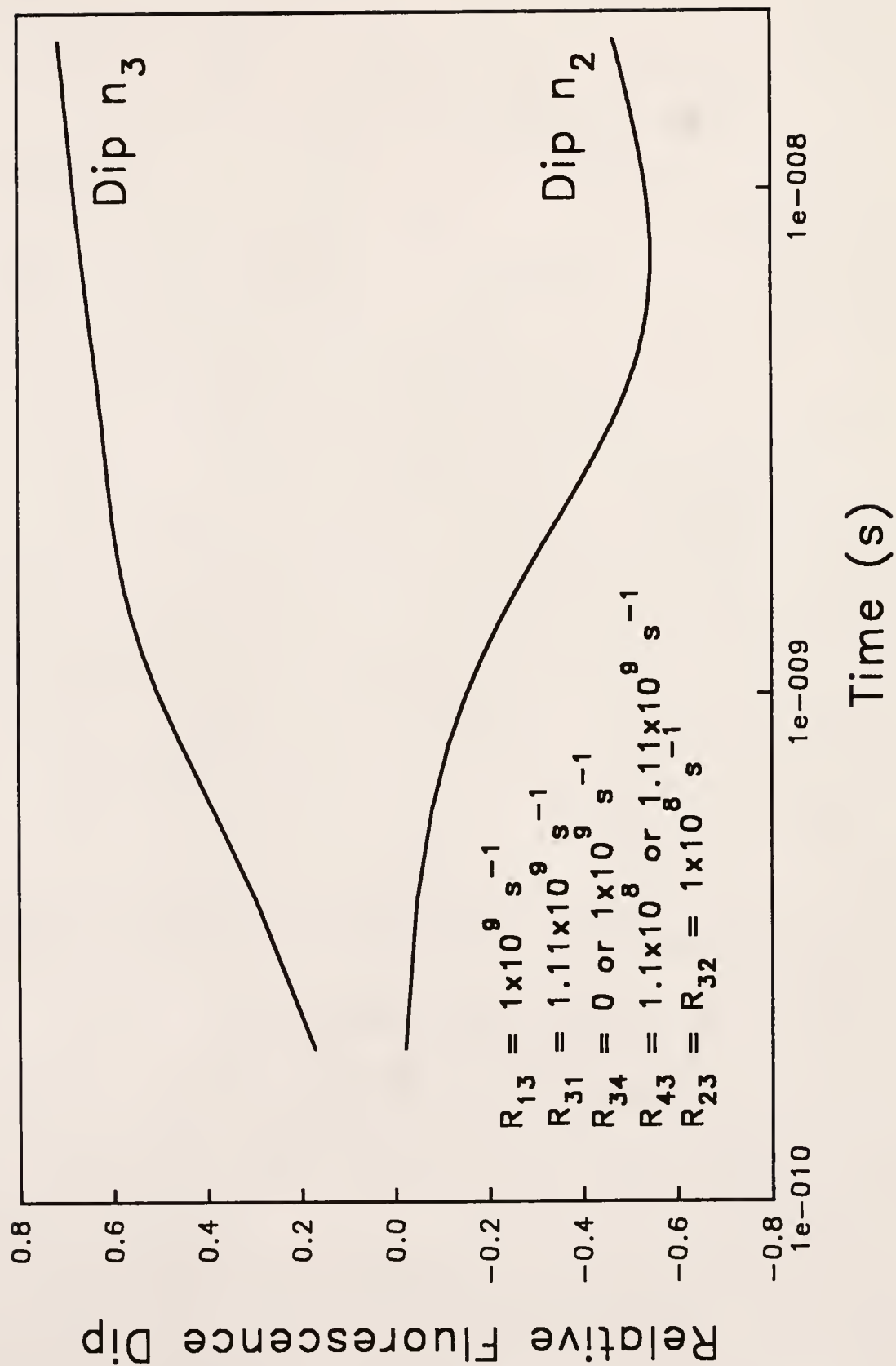
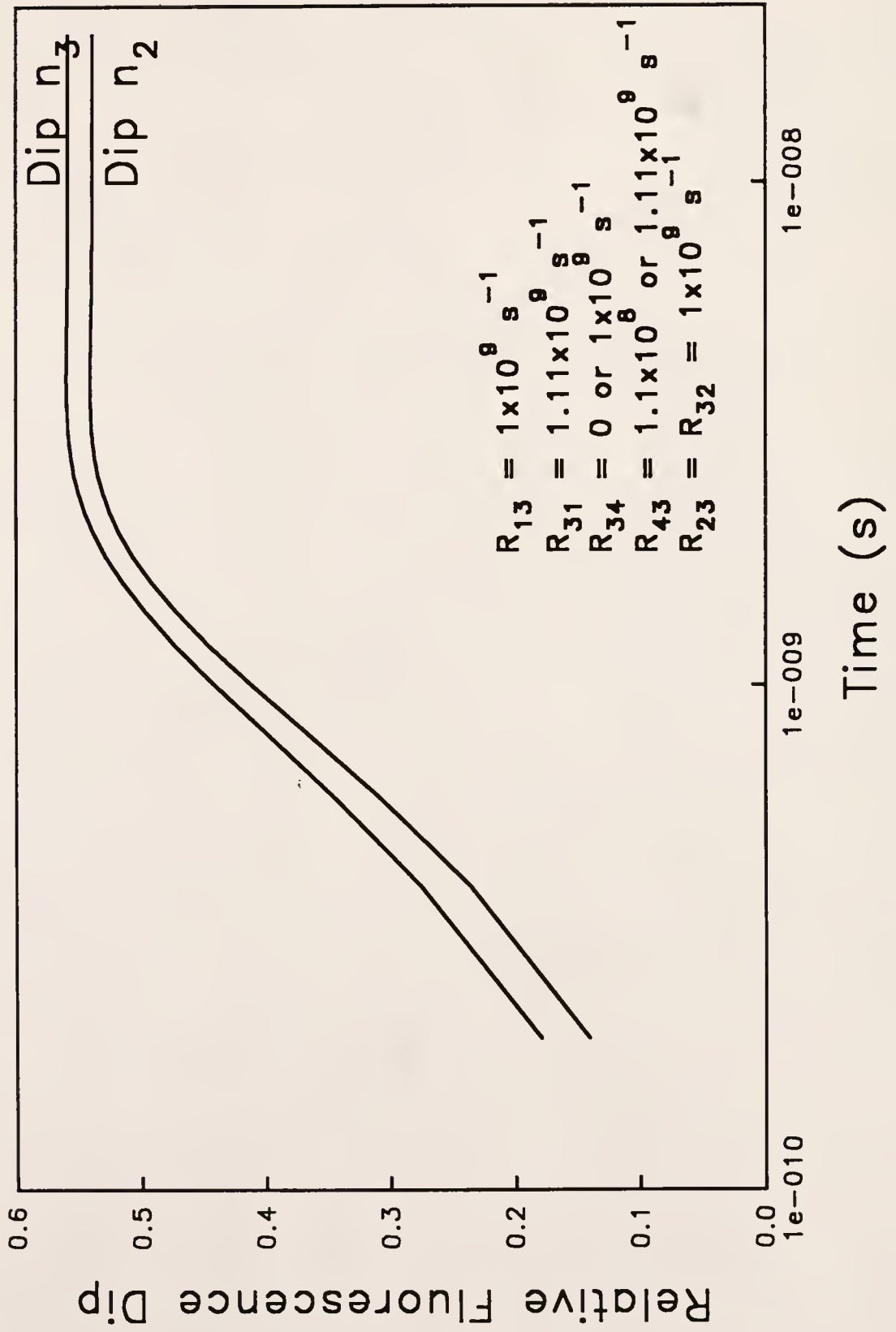


Figure 5-15 : Computer generated plots of the relative fluorescence dips of levels 2 and 3 as the result of laser excitation at first $\lambda_{1 \rightarrow 3}$ and then both $\lambda_{1 \rightarrow 3}$ and $\lambda_{3 \rightarrow 4}$ versus time with high collisional activity between levels 2 and 3.



but there are assumptions that can be made allowing for very reasonable estimations of the fluorescence dips.

Assuming, for example, that an atom suffers primarily metastable losses (insignificant ionization losses) (Figure 5-16) from the initially populated level. This atom will not achieve steady state conditions during the laser pulse since atoms populating the metastable level are not available to be recycled by the laser excitation as these population lifetimes are long compared to this pulse duration, resulting in a time dependence for the fluorescence dip measurement. The easiest way to monitor a time dependent fluorescence dip is to measure the time integrated fluorescence radiance. The expression for the maximum integrated fluorescence dip is

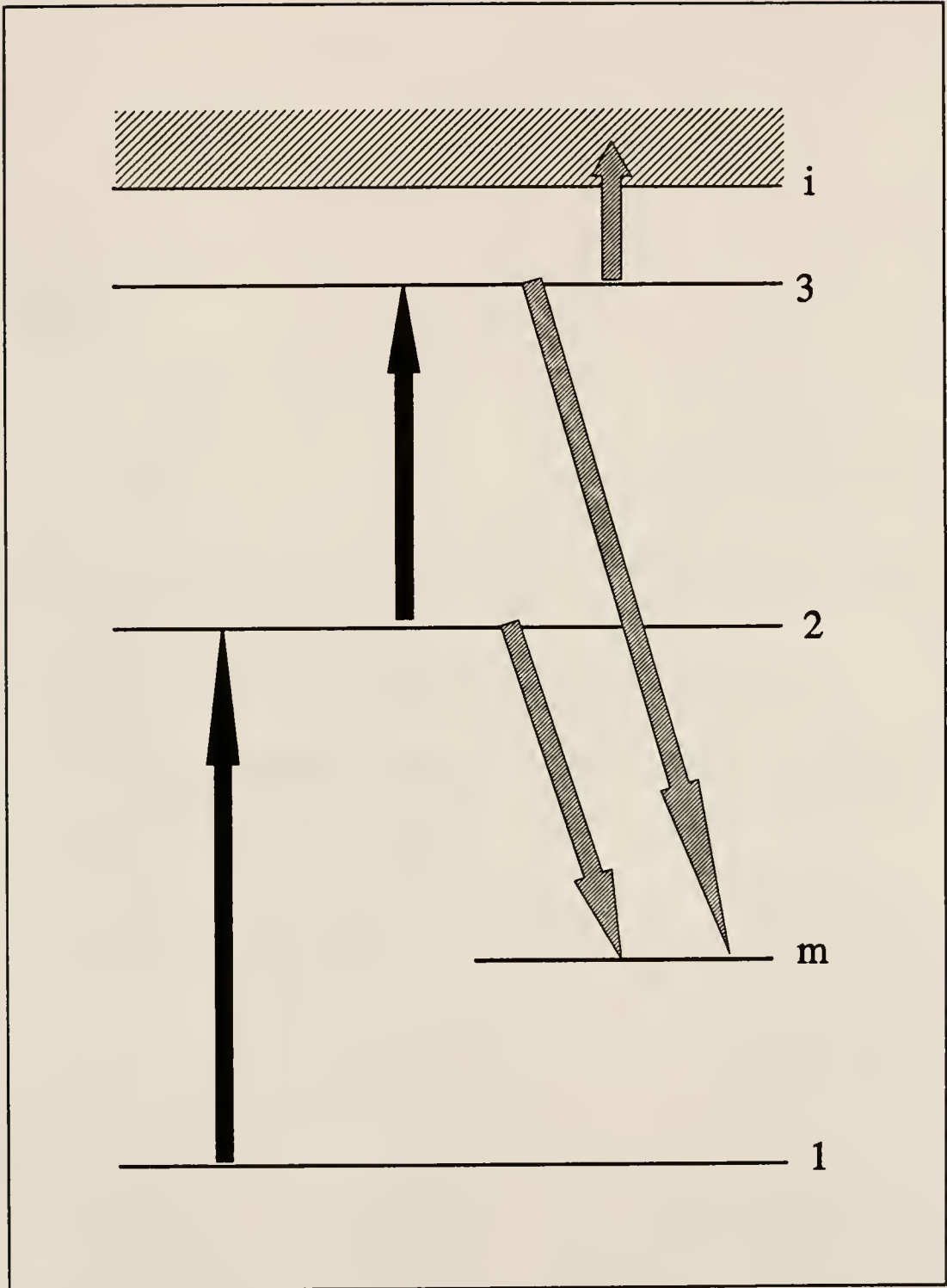
$$\Delta'_{\max} = 1 - \frac{1 - \exp\left(-\left(\frac{g_1 + g_2}{g_2}\right) B_{23} \rho_v(\nu_{23}) \delta t_1\right)}{\left(\frac{g_1 + g_2}{g_2}\right) B_{23} \rho_v(\nu_{23}) \delta t_1} \quad (5-53)$$

Numerical evaluation of this equation with empirical results allows determination of B_{23} , the Einstein coefficient of spontaneous absorption from level 2 to level 3. From this value, the absorption oscillator strength, f_{23} can be expressed as

$$f_{23} = \frac{h\nu_{23} m_e}{\pi e^2} B_{23} \quad (5-54)$$

The time integrated fluorescence dip is not difficult to perform. The boxcar gate width must be set at a width equalling the laser pulse duration for sampling of the fluorescence signal at different times. Assumptions for the model include that both lasers

Figure 5-16 : Diagram of a five level atom system including the potential for metastable and ionization losses.



are capable of saturating the two transitions for the duration of the rectangular shaped pulse.

If the atom suffers significant ionization losses, an alternative method for measurement of the fluorescence dip must be employed. Losses of the population through thermal or collisional promotion to the ionization continuum are important when dealing with some two step excitation schemes as they result in atoms being excited close to this ionization continuum. The approach for such a situation is somewhat more complex as is the instrumentation required, but results in temporal profiling of the fluorescence dip waveforms making it useful to evaluate the rates of decay for these fluorescence waveforms.

Considering a five level model with two of the levels being a metastable and the ionization continuum (Figure 5-16) and assuming saturation conditions attained through laser excitation for both transitions ($\lambda_{1\rightarrow2}$ and $\lambda_{2\rightarrow3}$), the time dependent populations of the atomic levels are

$$n_2(t) + n_3(t) = n_{23}(t) \quad (5-55)$$

$$n_3(t) = \left(\frac{g_3}{g_2 + g_3} \right) n_{23}(t) \quad (5-56)$$

$$n_2(t) = \left(\frac{g_2}{g_2 + g_3} \right) n_{23}(t) \quad (5-57)$$

and the temporal development of the metastable atom and the ion population densities are

$$\frac{dn_i}{dt} = R_i n_{23} \quad (5-58)$$

$$\frac{dn_m}{dt} = R_m n_{23} \quad (5-59)$$

where R_m and R_i are the total rates of relaxation into the metastable level and ionization continuum, respectively. The total atom population density, n_T , can be expressed as

$$n_T = n_1(t) + n_{23}(t) + n'_i(t) \quad (5-60)$$

where

$$n'_i(t) \equiv n_i(t) + n_m(t) \equiv n_i(t) \left(1 + \frac{R_m}{R_i} \right) \quad (5-61)$$

Using the previous relationships, the time dependence of the fluorescence of level 2 as a result of one and two step excitation is given by

$$I_F(t)_{(off)} = C_{n_T} \left(\frac{g_2}{g_1 + g_2} \right) \exp \left(- \left(\frac{g_2}{g_1 + g_2} \right) (R_{2m} + R_{2i}) t \right) \quad (5-62)$$

$$I_F(t)_{(on)} = C_{n_T} \left(\frac{g_2}{g_1 + g_2 + g_3} \right) \exp \left(- \left(\frac{g_2 + g_3}{g_1 + g_2 + g_3} \right) (R_m + R_i) t \right) \quad (5-63)$$

resulting in the time dependent relative fluorescence dip expression

$$\Delta'(t) = \frac{I_F(t)_{(off)} - I_F(t)_{(on)}}{I_F(t)_{(on)}} \quad (5-64)$$

which, at $t=0$, reduces to

$$\Delta'(0) = \frac{g_3}{g_1 + g_2 + g_3} \quad (5-65)$$

After time $t=0$, the fluorescence dip increases as a function of time due to the depletion caused by the ionization and metastable losses. When $\Delta'(t)$ reaches a maximum value (i.e. at time $t=t_{\max}$)

$$t_{\max} = \frac{1}{\left(\frac{g_2}{g_1+g_2}\right)(R_{2m}+R_{2i}) - \left(\frac{g_2+g_3}{g_1+g_2+g_3}\right)(R_m+R_i) \ln\left(G\left(\frac{R_{2m}+R_{2i}}{R_m+R_i}\right)\right)} \quad (5-66)$$

where

$$G = \frac{g_2 (g_1+g_2+g_3)^2}{(g_1+g_2)^2 (g_2+g_3)} \quad (5-67)$$

Inspection of the above equation shows that t_{\max} will decrease as the total rates of ionization and metastable losses increase. This makes sense since the fluorescence dip will decay at a faster rate with increasing losses from the fluorescent level, suggesting that the fluorescence dip value will reach its maximum early in the laser pulse. Inspection of the relative fluorescence dip expression (5-66) reveals that the relative dip will steadily approach the value of one.

The effect of ionization on the relative populations densities of the atomic levels is predicted through computer simulations using rate equations modeling (Figures 5-17 to 5-19). At low ionization (Figure 5-17), n_i , the atomic losses to the ionization continuum, does not play a role in the determination of the final population densities of the other levels. With moderate (Figure 5-18) and high (Figure 5-19) ionization losses, the relative population densities of the other levels are greatly affected such that a steady state assumption is no longer valid at even 20 ns after the laser pulse.

Figure 5-17 : Computer generated plots of the relative population densities of the atomic levels as the result of laser excitation at $\lambda_{1\rightarrow3}$ and $\lambda_{3\rightarrow4}$ versus time with low ionization losses from level 4 to level i.

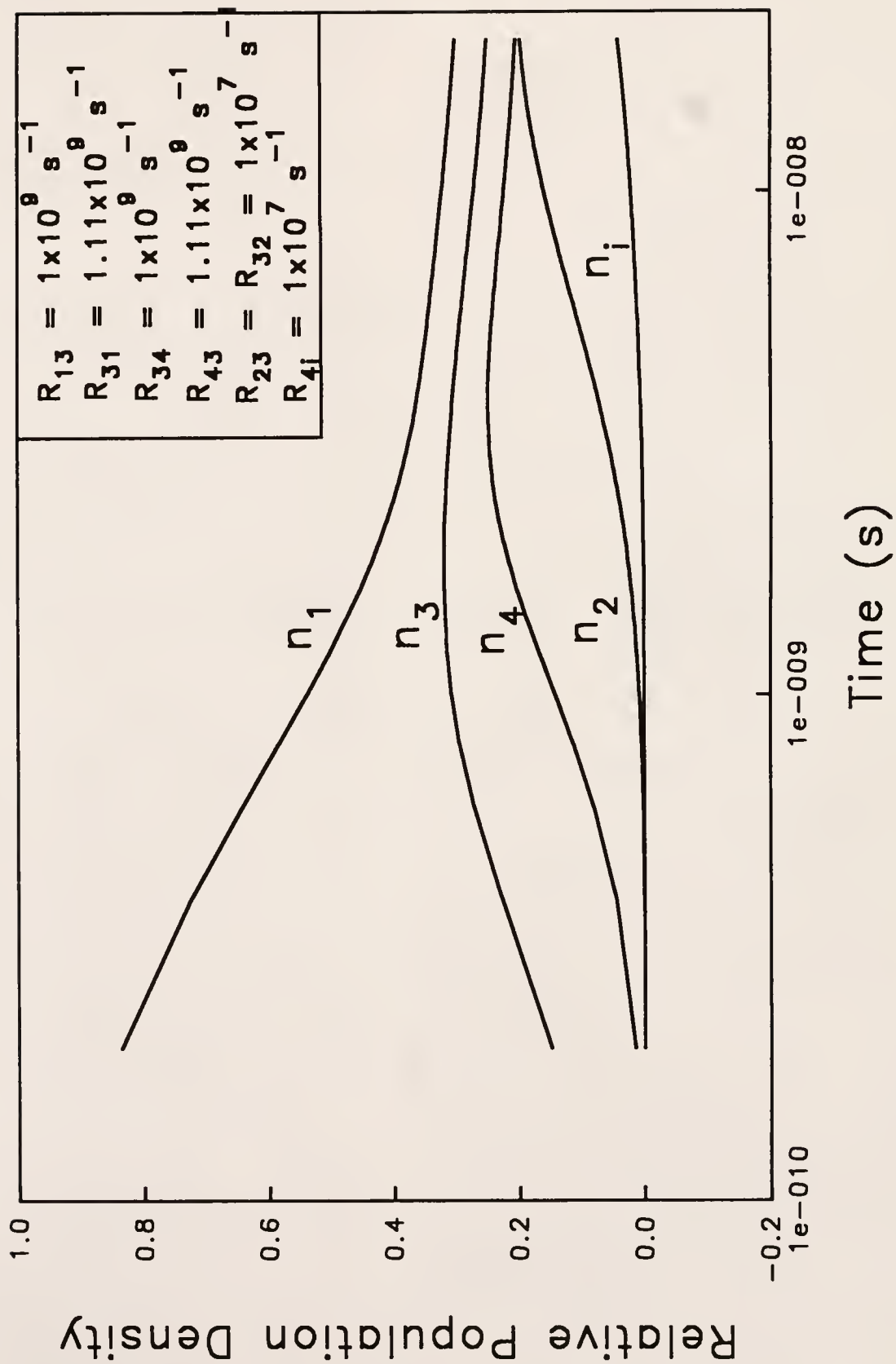


Figure 5-18 : Computer generated plots of relative population densities of atomic levels as the result of laser excitation at λ_{1-3} and λ_{3-4} versus time with moderate ionization losses from level 4 to level i.

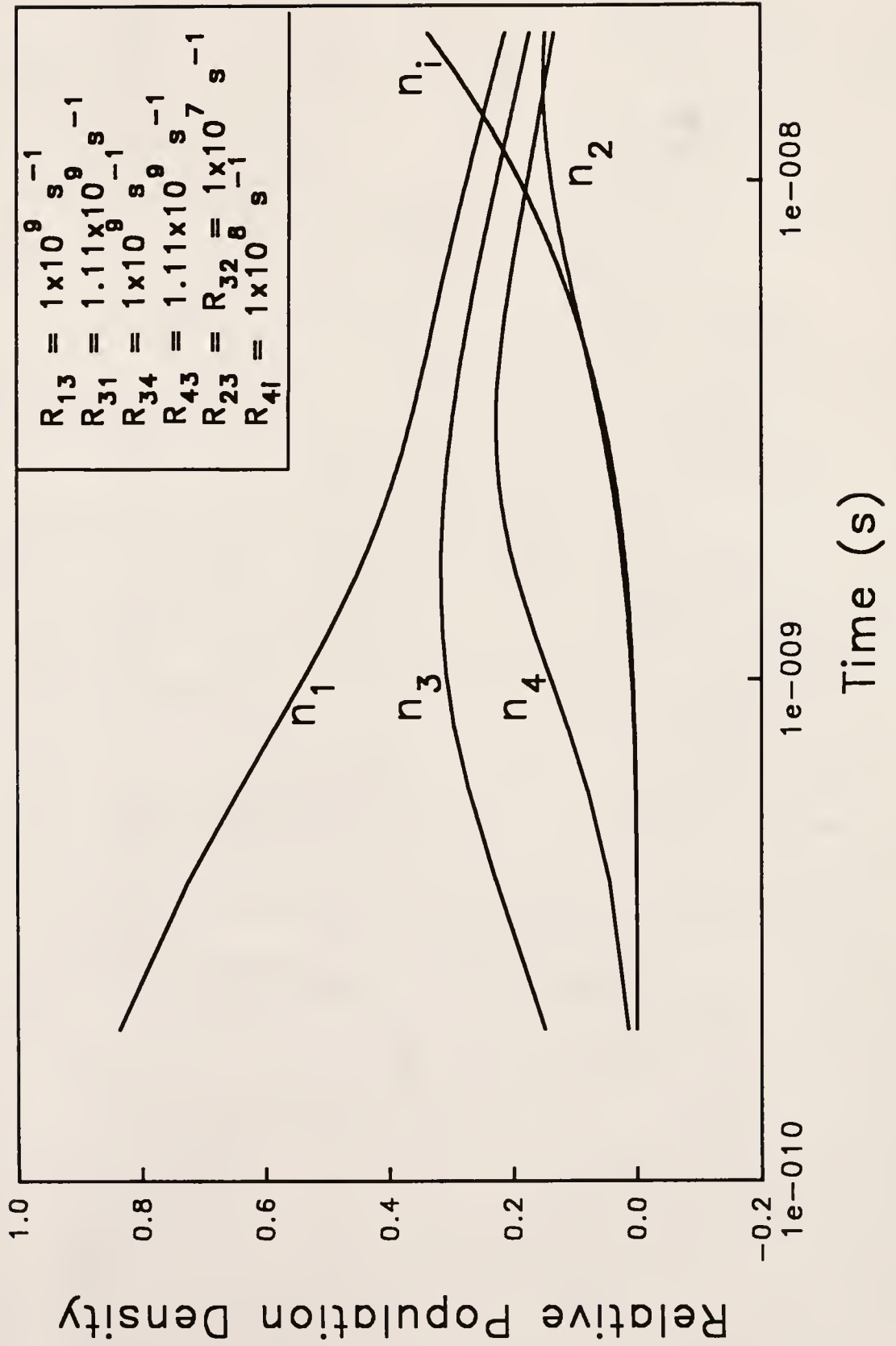
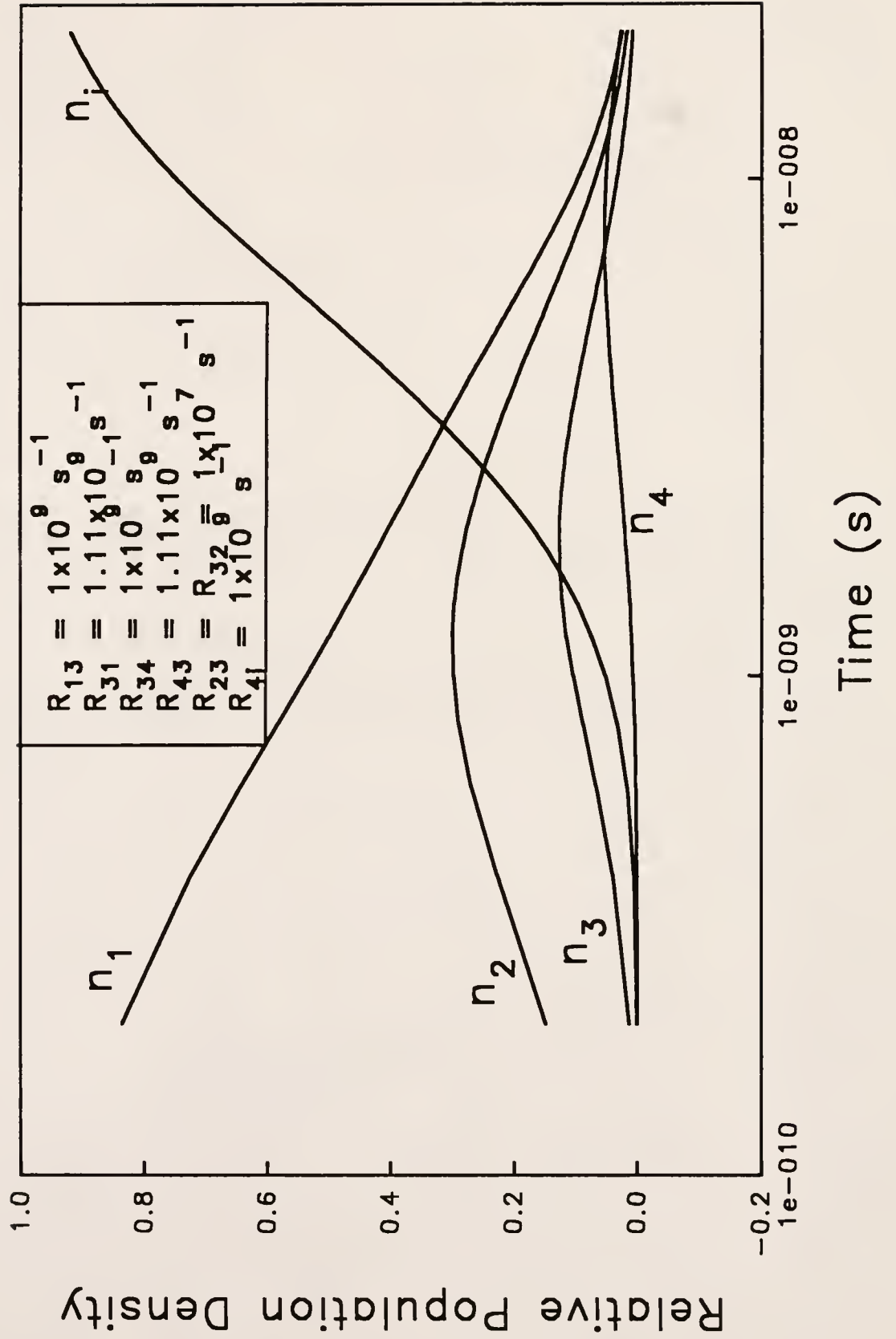


Figure 5-19 : Computer generated plots of relative population densities of atomic levels as the result of laser excitation at λ_{1-3} and λ_{3-4} versus time with high ionization losses from level 4 to level i.



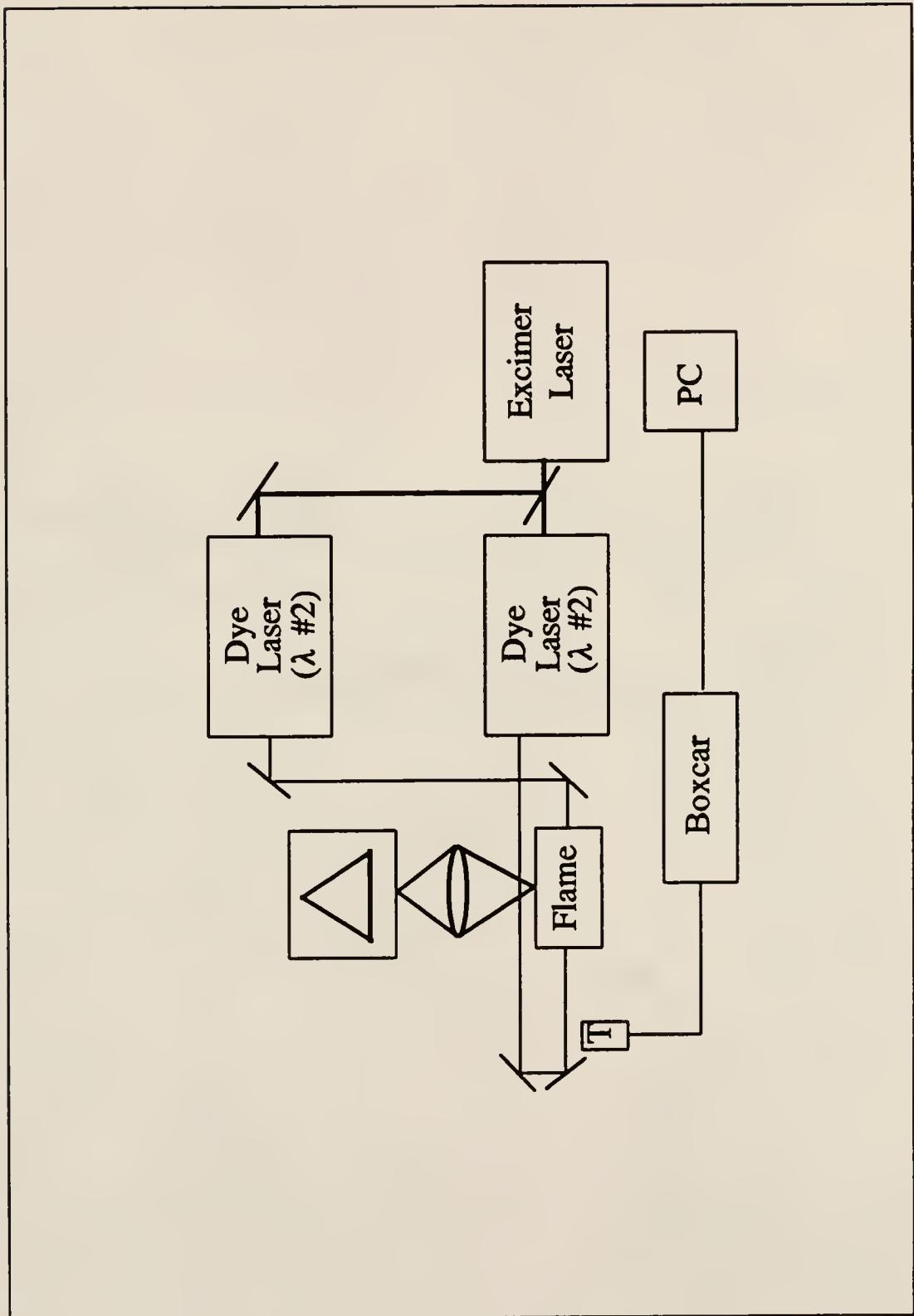
CHAPTER 6 EXPERIMENTAL

Instrumentation

The experimental instrumentation is shown in block diagrams of the experimental set-ups in Figures 6-1 and 6-2. A xenon chloride excimer laser (LPX-110i, Lambda Physik, Gottingen, FRG), typically operating at 30 Hz and 80 mJ/pulse, was used to pump one of two dye lasers to take the one step excitation fluorescence measurement, and both dye lasers simultaneously for the measurement of the fluorescence signal as the result of two step excitation (EPD-330, Lumonics Inc., Kanata, Ontario, Canada). The wavelength selection devices in these dye lasers were controlled with automatic scanning units (EPD-60, Lumonics Inc., Kanata, Ontario, Canada). The laser dyes used in this experiment were purchased from Exciton Inc. (Dayton, Ohio), and the solutions were prepared at concentrations suggested for use with this particular pump source in solvents purchased from Fisher Scientific (Fair Lawn, NJ). All of the dyes utilized in these studies (Coumarin 500, Coumarin 540A, DCM, and Oxazine 720) result in laser radiation from the dye laser in the visible range, so the ultraviolet radiation required for the first excitation step in all of the measurements taken was generated through the use of doubling crystals (KDP-C and KDP-D, Inrad, Northvale, NJ). Separation of the fundamental frequency from this generated ultraviolet beam was accomplished through

Figure 6-1 : Experimental set-up for analyte studies in the ICP (inductively coupled plasma) and ICP expansion.

Figure 6-2 : Experimental set-up for analyte studies in the air/acetylene flame.



the use of a UG-7 Schott glass filter (Corion Corp., Holliston, MA). To perform the saturation studies, the laser radiation was attenuated prior to introduction into the atom source through the use of calibrated neutral density filters (Corion Corp., Holliston, MA), also used to reduce the fluorescence being focussed onto the entrance slit of the monochromator in those cases where the photomultiplier tube (PMT) was experiencing saturation resulting in a nonlinear response from this detector. Laser radiation from the two dye lasers was directed through the use of quartz prisms and mirrors into the atom reservoir in which the analyte was being studied.

The first atom reservoir was an air/acetylene flame (Perkin-Elmer, Flanders, NJ). The flow rates were set to achieve to a maximum nonresonance fluorescence signal from the analyte species. The observation height was again set to achieve the maximum signal and was typically around 10 mm. Fluorescence emission from the flame was collected perpendicular to the laser excitation and focussed onto the entrance slit of a monochromator (Minimate, Spex, Metuchen, NJ) for detection by a PMT (R955, Hamamatsu Corp., Middlesex, NJ) which was biased at -900 V for monitoring the fluorescence emission as a result of pulsed excitation situated at the exit slit of the monochromator.

An inductively coupled plasma (ICP) atom reservoir was also implemented in this experimentation. This ICP was powered by a 27 MHz radio frequency generator (HFP 2500D, Plasma-Therm Inc., Kresson, NJ) and sustained by a 3 turn coil on the standard quartz torch (Precision Glassblowing, Englewood, CO). Argon gas flows were set based on the rates resulting in the greatest signal for a nonresonance fluorescence signal and

these flows were typically 15-20 L/min for the plasma support gas and 1 L/min for the auxiliary gas. A concentric nebulizer (Model TR-30-A3, J.E. Meinhard and Associates, Santa Ana, CA) was implemented for solution nebulization at a pressure of 30 psi. ICP forward power was set at 600 W with a reflected power of approximately 0-10 W. The observation height was experimentally determined in each case again maximizing nonresonance fluorescence signals and resulting in above torch heights of 10-15 mm. Fluorescence emission was again collected perpendicular to the laser excitation and focussed onto the entrance slit of the monochromator (Heath EU-700, Heath Corp., Benton Harbor, MI) and detected by a PMT again wired for pulsed response.

The third atom source used in this work was an inductively coupled plasma low pressure expansion sampling the existing ICP with a sampling orifice of 1 mm diameter at a height of typically 15-30 mm above the load coil into a quartz cylinder (diameter = 5 inches) resulting in pressures as low as 0.5 torr. The analyte population was sampled in the zone of silence which is an area of the expansion with a low analyte population as well as low collisional activity. The ICP was operated at forward powers of around 750-900 W (i.e. as low as possible to maintain a stable plasma in the presence of low pressure conditions) with reflected powers less than 25 W. This expansion chamber was water-cooled and grounded to the metal box housing the ICP.

For each atom reservoir/analyte combination, slit widths for the monochromator were determined with respect to the signal to noise ratio observed as well as the required resolution to independently monitor the resonance and nonresonance fluorescence signals. The PMT was terminated into a voltage by a 50 ohm resistor and its output sent into the

input of a boxcar averager (SR250, Stanford Research Systems, Palo Alto, CA) that was triggered externally by a photodiode (FND-100, EG&G, Salem, MA) monitoring the output of either the excimer laser or one of the dye lasers. The boxcar gate was adjusted to between 3 and 5 ns in width to collect the fluorescence peak signal. Synchronization of the fluorescence pulse with the boxcar gate was attained through adjustment of the time delay on the boxcar while viewing both the fluorescence peak and boxcar gate simultaneously on an oscilloscope (Tektronix 2430A, Tektronix Inc., Beaverton, OR) until observing temporal coincidence. The gate was scanned across the fluorescence signal peak while monitoring the signal collected using commercial data acquisition software (Stanford Research Systems, Palo Alto, CA) by a personal computer (IBM PC, IBM Inc., Boca Raton, FL).

Both temporal and spatial coincidence was required for the two beam portion of the fluorescence dip measurements. Temporal coincidence was achieved by delaying one of the beams from the dye lasers to insure that the beam lengths from the excimer to the atom source are equivalent. Spatial coincidence was achieved by directing both laser beams through a pair of iris diaphragms situated at either side of the atom source at the same height as the monochromator slit width.

Analyte Solutions

A standard stock solution for copper was made by dissolving the appropriate amount of copper powder in concentrated nitric acid (Fisher Scientific, Lawn Fair, NJ) and subsequently diluted to the desired volume with deionized water. A stock solution

of silver was made by dissolving the appropriate amount of silver nitrate (Fisher Scientific) in deionized water and diluting to the desired volume. For these studies, a solution concentration was chosen based on maximum fluorescence signal while still remaining in the linear range of a signal vs. concentration curve and attaining saturation conditions for both excitation steps.

Experimental Procedure

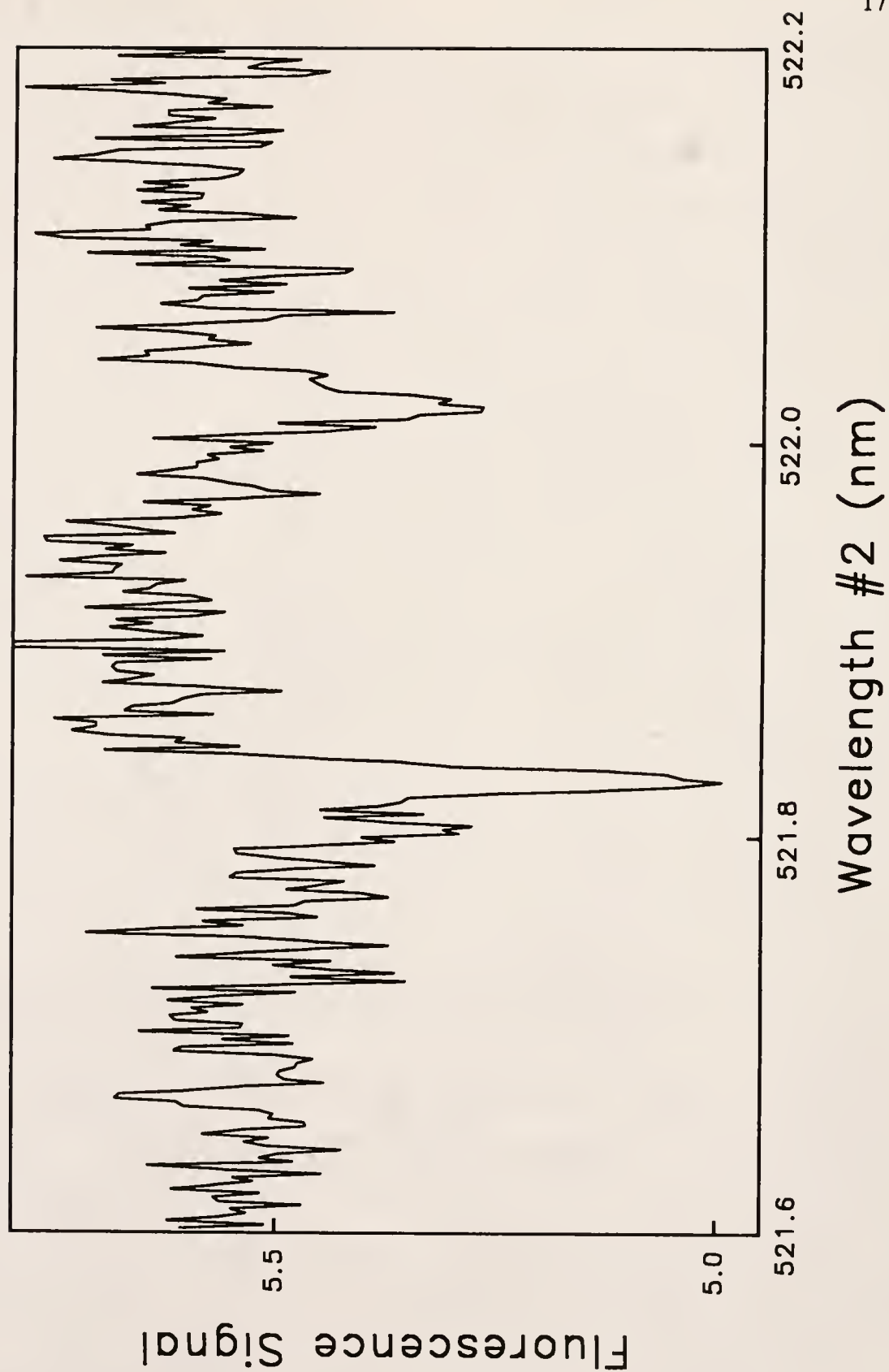
The fluorescence signal as the result of one step excitation was maximized by viewing the fluorescence peak on the oscilloscope while adjusting the wavelength of the radiation being emitted from the dye laser until the maximum signal was reached. Once this was done, several data points were collected by the boxcar set at 30 averages and this data was collected and saved using the Stanford software for both one step fluorescence and a blank signal resulting from the substitution of deionized water for the analyte with all other experimental conditions kept constant to allow for correction from laser scatter.

The two step fluorescence signal was collected through one of two different methods. The first method involved manual adjustment of the wavelength of the dye laser responsible for the second excitation step while viewing the fluorescence signal on an oscilloscope to minimize the signal (i.e. maximize the dip), and data was collected in the same manner as that for the one step case. Another method that was employed for measuring the two step signal was performed through computer control of the scanning unit for the dye laser producing the laser excitation for step 2. With analyte solution

being nebulized and the wavelength of the first dye laser set to achieve maximum fluorescence for one step excitation, the wavelength was scanned over a range encompassing the wavelength corresponding to the second transition. The signal was then collected using the Stanford software, and a representative resulting scan is shown in Figure 6-3.

The fluorescence dip was then calculated for each combination of first and second step excitation and both resonance and nonresonance fluorescence being monitored as the difference between the averaged signals for one and two step excitation or the difference between the averaged one step signal and the maximum dip (i.e. minimum signal) in the scanned cases. These data were averaged with other dip values obtained in the same fashion, and the reported errors in these measured dip signals corresponded to one standard deviation.

Figure 6-3 : Representative scan of λ_2 while holding λ_1 constant. In this example, copper is experiencing excitation at 324.754 nm while the second wavelength is scanned over the given range encompassing both second step transitions originating from the initially populated level in the low pressure ICP expansion.



CHAPTER 7 RESULTS AND DISCUSSION

Experiments Performed

The fluorescence from copper atoms (Figure 7-1) as the result of one step excitation at 327.396 nm was monitored at both 327.396 nm (resonance fluorescence) and 328.068 nm (nonresonance fluorescence). A second excitation step was then added at either 515.324 nm, directly depleting the initially populated level, or 522.007 nm or 547.115 nm, depleting the level dependent upon collisions from the initially directly populated level for its population, while continuing to monitor the fluorescence signal at either 327.396 nm or 324.754 nm. This same procedure was repeated for a first wavelength of 324.754 nm while monitoring fluorescence at both 324.754 nm (resonance fluorescence) and 327.396 nm (nonresonance fluorescence).

The same experimental work was performed on the silver atom, also approximated by a five level atomic system (Figure 7-2). The first step excitation was tuned to either 328.068 nm or 338.289 nm while monitoring both resonance and nonresonance fluorescence as the result of this one step excitation. A second excitation step was added at either, 520.907 nm, 546.549 nm, or 547.115 nm depleting either the level directly populated through the initial excitation step or thermally populated through collisional activity from this directly populated level as the result of the one laser

Figure 7-1 : The copper atom approximated as a five level system.

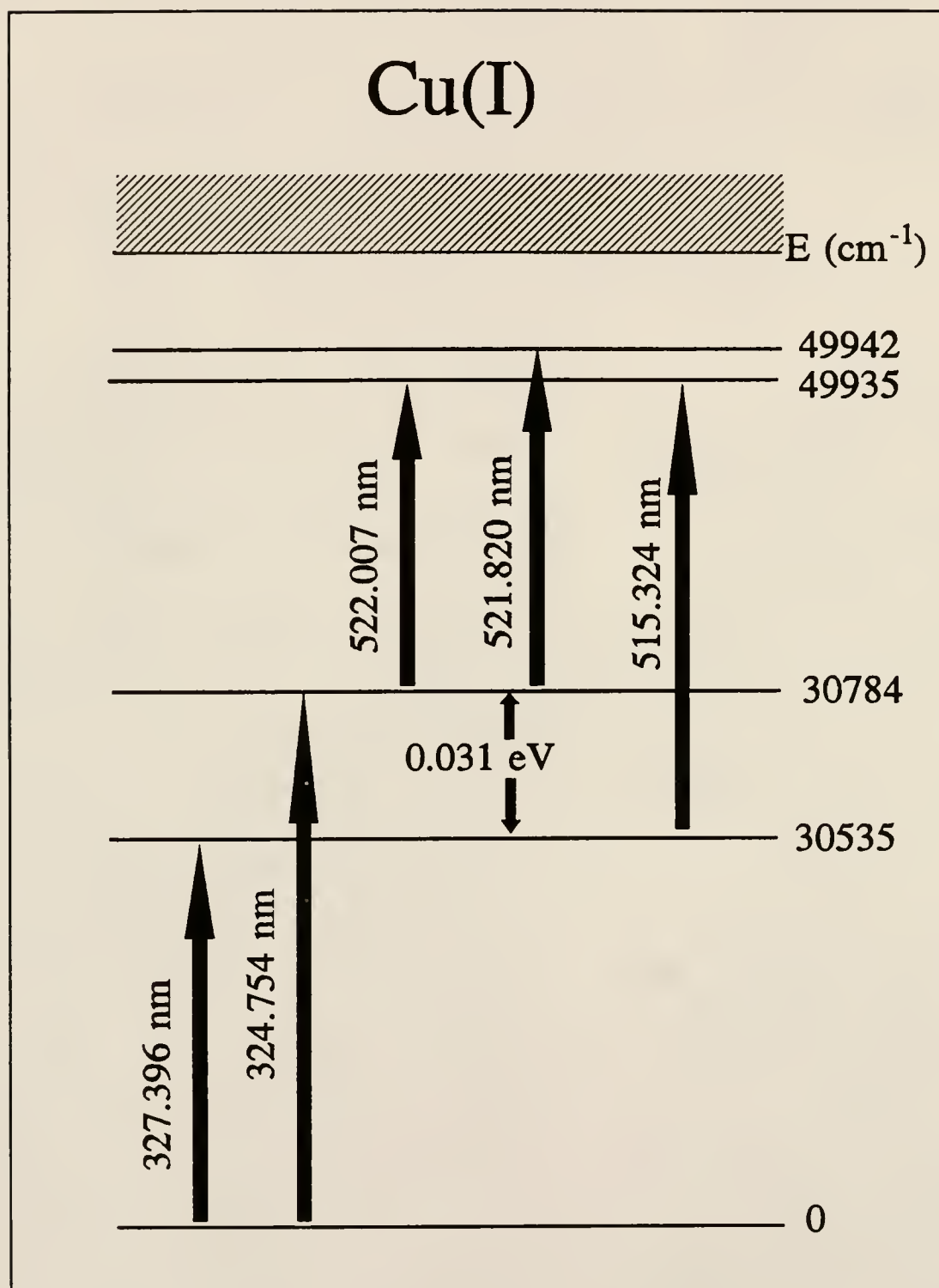


Figure 7-2 : The silver atom approximated as a five level system.

Ag(I)

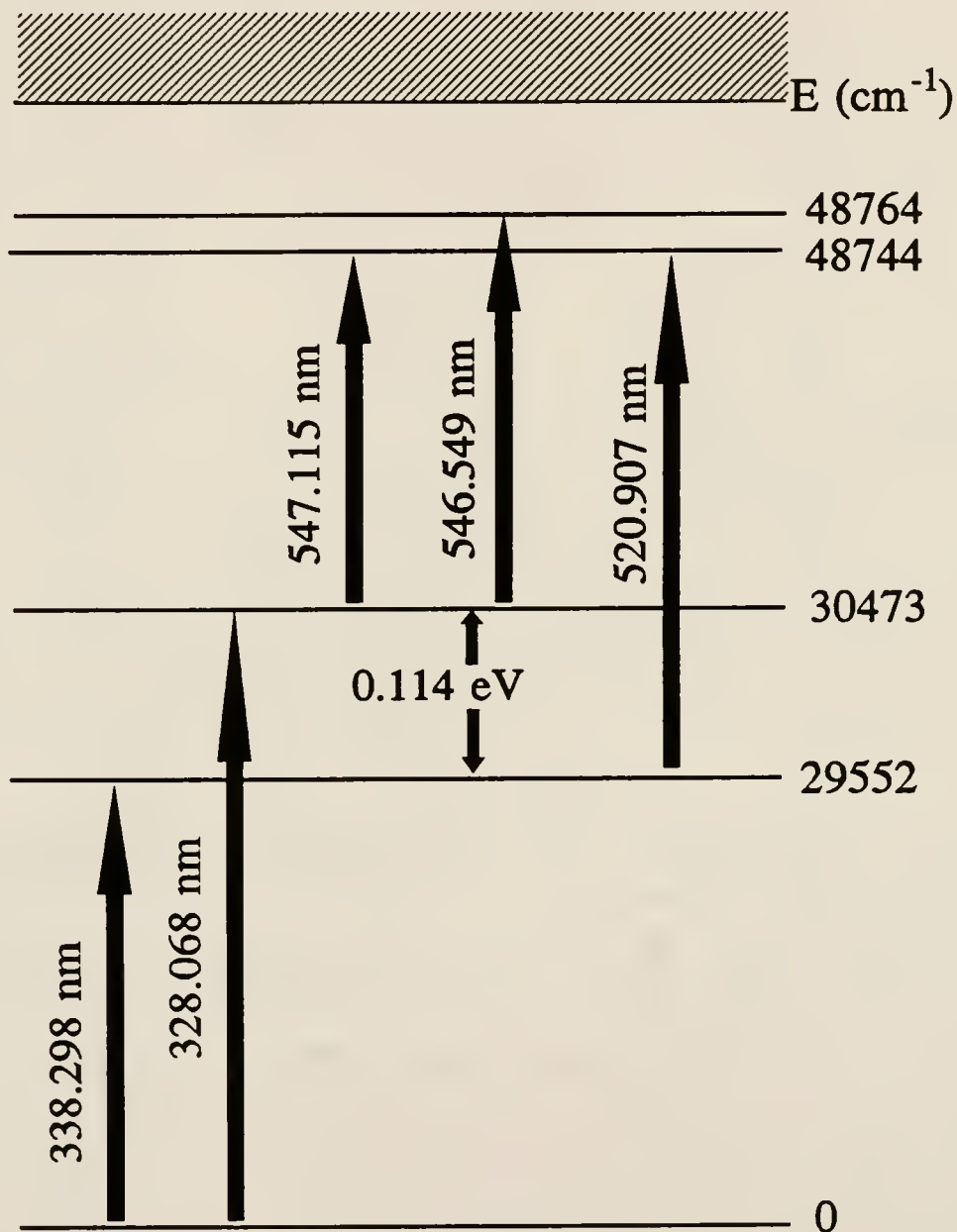
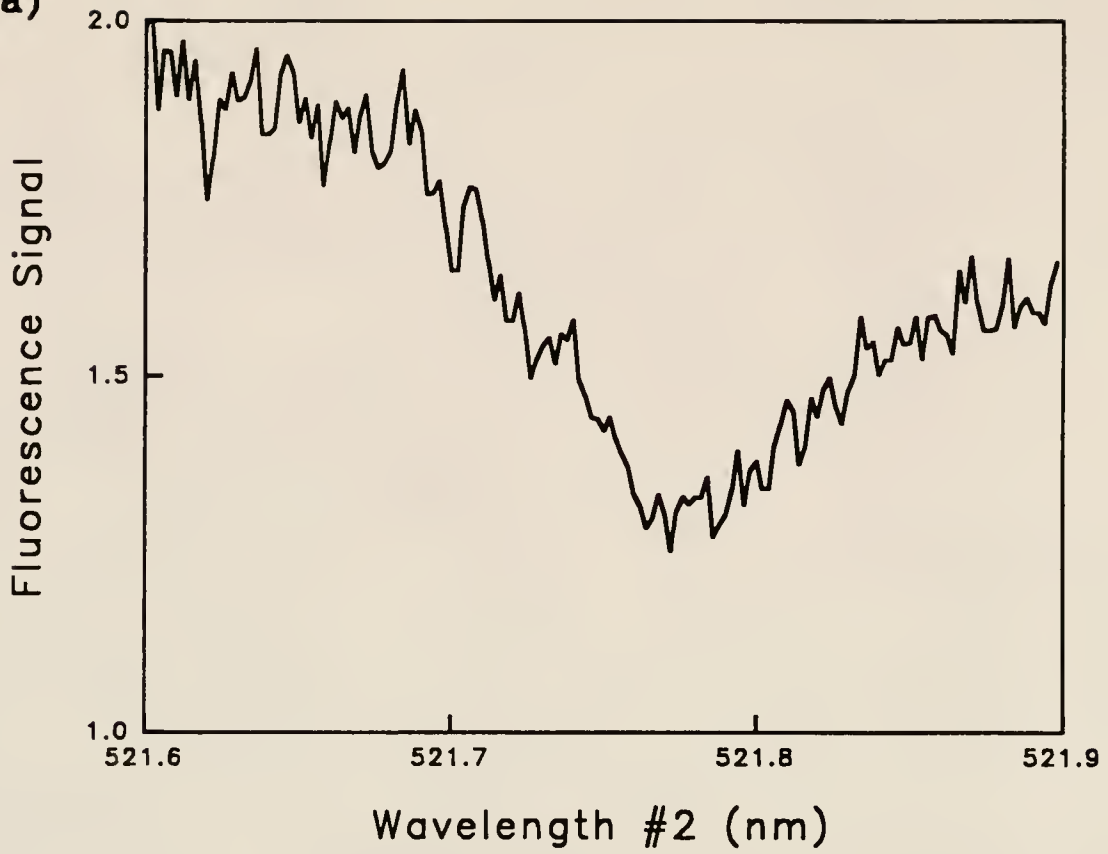


Figure 7-3 : Fluorescence signal versus wavelength of the second excitation wavelength and the resulting fluorescence dip for copper in the air/acetylene flame while holding λ_1 constant at 324.754 nm and monitoring both (a) resonance fluorescence and (b) nonresonance fluorescence.

(a)



(b)

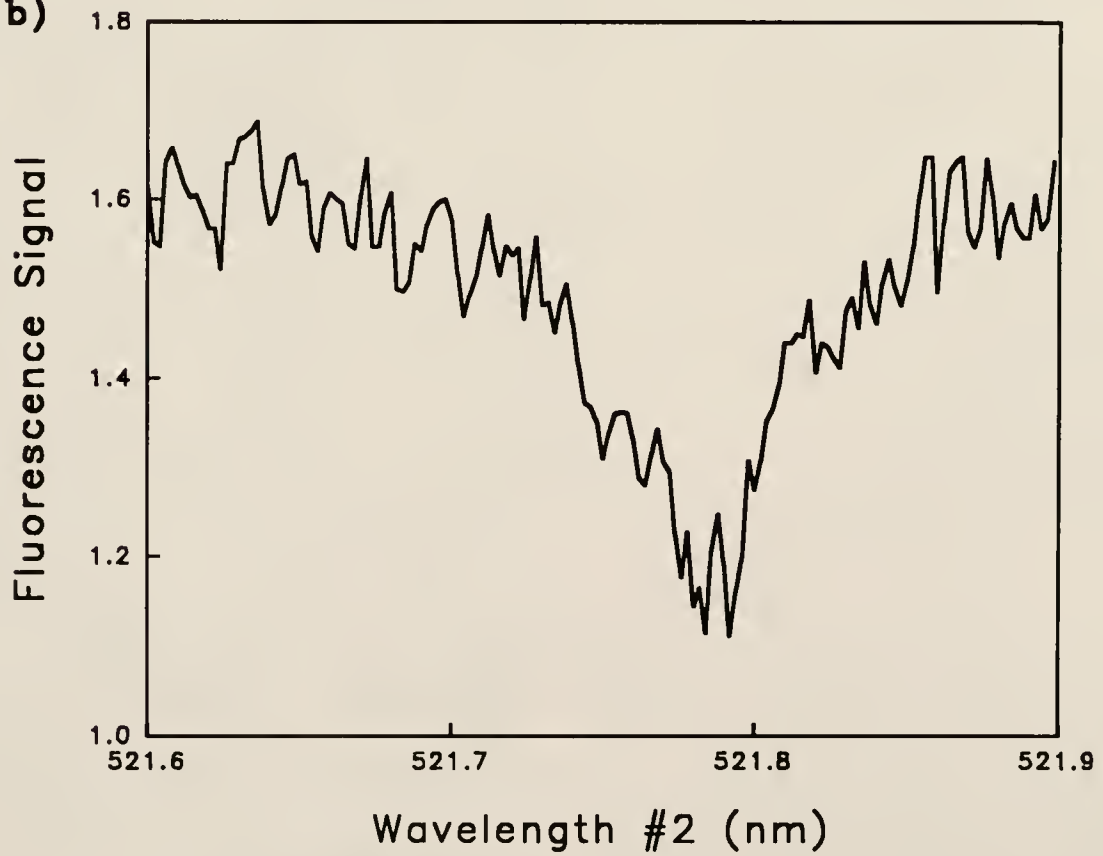


Figure 7-4 : Fluorescence signal versus wavelength of the second excitation wavelength and the resulting fluorescence dip for copper in the ICP while holding λ_1 constant at 324.754 nm and monitoring both (a) resonance fluorescence and (b) nonresonance fluorescence.

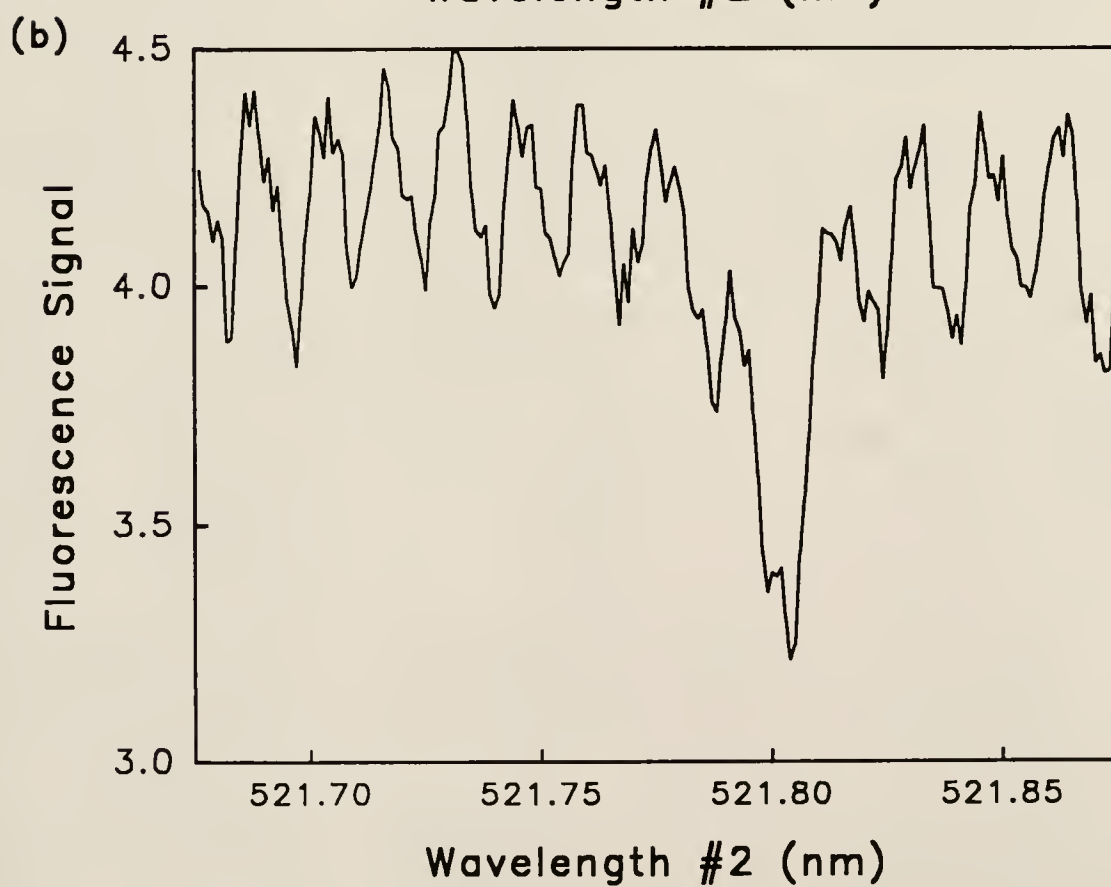
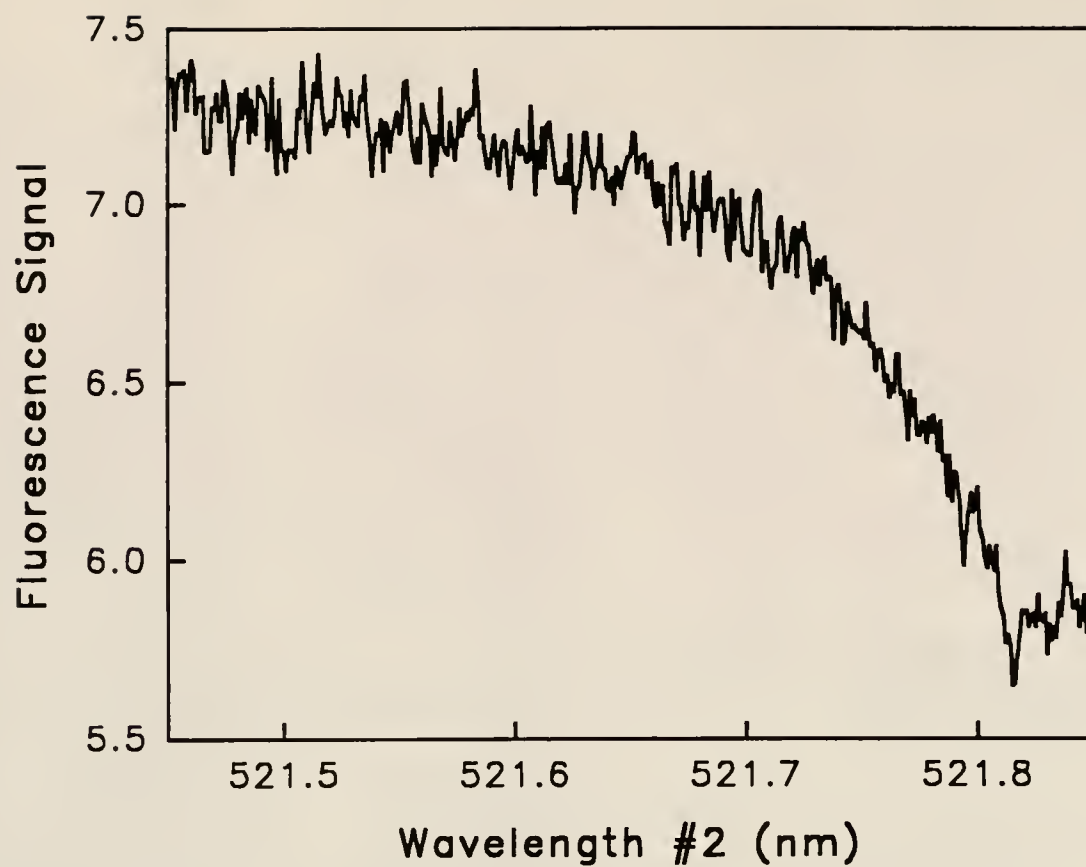
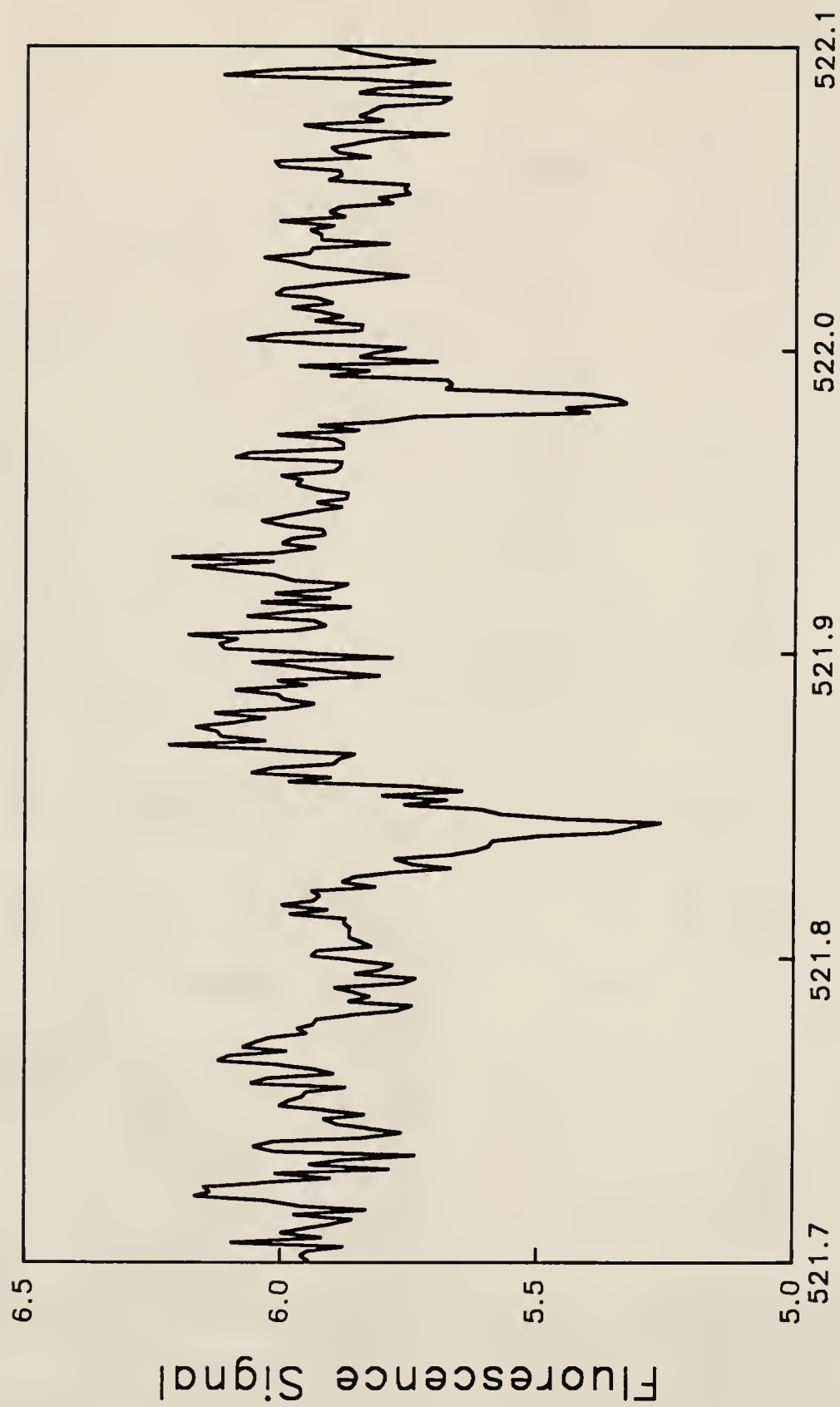


Figure 7-5 : Fluorescence signal versus wavelength for the second excitation wavelength and the resulting fluorescence dips for copper in the low pressure ICP expansion while holding λ_1 constant at 324.754 nm and monitoring the resonance fluorescence.



Wavelength #2 (nm)

excitation, again while monitoring both resonance and nonresonance fluorescence at either 324.754 nm or 327.396 nm.

Some representative scans are given in Figures 7-3 to 7-5. These scans were all performed with the same excitation and fluorescence scheme with the difference being the atom reservoir into which the analyte is being introduced. These different atom cells will, of course, have different noise characteristics which can be seen in these scans which were all performed using the same concentration of copper solution. While the fluorescence dips are not the same from atom source to atom source because of the different collisional environments, the differences in the noises in the various atomizers can be seen.

The data were collected for both one and two step excitation schemes as previously explained, and the relative fluorescence dips were calculated with the errors involved in the measurement expressed as one standard deviation (Tables 7-1 to 7-6). The comparison of these empirical data to the theoretical values within experimental error was good. It was only possible to calculate theoretical fluorescence dips for excitation and fluorescence schemes where the second excitation step was tuned to directly deplete the initially populated level, and then only when the fluorescence signal from that level was being monitored, because of the implementation of the rate equations modeling (Figure 7-6).

Table 7-1

Ag(I) Fluorescence Dips in a Flame

λ_1 (nm)	λ_2 (nm)	λ_{η} (nm)	Δ' (Theory)	Δ' (Observed)
328.068	546.549	328.068	0.56	0.31 ± 0.05
328.068	546.549	338.289	—	0.18 ± 0.04
328.068	547.115	328.068	0.56	0.43 ± 0.03
328.068	547.115	338.289	—	0.20 ± 0.04
328.068	520.907	328.068	—	0.07 ± 0.03
328.068	520.907	338.289	—	0.63 ± 0.05
338.298	546.549	338.289	—	0.11 ± 0.02
338.298	546.549	328.068	—	0.40 ± 0.04
338.298	547.115	338.289	—	0.11 ± 0.04
338.298	547.115	328.068	—	0.28 ± 0.04
338.298	520.907	338.289	0.56	0.64 ± 0.05
338.298	520.907	328.068	—	0.28 ± 0.05

Table 7-2

Cu(I) Fluorescence Dips in a Flame

λ_1 (nm)	λ_2 (nm)	λ_n (nm)	Δ' (Theory)	Δ' (Observed)
327.396	515.324	327.396	0.56	0.49 ± 0.02
327.396	515.324	324.754	0.56	0.36 ± 0.04
327.396	521.820	327.396	0.56	0.12 ± 0.05
327.396	521.820	324.754	0.56	0.45 ± 0.06
327.396	522.007	327.396	0.56	0.10 ± 0.04
327.396	522.007	324.754	0.56	0.37 ± 0.06
324.754	521.820	324.754	0.56	0.53 ± 0.05
324.754	521.820	327.396	0.56	0.51 ± 0.08
324.754	522.007	324.754	0.56	0.38 ± 0.03
324.754	522.007	327.396	0.56	0.33 ± 0.05
324.754	515.324	324.754	0.56	0.13 ± 0.04
324.754	515.324	327.396	0.56	0.41 ± 0.08

Table 7-3

Ag(I) Fluorescence Dips in the ICP

λ_1 (nm)	λ_2 (nm)	λ_n (nm)	Δ' (Theory)	Δ' (Observed)
328.068	546.549	328.068	0.63	0.62 ± 0.01
328.068	546.549	338.289	—	-0.56 ± 0.05
328.068	547.115	328.068	0.63	0.57 ± 0.01
328.068	547.115	338.289	—	-0.55 ± 0.04
328.068	520.907	328.068	—	0.09 ± 0.01
328.068	520.907	338.289	—	0.79 ± 0.02
338.298	546.549	338.289	—	-0.12 ± 0.03
338.298	546.549	328.068	—	0.52 ± 0.03
338.298	547.115	338.289	—	$0.06 \pm 0.00_4$
338.298	547.115	328.068	—	$0.56 \pm 0.00_1$
338.298	520.907	338.289	0.71	0.71 ± 0.04
338.298	520.907	328.068	—	-0.82 ± 0.12

Table 7-4

Cu(I) Fluorescence Dips in the ICP

λ_1 (nm)	λ_2 (nm)	λ_n (nm)	Δ' (Theory)	Δ' (Observed)
327.396	515.324	327.396	0.71	0.74 ± 0.04
327.396	515.324	324.754	—	0.64 ± 0.01
327.396	521.820	327.396	—	0.03 ± 0.06
327.396	521.820	324.754	—	0.77 ± 0.01
327.396	522.007	327.396	—	0.06 ± 0.04
327.396	522.007	324.754	—	0.62 ± 0.03
324.754	521.820	324.754	0.63	$0.66 \pm 0.00_3$
324.754	521.820	327.396	—	0.61 ± 0.07
324.754	522.007	324.754	0.63	0.64 ± 0.04
324.754	522.007	327.396	—	0.51 ± 0.01
324.754	515.324	324.754	—	0.02 ± 0.01
324.754	515.324	327.396	—	0.68 ± 0.01

Table 7-5

Ag(I) Fluorescence Dips in the ICP
Expansion

λ_1 (nm)	λ_2 (nm)	λ_n (nm)	Δ' (Theory)	Δ' (Observed)
338.298	520.907	338.298	0.50	0.46 ± 0.04
338.298	520.907	328.068	—	No Dip ^a
338.298	546.549	338.298	—	No Dip ^b
338.298	546.549	328.068	—	No Dip ^a
338.298	547.115	338.298	—	No Dip ^b
338.298	547.115	328.068	—	No Dip ^a
328.068	546.549	328.068	0.50	0.46 ± 0.04
328.068	546.549	338.298	—	No Dip ^a
328.068	547.115	328.068	0.40	0.35 ± 0.04
328.068	547.115	338.298	—	No Dip ^a
328.068	520.907	328.068	—	No Dip ^b
328.068	520.907	338.298	—	No Dip ^a

^a No nonresonance fluorescence

^b Depleting non-connected level

Table 7-6

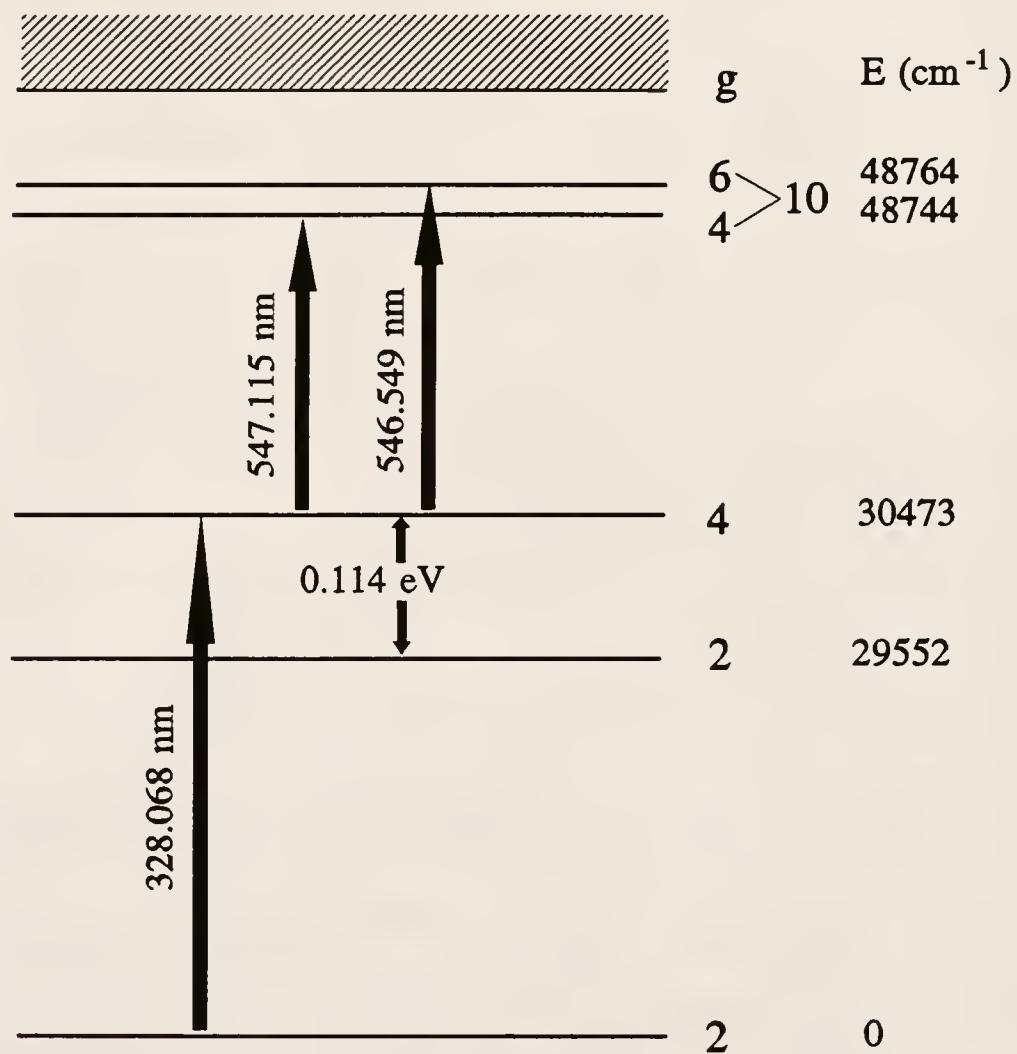
Cu(I) Fluorescence Dips in the ICP
Expansion

λ_1 (nm)	λ_2 (nm)	λ_n (nm)	Δ' (Theory)	Δ' (Observed)
327.396	515.324	327.396	0.50	0.46 ± 0.04
327.396	515.324	324.754	—	No Dip ^a
327.396	521.820	327.396	—	No Dip ^b
327.396	521.820	324.754	—	No Dip ^a
327.396	522.007	327.396	—	No Dip ^b
327.396	522.007	324.754	—	No Dip ^a
324.754	521.820	324.754	0.50	0.43 ± 0.09
324.754	521.820	327.396	—	No Dip ^a
324.754	522.007	324.754	0.40	0.33 ± 0.09
324.754	522.007	327.396	—	No Dip ^a
324.754	515.324	324.754	—	No Dip ^b
324.754	515.324	327.396	—	No Dip ^a

^a No nonresonance fluorescence^b Depleting non-connected level

Figure 7-6 : Example of a theoretical maximum relative fluorescence dip for copper assuming the two uppermost excited levels behave as one level and the two intermediate levels act independent of each other.

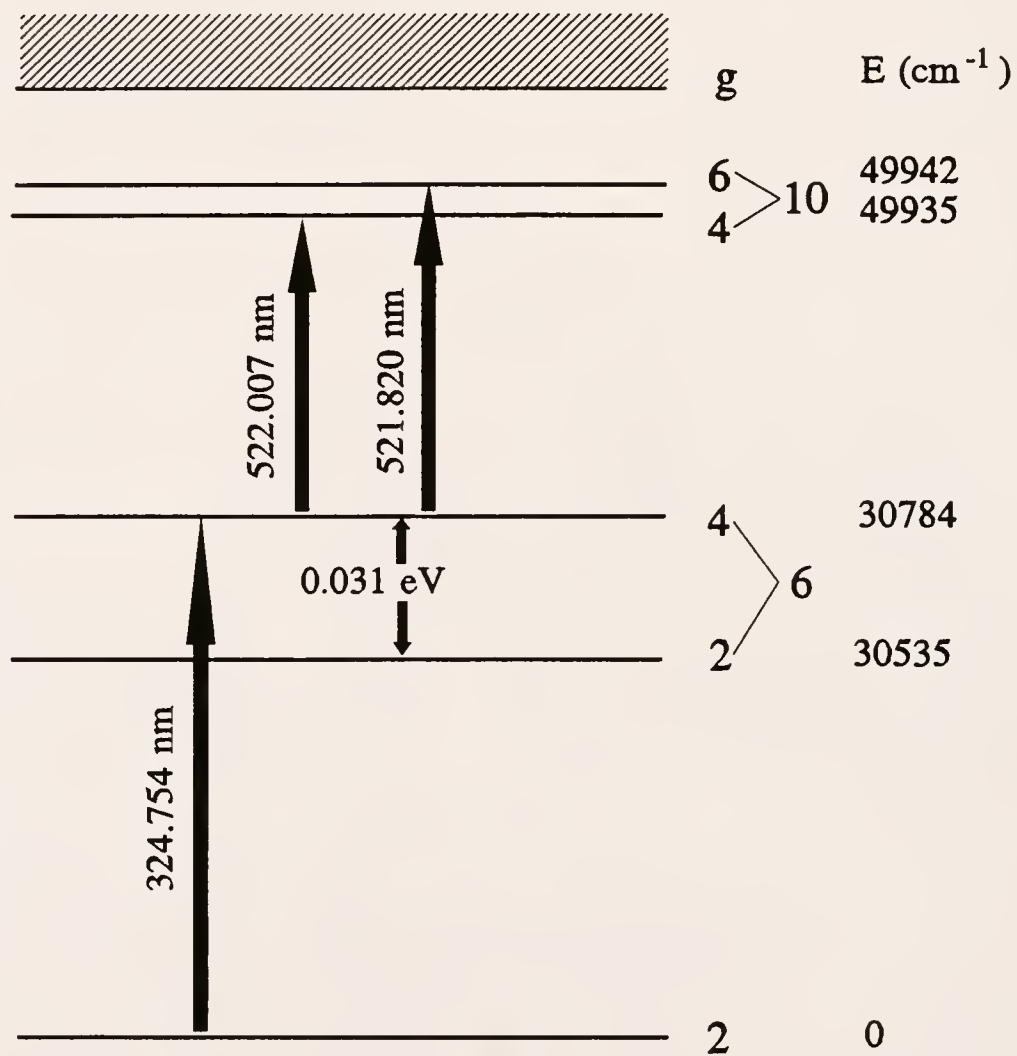
Ag(I)



$$\Delta' = \frac{g_4 \text{ (eff)}}{g_1 + g_3 + g_{4(\text{eff})}} = \frac{10}{2+4+10} = 0.63$$

Figure 7-7 : Example of a theoretical maximum relative fluorescence dip for copper assuming the two uppermost excited levels behave as one as well as the two intermediate levels.

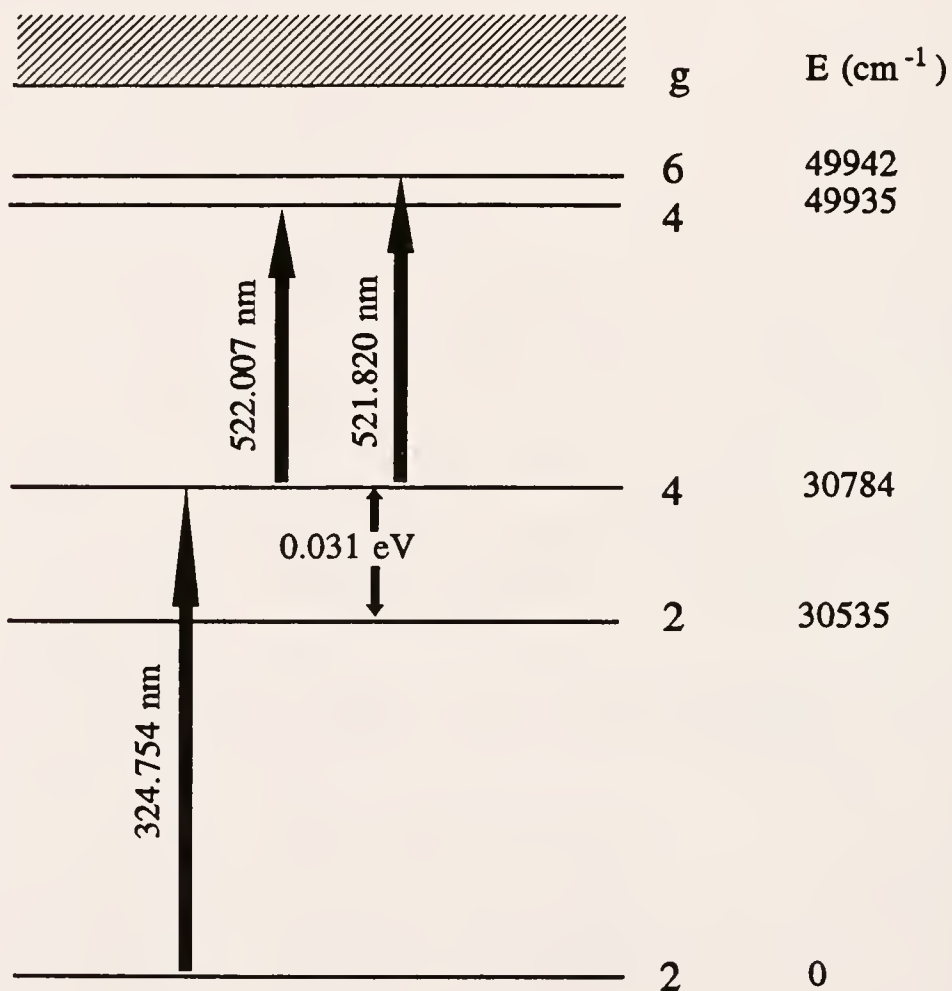
Cu(I)



$$\Delta' = \frac{g_1 + g_{2+3} + g_{4(\text{eff})}}{g_1 + g_{2+3} + g_{4(\text{eff})}} = \frac{10}{2+6+10} = 0.56$$

Figure 7-8 : Example of a theoretical maximum fluorescence dip for copper assuming the two uppermost levels act independent of each other as well as the two intermediate levels.

Cu(I)



$$\Delta' = \frac{g_4}{g_1 + g_3 + g_4} = \frac{6}{2+4+6} = 0.50$$

$$\Delta' = \frac{g_4}{g_1 + g_3 + g_4} = \frac{4}{2+4+4} = 0.40$$

Discussion

The different theoretically calculated values for the three different atom reservoirs can be illustrated through Figures 7-6 to 7-8. Because different collisional environments were implemented in this experimentation (i.e. the air/acetylene flame, the ICP, and a low pressure ICP expansion), different atomic levels needed to be taken into consideration when calculating the effective statistical weights to be used in the fluorescence dip expression, thereby affecting the theoretically calculated fluorescence dip.

In Figure 7-7, the atom reservoir of use was the air/acetylene flame, which is known to be a collisionally active atom source. The abundance of collisions in this atom cell caused the atomic levels to have a substantial collisional relationship. Using this assumption, an effective statistical weight was calculated for these intermediate levels simply by adding the relative statistical weights of the levels and using this new value in the fluorescence dip expression to calculate a theoretical value (Figure 7-7). In the case of copper in the air/acetylene flame, this was a good approximation because the close electronic spacing of these intermediate levels in conjunction with an environment rich in collisions caused equal sharing of the excited state atom population between these two levels.

In the case of silver in the air/acetylene flame, this approximation was not a good one as was seen through a comparison of observed to theoretical fluorescence dip values. Since these measurements were taken in the same collisional environment as the copper data, it must be assumed that the difference in dip values was due to the greater

electronic spacing between the two intermediate levels of silver (0.114 eV) as compared to the spacing in copper (0.031 eV). To compensate for this larger spacing, the two intermediate levels were considered to behave separately when calculating the fluorescence dip (Figure 7-6). As was seen through comparison of these values, this was also not necessarily a valid treatment for the modeling of silver in an air/acetylene flame. This led to the conclusion that the large spacing between the intermediate levels was large enough to consider them as separate levels, yet the high collisional environment of the air/acetylene flame induced a relationship in population between these levels to some extent. This illustrated the effect of different atomic systems and experimental parameters on the fluorescence dip and, therefore, the information that can be obtained through the fluorescence dip measurement.

In the ICP atom reservoir, collisional activity between the two intermediate levels was not appreciably affected by the atom source, since the argon ICP is a low collision environment relative to the air/acetylene flame. This was seen through the agreement within experimental error between the observed relative fluorescence dips and the theoretically calculated fluorescence dips assuming negligible mixing between the intermediate, excited state levels. There must be some relationship between these levels, however, in order to be able to monitor the nonresonance fluorescence signal, although this signal was present at a magnitude substantially less than that for the resonance transition. The fact that some collisional mixing does occur was supported by the fact that the two uppermost excited state levels (considered level 4) still behaved as one level in this atom reservoir. This was the assumption made when calculating the theoretical

relative fluorescence dips using an effective statistical weight, the sum of the actual statistical weights of the two levels (Figure 7-6), which was obviously valid examining the agreement between the experimental and theoretical values.

When implementing the ICP low pressure expansion, it was expected that this virtually collision free environment would have a great effect on the fluorescence dip measurement, which was, in fact, the case. There was no nonresonance fluorescence signal detected in introducing either of the first excitation steps. In the implementation of the ICP, there was enough of a relationship to monitor nonresonance fluorescence, but not enough to consider the levels substantially collisionally related, while in the low pressure ICP expansion, there was little to no relationship between the two intermediate levels at all. In addition, in this atom source it was no longer valid to assume a collisional relationship between the two uppermost excited levels as was noted through poor agreement between the experimentally determined values and the calculated fluorescence dips implementing this assumption. If, however, the fluorescence dips were calculated assuming no collisional activity between these highest excited levels (Figure 7-8), agreement within experimental error for the observed and theoretical dips was good.

Theoretical Modeling

The computer simulations presented in this section were performed utilizing the rate equations approximation while varying the relationships between the levels to examine the effect that these different associations had upon the relative population

densities of the atomic levels and, consequently, the fluorescence dip. Unless otherwise indicated on the computer generated plots and in the absence of any external excitation, excitation upwards from one atomic level to another or from an atomic level to the ionization continuum was neglected. In the absence of laser excitation, de-excitation rates from the uppermost levels to either intermediate level or from one of the intermediate levels to the ground state were set at $1.1 \times 10^8 \text{ s}^{-1}$, a typical Einstein coefficient of spontaneous emission. Laser radiation was assumed to induce an excitation rate of $1 \times 10^9 \text{ s}^{-1}$, a value easily resulting in saturation conditions for the transition corresponding to the wavelength of the excitation. The collisional relationship between the two intermediate levels was the parameter being examined in this experimentation, and the values representing these associations are given on the plots. These plots are presented more for the comparison of trends in the behavior of the atomic levels than for the calculation of the actual population densities. The relationships between the atomic levels in copper and silver are different, and, therefore, these plots would have to be separately determined for both of these elements, yielding the same information obtainable from the fluorescence dip calculation assuming saturation, steady state conditions. In any of the proposed excitation and fluorescence schemes, it was still not possible to theoretically determine the fluorescence dips for a nonresonant signal or when the level being depopulated through the introduction of the second excitation step is different from the level directly populated by the first excitation step. At this time, it was only possible to investigate tendencies toward certain behaviors, but not the actual

values for physical parameters for these atoms in these various atom sources because of the number of unknown quantities involved in these determinations.

The collisional relationships were varied for all possible excitation and fluorescence combinations, and the computer generated data were plotted as a function of time. The rate equations approximation cannot be trusted at the beginning of the interaction, but only steady state trends were being examined in this dissertation, so, while it is helpful to see how the atomic populations reach their steady state values, accurate time dependence values were not crucial. These time dependent curves are labeled either dip n_2 or dip n_3 . These values are defined at this time as the fluorescence dips predicted while monitoring the fluorescence dips for either level 2 or level 3, respectively.

Excitation at $\lambda_{1 \rightarrow 3}$ and $\lambda_{3 \rightarrow 4}$

Computer simulations of relative fluorescence dips were performed for the $\lambda_{1 \rightarrow 3}$ and $\lambda_{3 \rightarrow 4}$ excitation scheme and the relative population densities for all of the atomic levels experiencing both one and two step excitation were calculated. From this information, the fluorescence dips were calculated and the inequality in the statistical weights of the levels involved in the excitation scheme was compensated for. This compensation was effected by multiplying the relative fluorescence dip calculated from the relative population densities by a weighting factor corresponding to the statistical weights of the levels (i.e. $g_3/(g_1 + g_2 + g_3)$) involved in the excitation scheme. This correction allowed for actual calculation of the steady state dip for level 3, but not level

2 as it was not possible to include this level in the statistical weight expression. In this case, it is still useful to examine the comparison of the dips for levels 2 and 3, so, in order to keep their relationship constant, both of the dips were multiplied by this weighting factor. This does not result in absolute values for the fluorescence dip in the nonresonance case, but the relative behavior of the dips for the two levels remained constant. For silver, these simulations were compared to the excitation schemes with a first excitation wavelength of 328.068 nm and a second step wavelength of either 546.459 nm or 547.115 nm. For copper, these excitation wavelengths were 324.754 nm for $\lambda_{1 \rightarrow 3}$ and either 522.007 nm or 521.820 nm for $\lambda_{3 \rightarrow 4}$.

At low collisional mixing between the intermediate levels (Figure 7-9), a large inverted dip was predicted for the nonresonance fluorescence signal while a positive dip of about 40 to 50 percent was present for the fluorescence monitored from the level directly populated through laser excitation. This scheme most closely approximated the behavior in the low pressure ICP expansion with the exception of the fact that no nonresonance fluorescence signal was observed, experimentally, in any of the excitation schemes in this atom source. That does not necessarily mean that there were no collisions in this atom reservoir, simply that the nonresonant level, level 2, was populated to a very low extent through collisions from level 3 and, therefore, the resulting signal was not seen. This prediction of a large inverted (negative) dip for the nonresonant level was reasonable since, at low collisional activity, the rate of spontaneous de-excitation from the uppermost excited level to the nonresonant level could easily be assumed to be substantially greater than the collisional relationship between the intermediate levels.

With the collisional mixing (Figure 7-10) increased by an order of magnitude, an inverted fluorescence dip was still present, but not to the same extent since the collisional activity was greater. This simulation most closely approximates the behavior of silver in the ICP because with this combination, the resonance fluorescence dip was about 60 percent with the nonresonance fluorescence dip being about -55 percent as was predicted through this rate equations modeling.

After the collisional relationship between these levels was again increased by five times greater than that in Figure 7-10 (Figure 7-11), an inverted dip was no longer present for the nonresonance fluorescence signal as the collisional coupling constant became greater than the coefficient of spontaneous emission from level 4 to level 2. While silver in the ICP was modeled through a scheme with less collisional activity, silver in the air/acetylene flame was more closely approximated by this scheme demonstrating the effect of atomization environments on the fluorescence dip measurement. The rate of collisional mixing in this case was such that the relative fluorescence dip for the directly populated level (level 3) was about 35 to 45 percent with a nonresonance relative fluorescence dip of close to 20 percent showing that the levels were mixed enough such that no inverted dips were present, but not collisionally coupled to an extent that they behaved in a similar manner which would result in equal fluorescence dips for both levels.

Another experimental scheme that was closely modeled by this computer simulation was copper in the ICP. While the study of silver in the ICP was

approximated by the previous computer simulation (Figure 7-7), copper in the same atom source experiences more of a collisional coupling in the same environment due to the lower amount of electronic spacing between the intermediate levels than for the comparable levels in silver.

By increasing the collisional relationship between levels 2 and 3 by yet another five times (Figure 7-12), the resulting computer generated relative fluorescence dips approximated those for copper in the air/acetylene flame. This atomic system and atom source combination resulted in the greatest amount of coupling between these intermediate levels since it involved the study of the atom with the lower amount of electronic spacing between the intermediate, excited state levels in the most collisionally rich environment. In this case, the resonance and nonresonance fluorescence dips for a given excitation scheme were equal, demonstrating that the collisional mixing resulted in close to complete coupling of the levels 2 and 3 causing them to behave as one level.

Excitation at $\lambda_{1 \rightarrow 2}$ and $\lambda_{2 \rightarrow 4}$

The relative fluorescence dips for both levels 2 and 3 were modeled for this excitation scheme again using the rate equations theory to solve for the relative population densities and calculating the relative fluorescence dips while compensating for the inequality in the statistical weights of the levels involved in the excitation scheme as previously described. The excitation wavelengths for this scheme in silver were 338.298 nm for $\lambda_{1 \rightarrow 2}$ and 520.907 nm for $\lambda_{2 \rightarrow 4}$ and in copper were 327.396 nm for $\lambda_{1 \rightarrow 2}$ and 515.324 nm for $\lambda_{2 \rightarrow 4}$.

At a low collisional mixing rate between levels 2 and 3 (Figure 7-13), again it would appear that it was the data that were taken in the ICP expansion that were most closely being modeled in this case. While, again, the nonresonance fluorescence signal was not observable experimentally, a large inverted dip was predicted for level 3, the level not directly populated through laser excitation. The predicted fluorescence dip for the resonant level, level 2, was around 50 percent, closely modeling the experimentally determined values.

An order of magnitude increase in the collisional mixing between levels 2 and 3 (Figure 7-14) still resulted in an inverted dip for the nonresonance fluorescence signal, with a positive dip for the resonance fluorescence signal of about the same deviation from zero. This most closely modeled the data taken for silver in the ICP which stands to reason since this was the atom with the greatest electronic spacing between the intermediate levels examined in a relatively low collision environment.

As this collisional relationship increased by another order of magnitude (Figure 7-15), the collisional coupling from level 2 to level 3 seemed to take precedence over emission from level 4 to level 3 as a mechanism to populate level 3. This resulted in a positive dip for the nonresonance fluorescence signal. This fluorescence dip did not equal that of the fluorescence dip of the resonance signal as the mixing at this point was not great enough to consider the levels substantially coupled. This computer simulation approximated the results for both silver in the air/acetylene flame (i.e. the greatest spacing with the greatest collisional environment) and copper in the ICP (i.e. the smaller spacing in the relatively collisional free environment) demonstrating how electronic

spacing between the levels worked together with the collisional medium in which the analyte is present in determining the magnitude of the fluorescence dip.

Increasing the collisional coupling between levels 2 and 3 yet another order of magnitude (Figure 7-16), the two intermediate, excited state levels began to behave as one level as the dips became close to equal with each other. This approximated the behavior of copper in the air/acetylene flame.

Something that should be pointed out at this time was seen through the comparison of Figures 7-12 and 7-16 and the information that can be derived from this association. In both cases, the collisional coupling rate was great enough between the two levels to cause them to behave in almost an identical manner. The important aspect here was that the collisional rate required to obtain this relationship was an order of magnitude greater in the case of Figure 7-16 than in Figure 7-12. This can be explained through the basic fact that in the case of Figure 7-12, collisions involving de-excitation were involved whereas in Figure 7-16, collisions to a more highly excited level, a less favorable process, were required for the population of the nonresonant level. This resulted in the requirement of more collisions to completely couple the two intermediate levels when upwards collisions were required.

Excitation at $\lambda_{1 \rightarrow 2}$ and $\lambda_{3 \rightarrow 4}$

The type of scheme discussed in this section involved excitation with a first step and then direct de-excitation of a thermally assisted level while the fluorescence signal from both intermediate levels was monitored. In these excitation and fluorescence schemes, it was not possible to correctly compensate for the inequalities of the statistical

weights of the levels involved in the excitation scheme because the level being depopulated through introduction of the second step was different from the one initially populated by the first excitation step. In these cases, the fluorescence dip values were corrected with an averaged statistical weight value for the two intermediate, and this resulted in values which may differ from those experimentally determined, but the general behaviors and trends can be compared to experimental data.

The scheme discussed here for silver involved excitation at 338.298 nm for $\lambda_{1 \rightarrow 2}$ and either 546.549 nm or 547.115 nm for $\lambda_{3 \rightarrow 4}$, and for copper the wavelengths for excitation were 327.396 nm for $\lambda_{1 \rightarrow 2}$ and either 521.820 nm or 522.007 nm for $\lambda_{3 \rightarrow 4}$. In these types of cases where the two excitation steps did not have an excited state level in common, comparison to the data collected in the low pressure ICP expansion could not be performed for two reasons. First, there was no nonresonance fluorescence signal detected, so the effect of the introduction of the second excitation step depleting this level could not be determined. Second, the second excitation step did not affect the population of the directly populated level as the result of the first excitation step since collisional coupling was negligible.

At low collisional coupling between levels 2 and 3 (Figure 7-17), the rate equations approach approximated both copper and silver in the ICP. Since there was little relationship between levels 2 and 3, the introduction of the second excitation step depopulating level 3 had little if any effect upon the fluorescence signal originating from level 2. Level 3, on the other hand, may not have a very high population resulting from

collisions upwards from level 2, but that population was greatly depleted through the introduction of the second excitation step originating at level 3.

With an increased collisional rate between these two intermediate levels by an order of magnitude (Figure 7-18), the data collected in the examination of both copper and silver in the air/acetylene flame were closely approximated with a greater affect on the fluorescence dip from level 2 and a lesser effect upon the fluorescence dip from level 3 since, as the relationship between the levels became greater, the levels behaved more and more like each other.

Excitation at $\lambda_{1 \rightarrow 3}$ and $\lambda_{2 \rightarrow 4}$

Again, the excitation scheme presented here could not be used to compare to empirical data in the ICP expansion chamber for the reasons mentioned earlier. Also mentioned earlier was the method in which the inequalities of the statistical weights of the atomic levels was compensated for and the indication that the fluorescence dip predictions in these cases could not be modeled directly, but that the comparison of trends were applicable to experimentally determined values. The excitation scheme discussed in this section involved silver wavelengths of 328.068 nm for $\lambda_{1 \rightarrow 3}$ and 520.907 nm for $\lambda_{2 \rightarrow 4}$, and copper wavelengths of 324.754 nm for $\lambda_{1 \rightarrow 3}$ and 515.324 nm for $\lambda_{2 \rightarrow 4}$.

At low collisional coupling rates between levels 2 and 3 (Figure 7-19), the rate equations modeling approximated the behavior seen in the case of both copper and silver in the ICP. Again, there was little effect upon level 3 since the population of level 2 was

the one directly depleted through the introduction of the second excitation step. This directly depleted level, while probably not greatly populated from collisions between these intermediate levels, experienced a large dip with the introduction of the second excitation step directly depopulating this level.

When this collisional relationship was increased by an order of magnitude (Figure 7-20), the theoretical fluorescence dips more closely resembled the experimental data for both copper and silver in the air/acetylene flame. Again, as the two levels were more closely related through collisions, the more they tended to behave in a similar fashion, explaining why the fluorescence dip for level 3 increased with an increasing fluorescence dip in level 2.

Saturation Through Laser Excitation

As was discussed when addressing the rate equations approximation as an approach through which to model the experiments presented in this dissertation, saturation of the transitions probed through laser excitation was required in order to assume steady state conditions and, subsequently, to utilize the maximum fluorescence dip expression in calculating the theoretical fluorescence dips. This was typically a valid assumption when implementing laser radiation as the source for excitation. In the work presented in this dissertation, however, this proved to be a very large problem. Frequency doubling was required to obtain the ultraviolet wavelengths for the first excitation step in all cases, and, while, for the doubling efficiency for the nonlinear optics used in this process doubling was reported as being as high as 10 percent, this

Figure 7-9 : Computer generated plots of the relative fluorescence dips as the result of excitation first at $\lambda_{1 \rightarrow 3}$ and then at both $\lambda_{1 \rightarrow 3}$ and $\lambda_{3 \rightarrow 4}$ for levels 2 and 3 versus time with low collisional activity between levels 2 and 3.

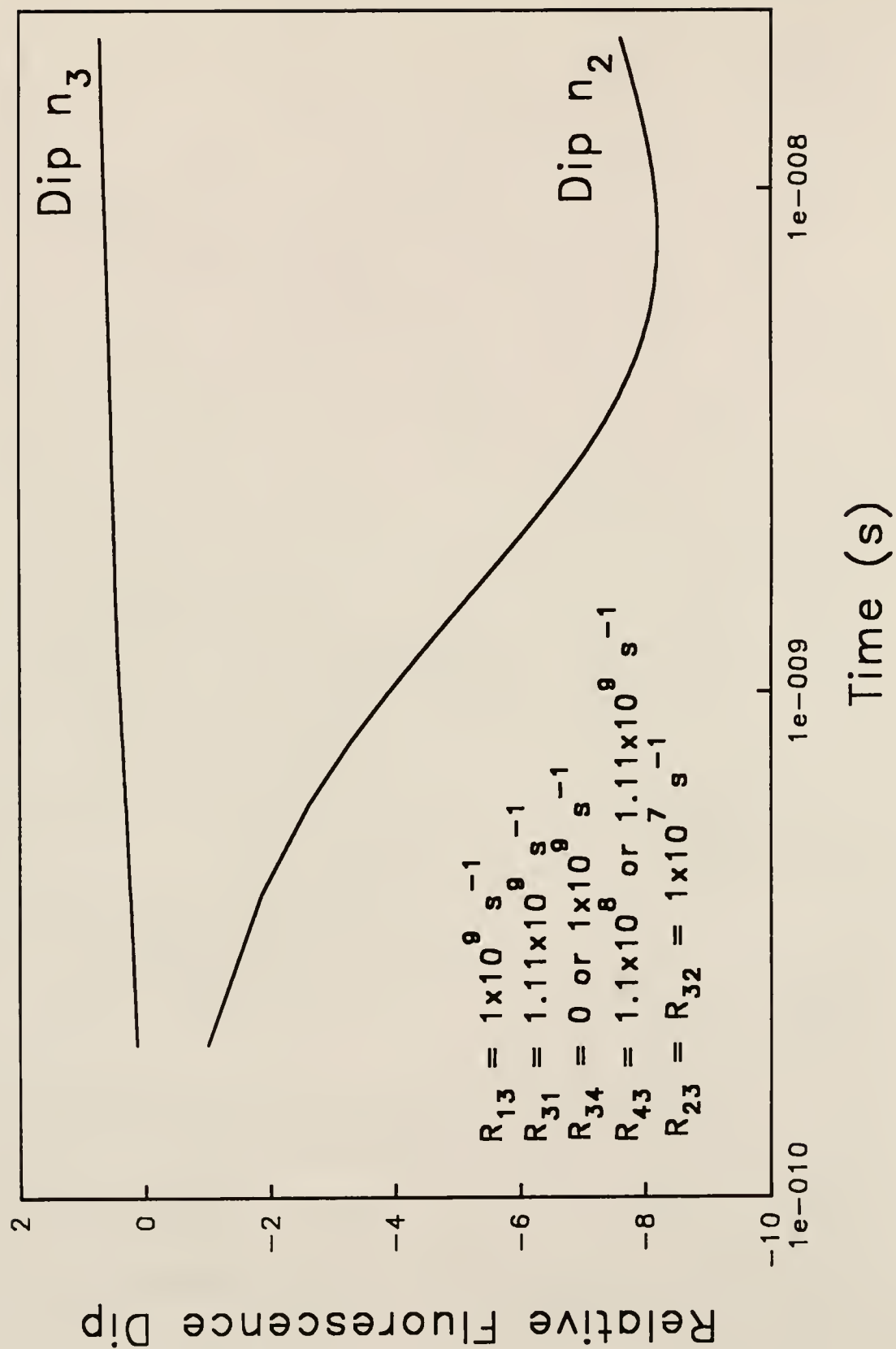


Figure 7-10 : Computer generated plots of the relative fluorescence dips as the result of excitation at first $\lambda_{1\rightarrow3}$ and then at both $\lambda_{1\rightarrow3}$ and $\lambda_{3\rightarrow4}$ for levels 2 and 3 versus time with moderate collisional activity between levels 2 and 3.

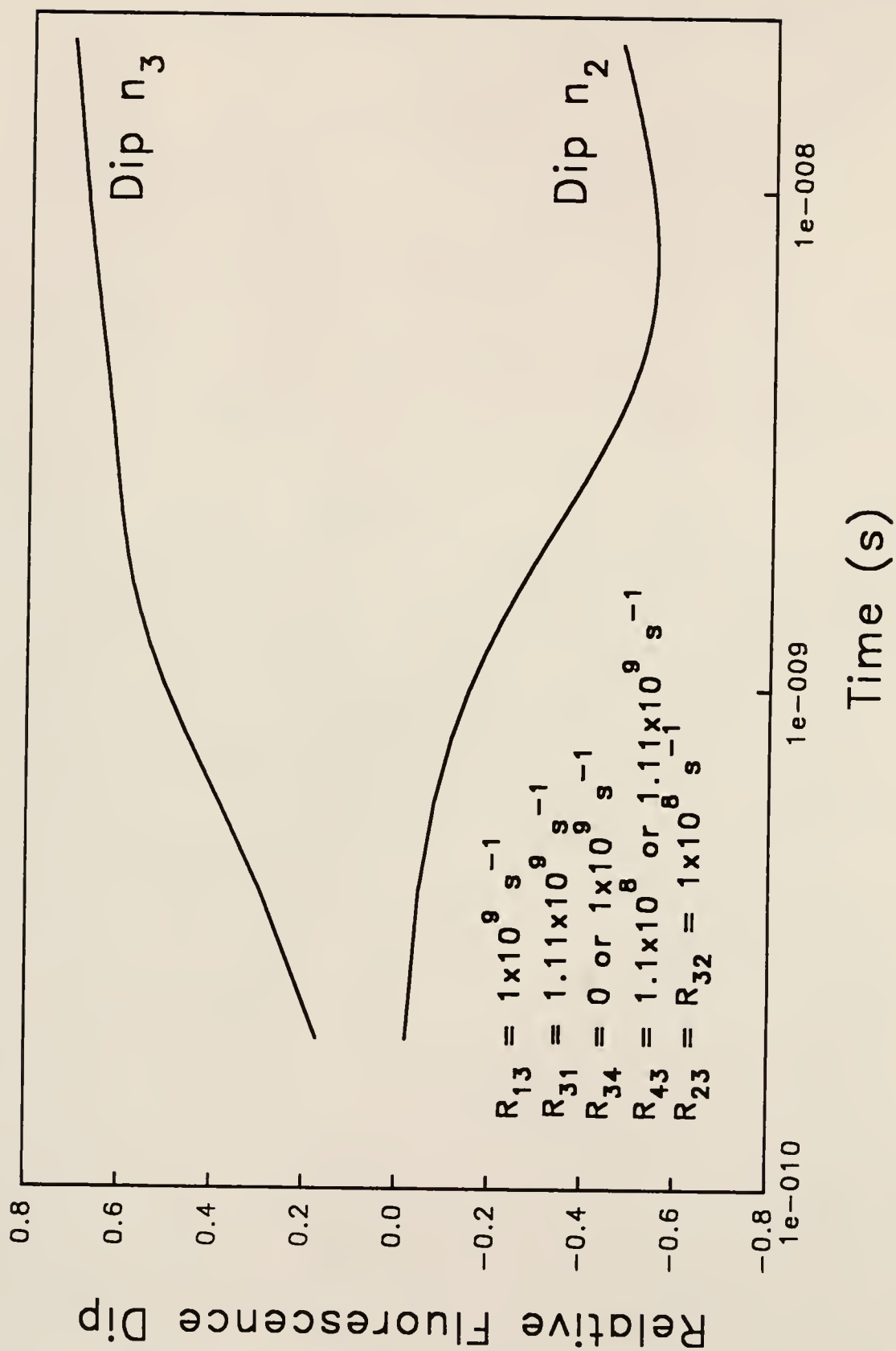


Figure 7-11 : Computer generated plots of the relative fluorescence dips as the result of excitation at first λ_{1-3} and than at both λ_{1-3} and λ_{3-4} for levels 2 and 3 versus time with moderate to high collisional activity between levels 2 and 3.

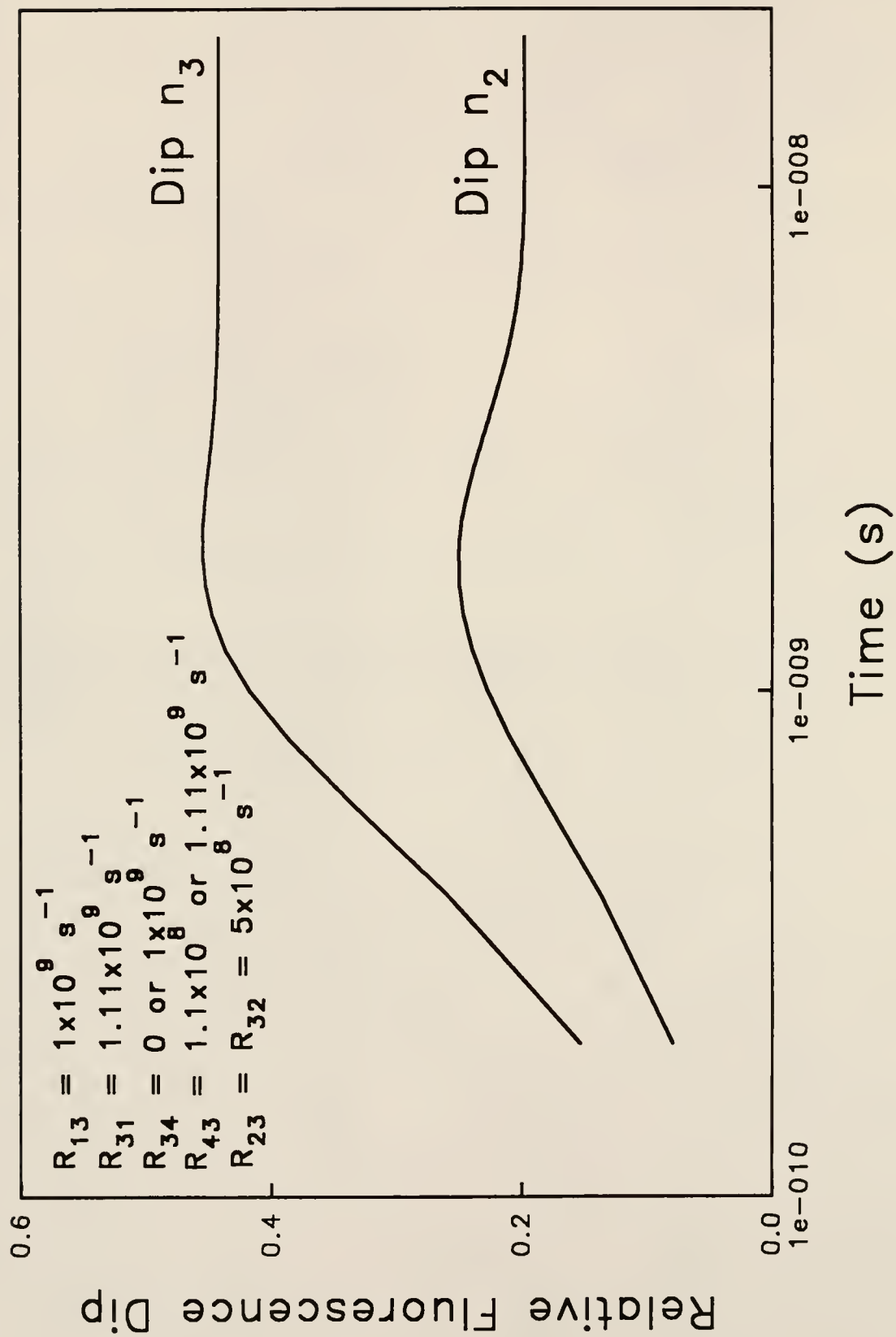


Figure 7-12 : Computer generated plots of the relative fluorescence dips as the result of excitation first at $\lambda_{1 \rightarrow 3}$ and then at both $\lambda_{1 \rightarrow 3}$ and $\lambda_{3 \rightarrow 4}$ for levels 2 and 3 versus time with high collisional activity between levels 2 and 3.

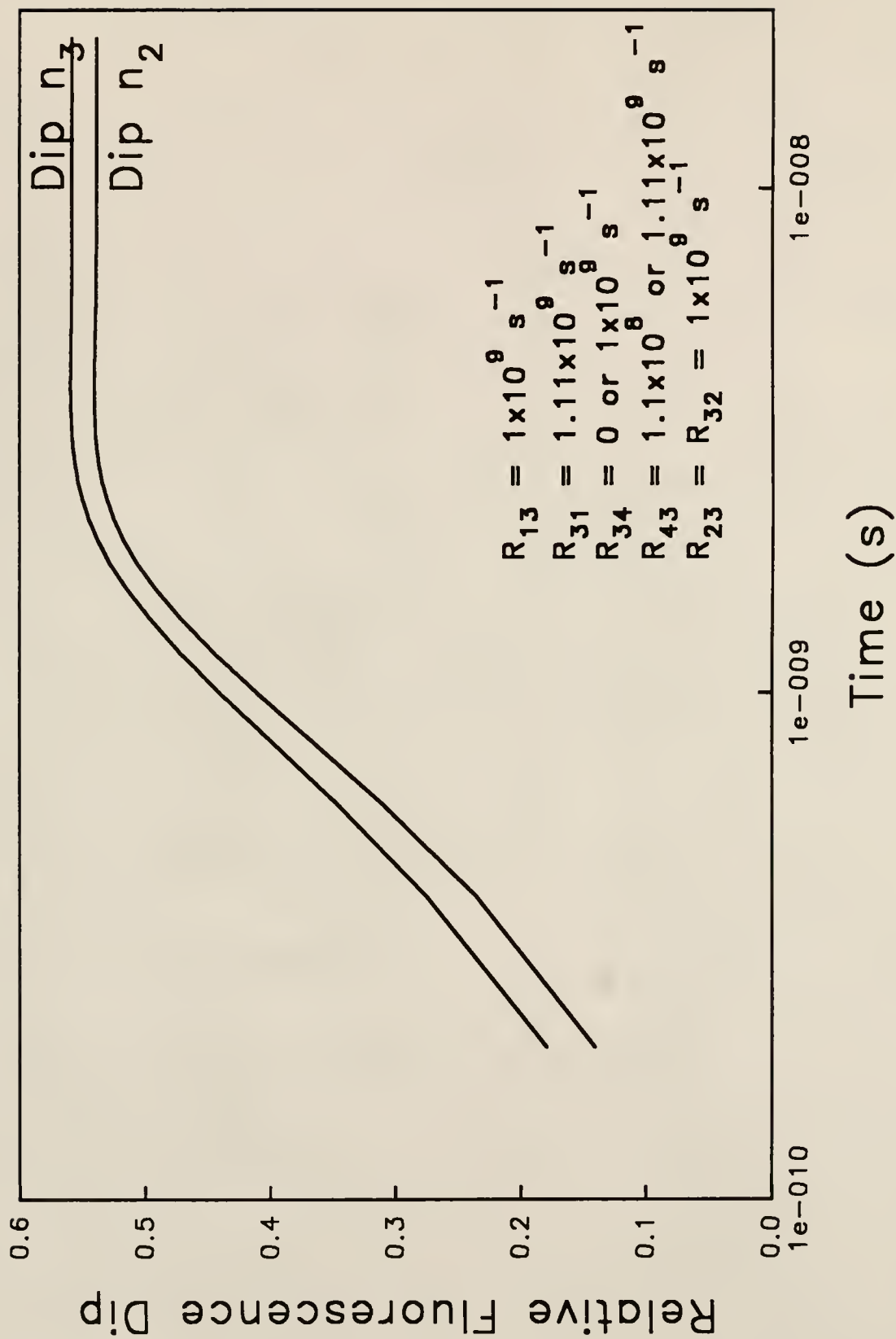


Figure 7-13 : Computer generated plots of the relative fluorescence dips as the result of excitation first at $\lambda_{1 \rightarrow 2}$ and then at both $\lambda_{1 \rightarrow 2}$ and $\lambda_{2 \rightarrow 4}$ for levels 2 and 3 versus time with low collisional activity between levels 2 and 3.

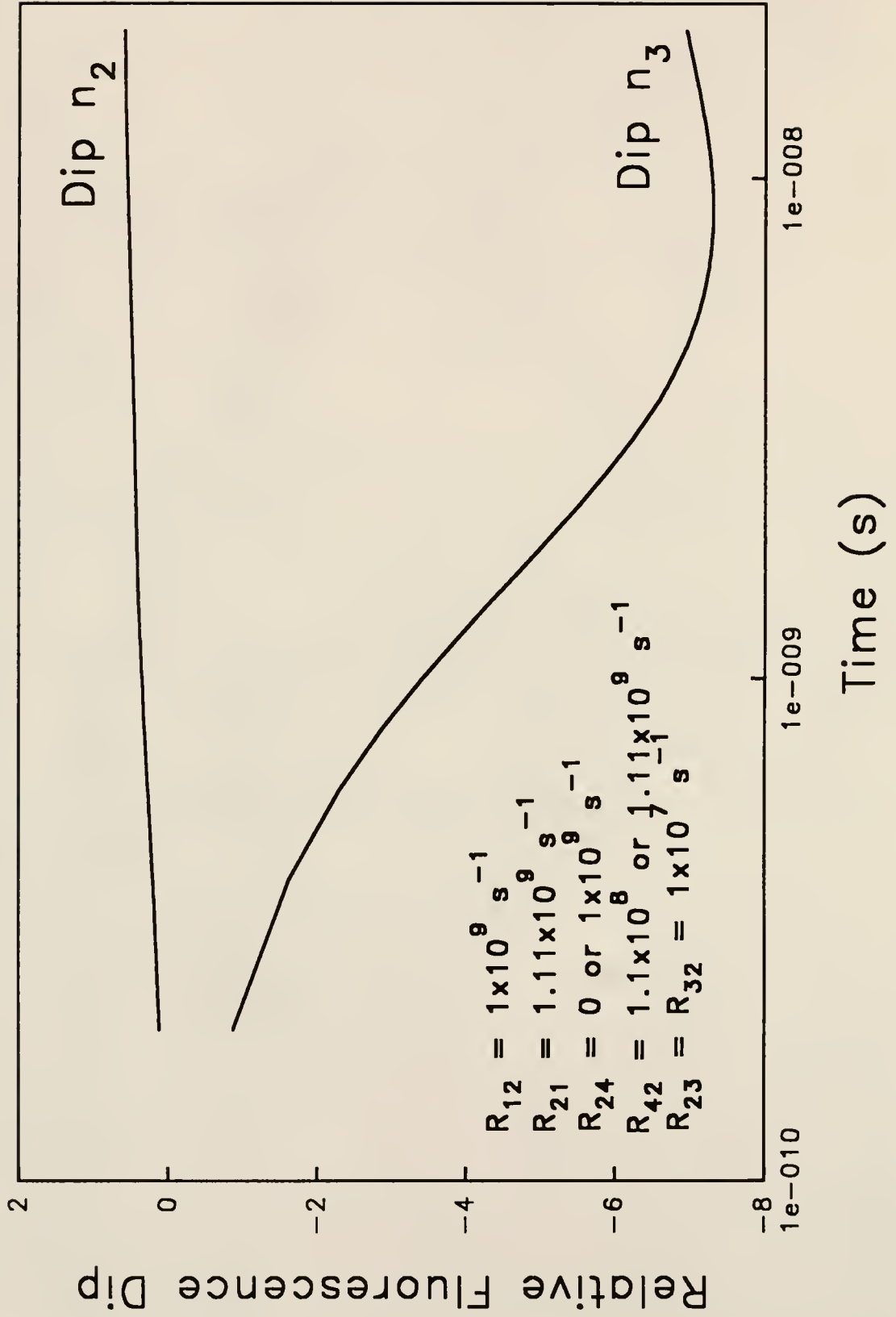


Figure 7-14 : Computer generated plots of the relative fluorescence dips as the result of excitation at first $\lambda_{1 \rightarrow 2}$ and then at both $\lambda_{1 \rightarrow 2}$ and $\lambda_{2 \rightarrow 4}$ for levels 2 and 3 versus time with moderate collisional activity between levels 2 and 3.

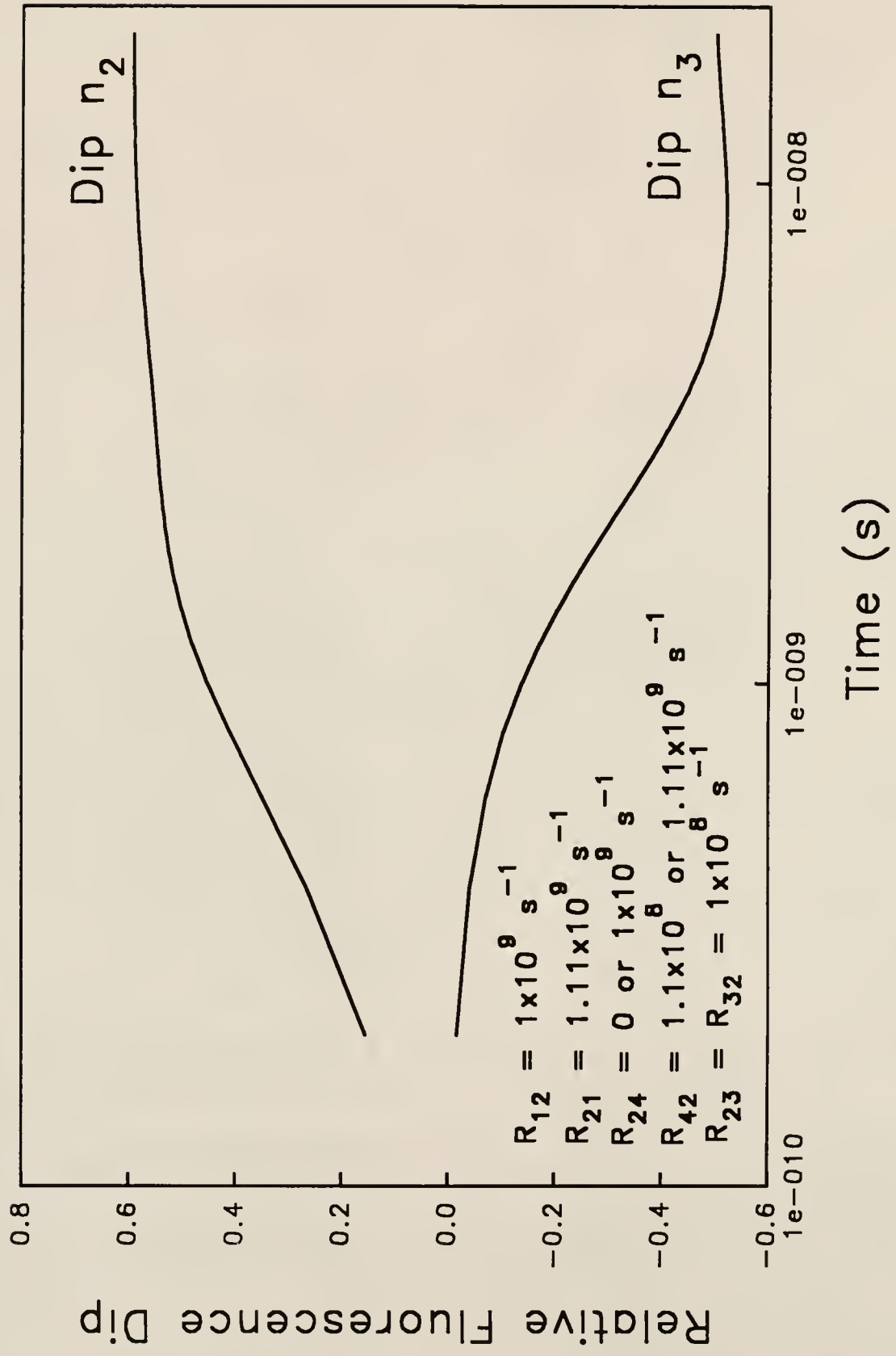


Figure 7-15 : Computer generated plots of the relative fluorescence dips as the result of excitation at first $\lambda_{1 \rightarrow 2}$ and then at both $\lambda_{1 \rightarrow 2}$ and $\lambda_{2 \rightarrow 4}$ for levels 2 and 3 versus time with high collisional activity between levels 2 and 3.

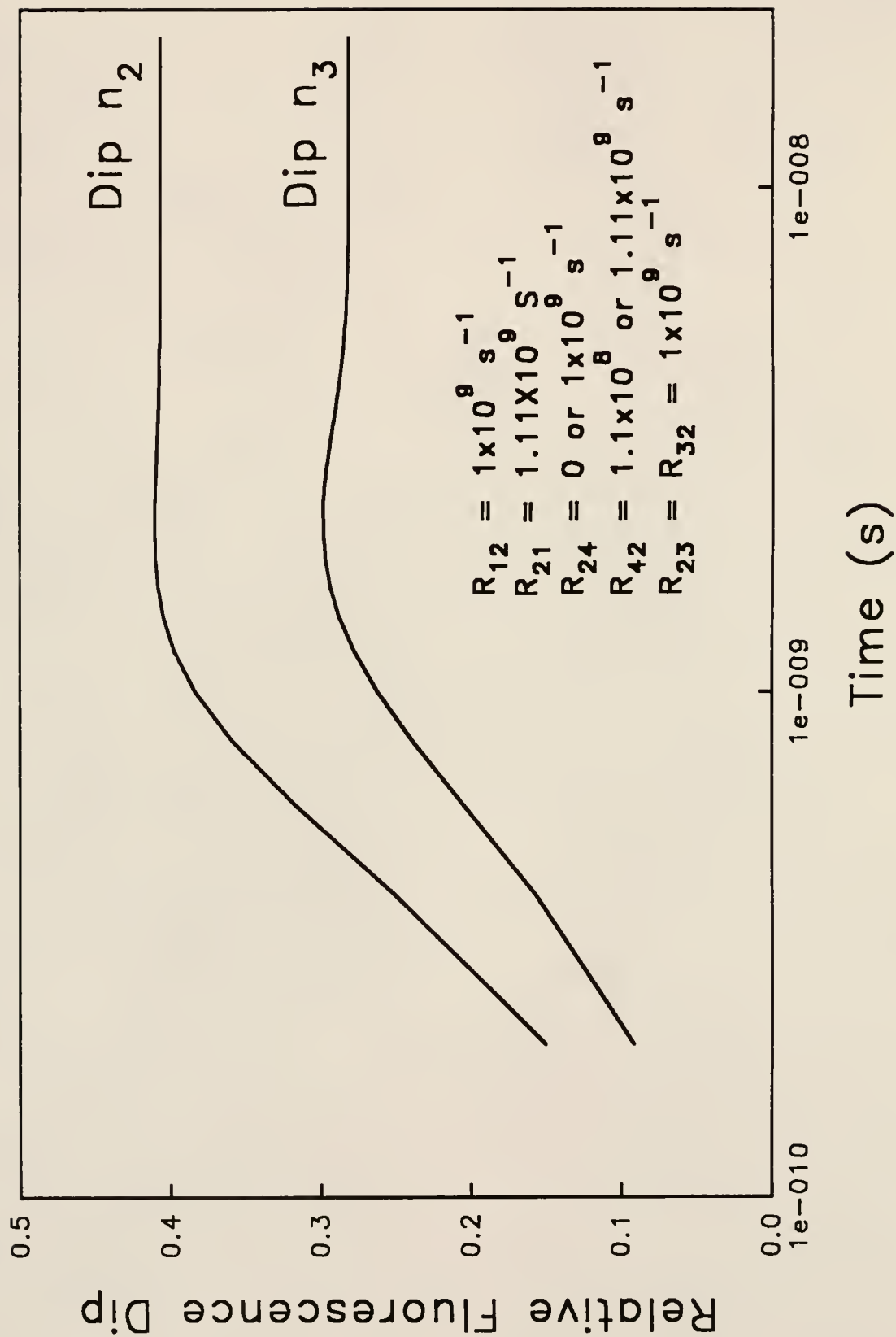


Figure 7-16 : Computer generated plots of the relative fluorescence dip as the result of excitation at first $\lambda_{1 \rightarrow 2}$ and then at both $\lambda_{1 \rightarrow 2}$ and $\lambda_{2 \rightarrow 4}$ for levels 2 and 3 versus time with very high collisional activity between levels 2 and 3.

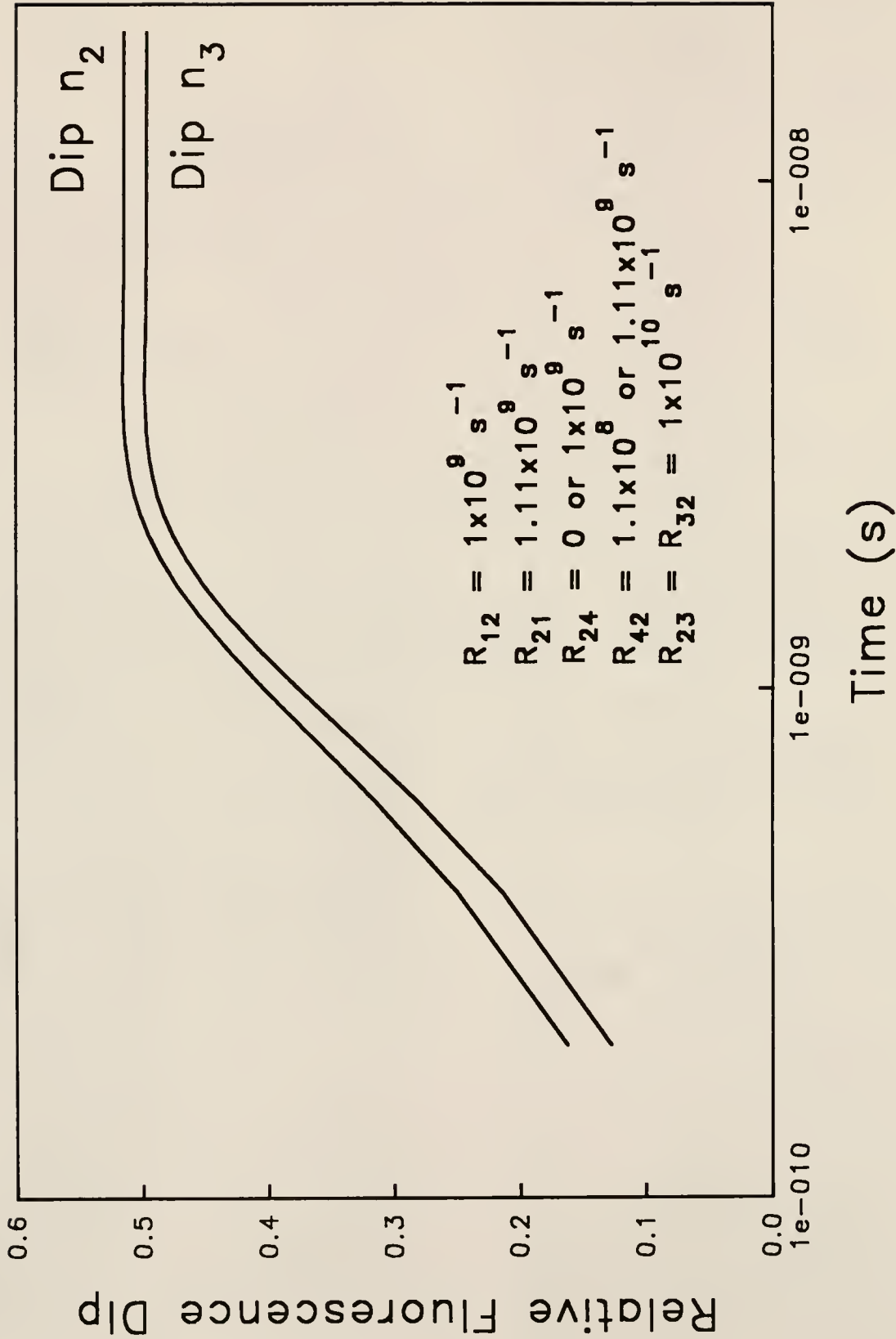


Figure 7-17 : Computer generated plots of the relative fluorescence dips as the result of excitation at first $\lambda_{1\rightarrow2}$ and then at both $\lambda_{1\rightarrow2}$ and $\lambda_{3\rightarrow4}$ of levels 2 and 3 versus time with low collisional activity between levels 2 and 3.

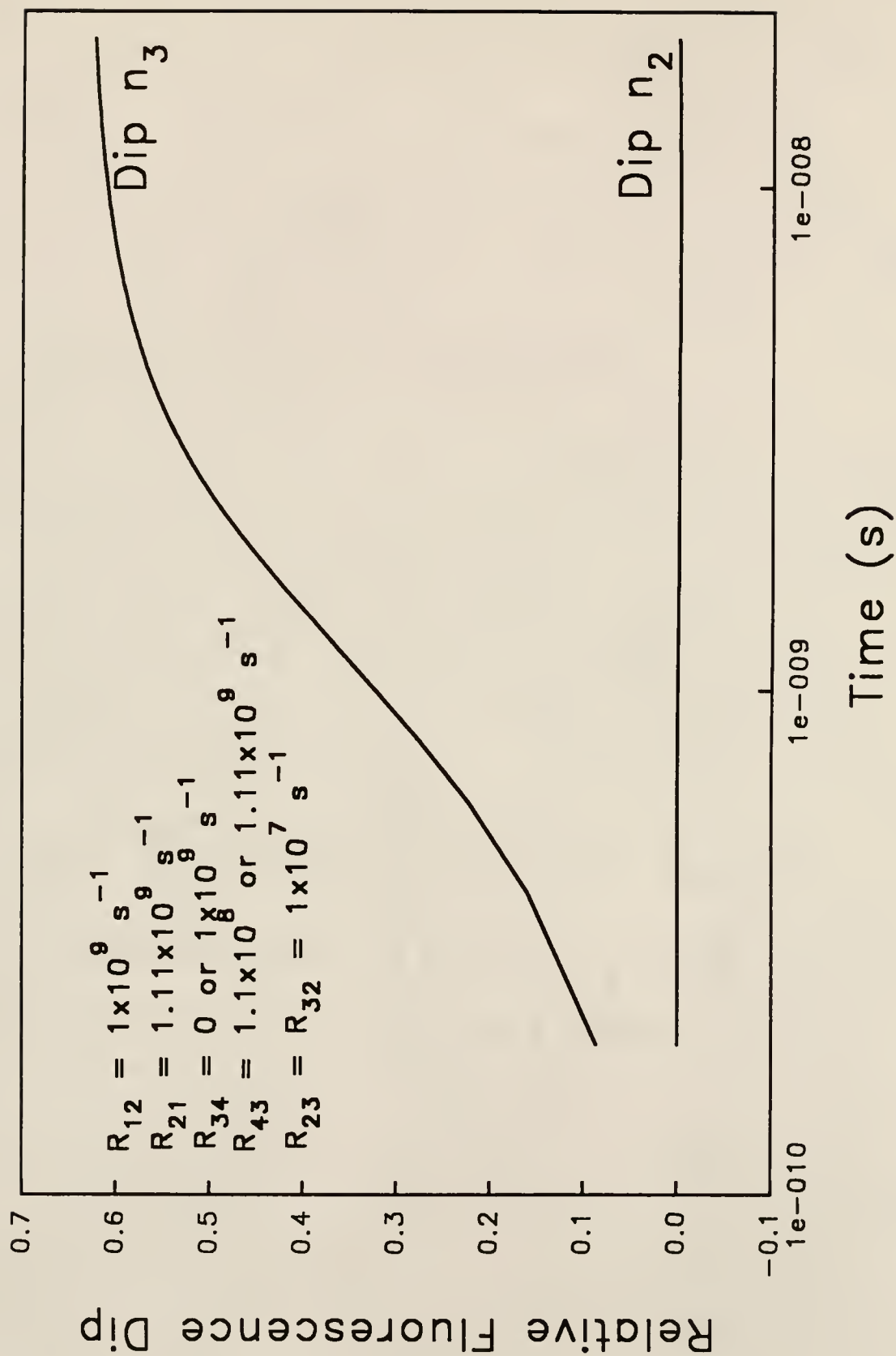


Figure 7-18 : Computer generated plots of the relative fluorescence dips as the result of excitation at both $\lambda_{1 \rightarrow 2}$ and then at both $\lambda_{1 \rightarrow 2}$ and $\lambda_{3 \rightarrow 4}$ for levels 2 and 3 versus time with moderate collisional activity between levels 2 and 3.

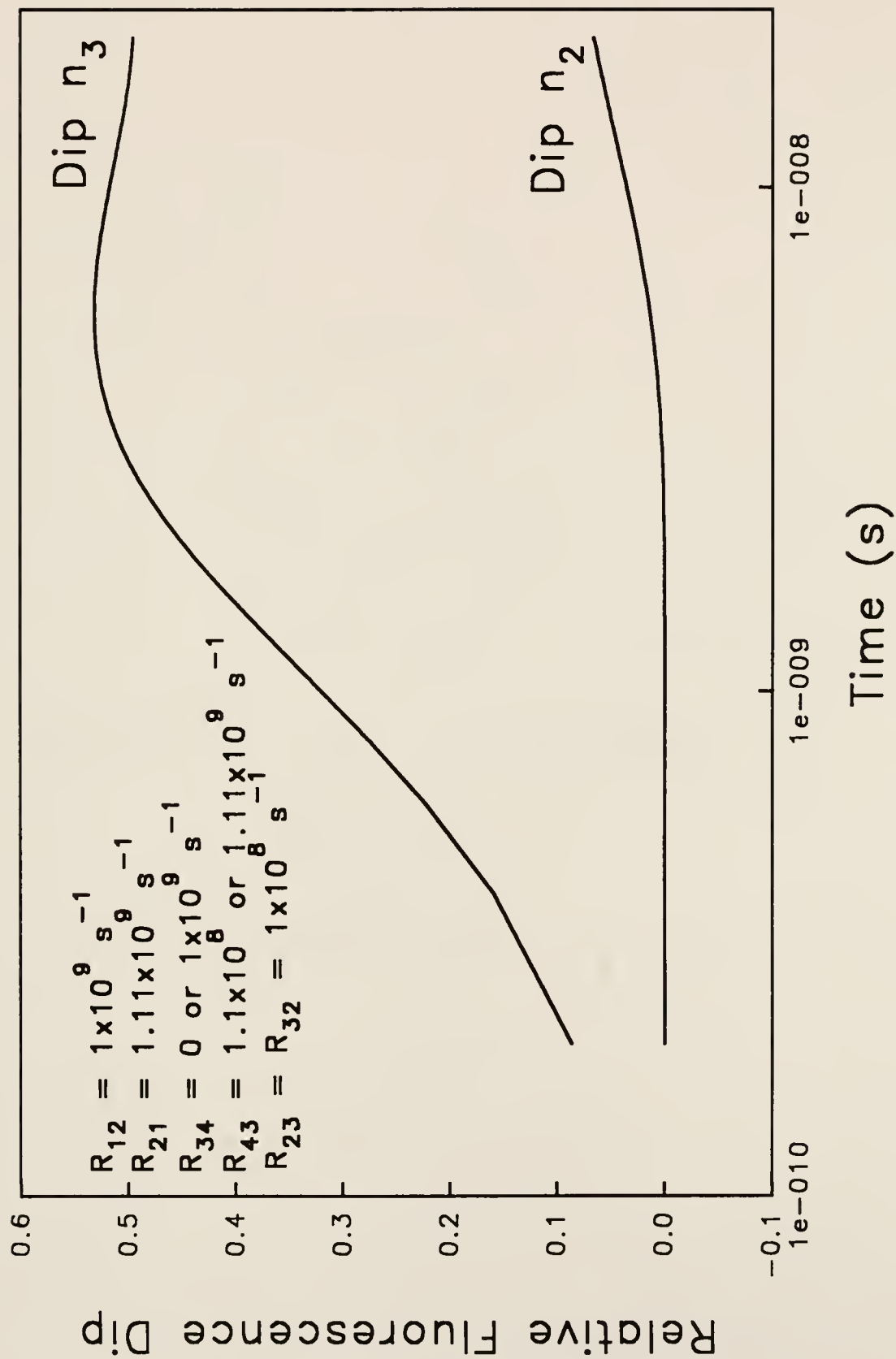


Figure 7-19 : Computer generated plots of the relative fluorescence dips as the result of excitation at first $\lambda_{1 \rightarrow 3}$ and then at both $\lambda_{1 \rightarrow 3}$ and $\lambda_{2 \rightarrow 4}$ for levels 2 and 3 versus time with low collisional activity between levels 2 and 3.

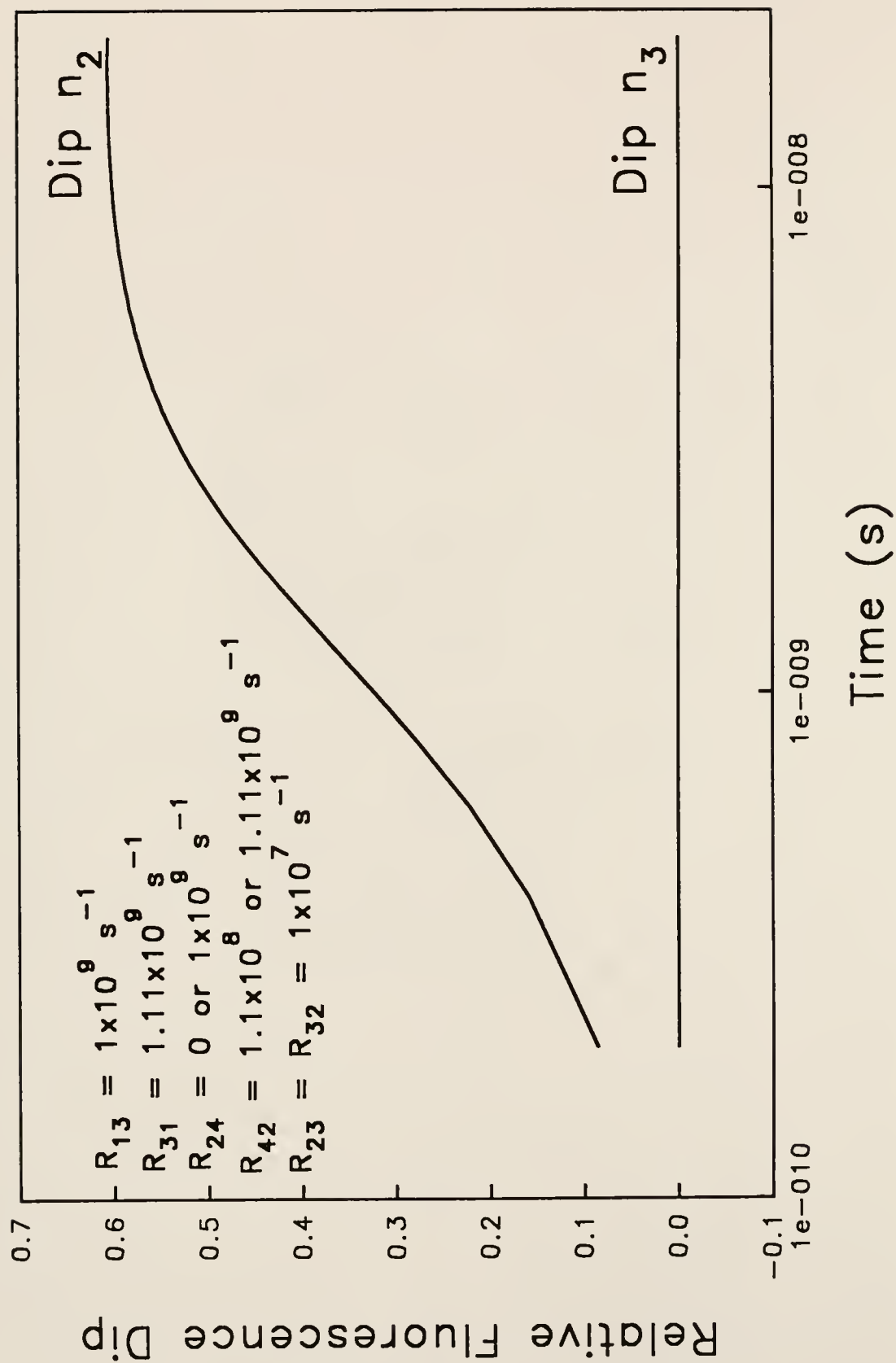
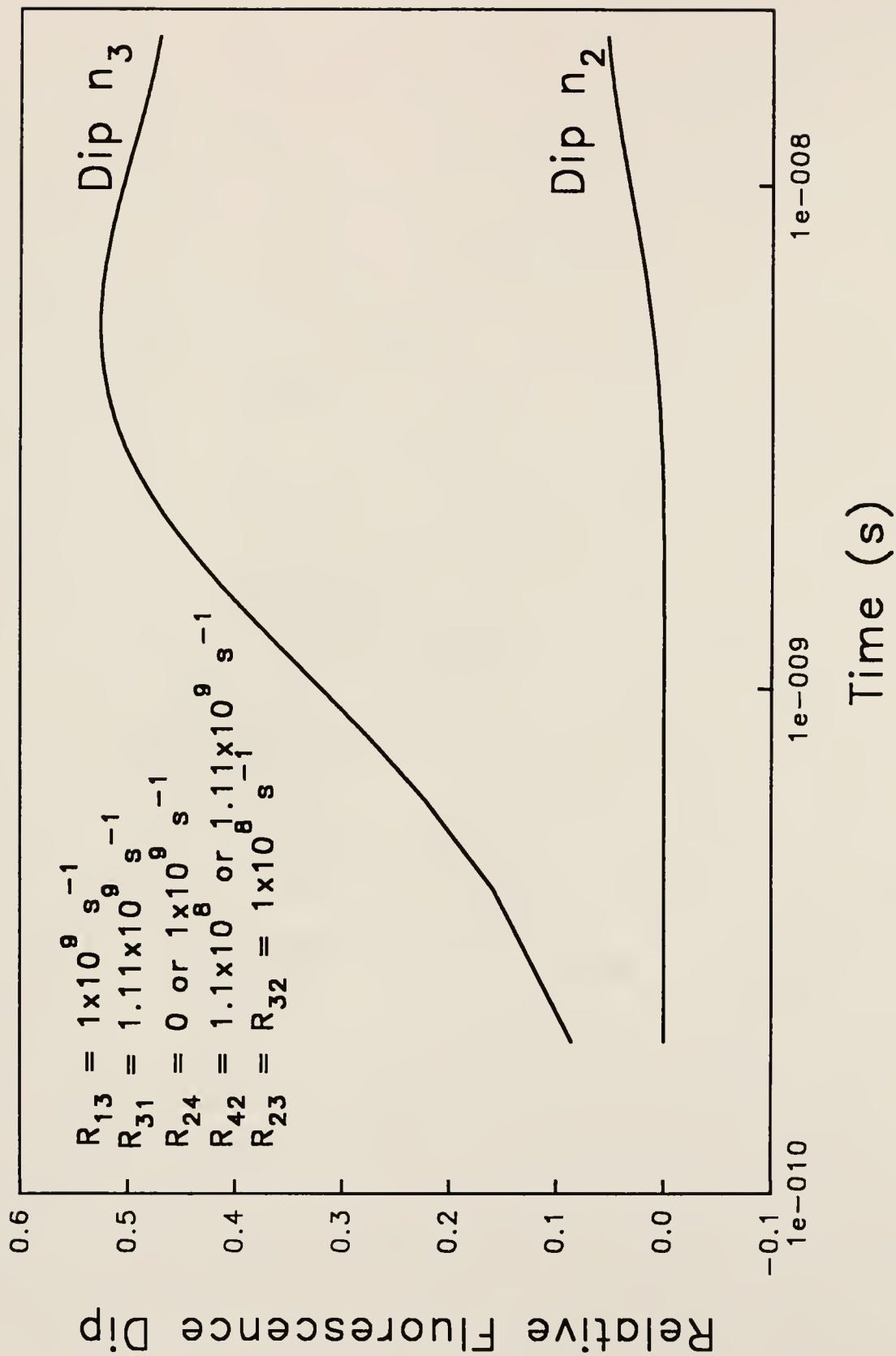


Figure 7-20 : Computer generated plots of the relative fluorescence dips as the result of excitation at first $\lambda_{1 \rightarrow 3}$ and then at both $\lambda_{1 \rightarrow 3}$ and $\lambda_{2 \rightarrow 4}$ for levels 2 and 3 versus time with moderate collisional activity between levels 2 and 3.



value was found experimentally to be closer to 1 percent, resulting in sometimes saturation conditions. This experimental parameter was, therefore, monitored quite closely, and data were only recorded when saturation conditions had been attained.

In the case of the laser responsible for the second excitation step, the laser power was measured at several orders of magnitude above that of the first excitation step, and it was assumed that this power was enough to result in saturation conditions for the transition corresponding to this excitation wavelength. This did, indeed, prove to be the case for fluorescence dip measurements taken in the ICP and ICP expansion atom sources as can be seen through the agreement of the experimental values to the theoretical values, calculated assuming saturation conditions, within experimental error (Figures 7-6 to 7-9). In the air/acetylene flame atom reservoir, however, this was not the case for the acetylene flame is the most collision rich environment used in this work, it stands to reason that the fluorescence dips with 521.820 nm as the second excitation wavelength should be equal to those with 522.007 nm with all other experimental conditions held constant. This was not the case for copper in the flame atom source, and the hypothesized explanation was that the 522.007 nm transition was not being saturated through this laser excitation. The air/acetylene flame is an atom reservoir which induces a large amount of quenching in the atom system, and this process obviously occurred to a great enough extent to prevent saturation of this transition. The 521.820 nm transition, however, does yield results agreeing with theoretical values within experimental error indicating that this transition was enjoying saturation or near saturation conditions. The probability of this transition is approximately an order of magnitude greater than that for

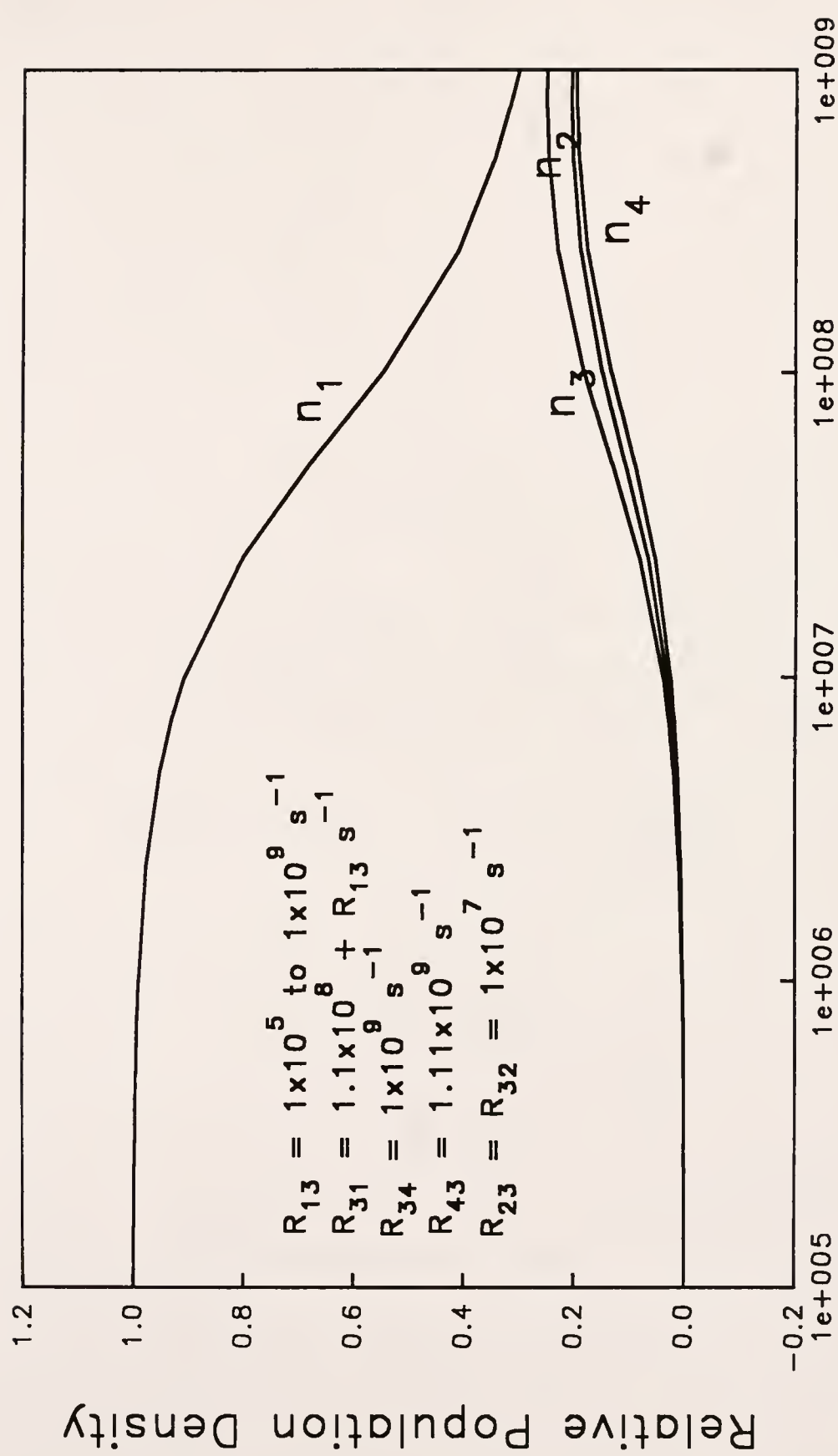
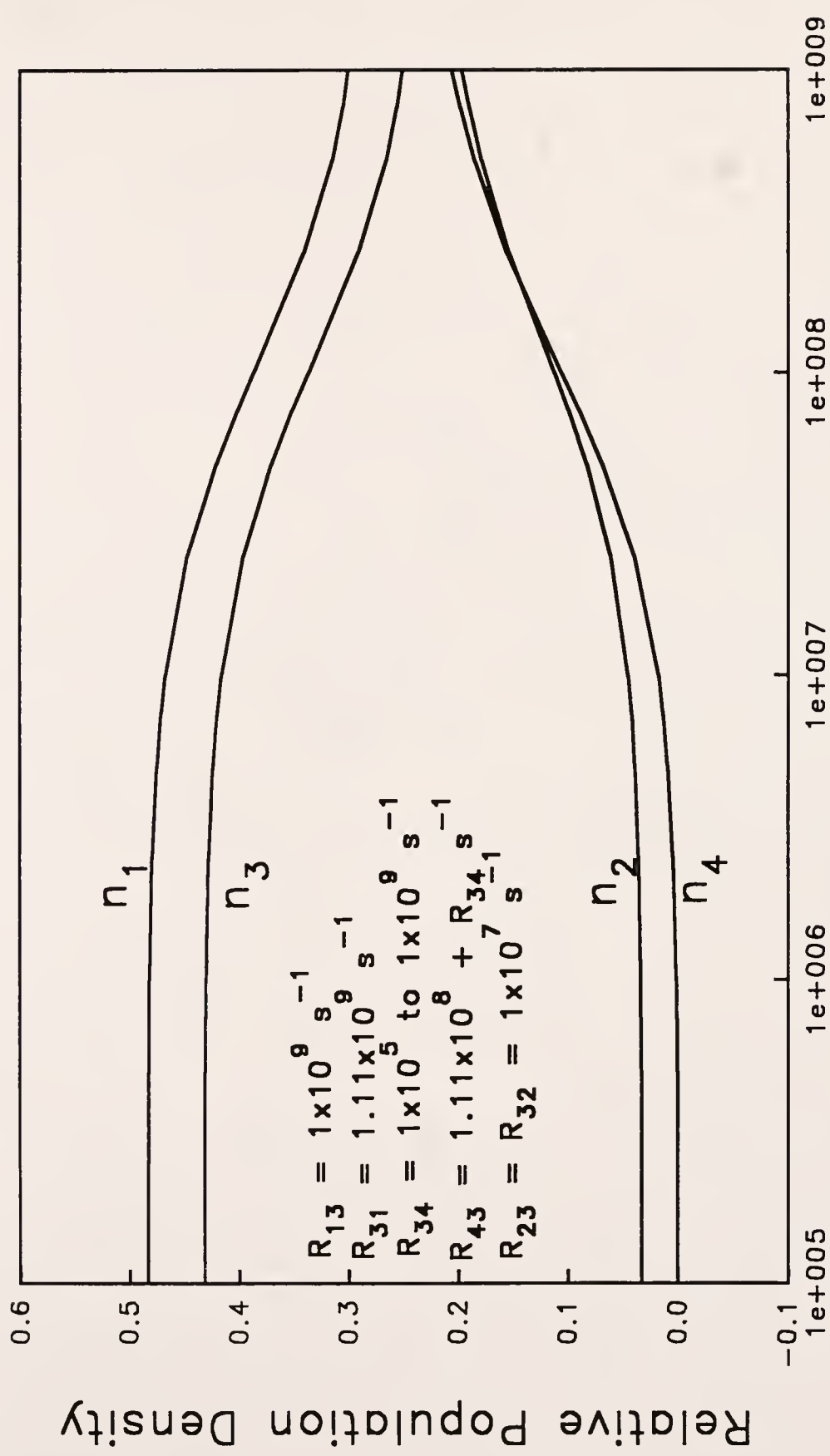


Figure 7-22 : Computer generated plots of the relative population densities of atomic levels experiencing laser excitation at $\lambda_{1\rightarrow3}$ and $\lambda_{3\rightarrow4}$ as a function of the rate of excitation for $\lambda_{3\rightarrow4}$.



the 522.007 nm transition, which explains why one transition was saturated and the other was not.

This discrepancy between experimental and theoretical values demonstrates the failure to saturate an atomic transition and the result on the fluorescence dip measurement when implementing the rate equations approach with the assumption that these saturation conditions do exist. The effect that the spectral energy density has upon the relative population densities was examined and is presented in Figures 7-21 and 7-22.

In Figure 7-21, the excitation rate from level 1 to level 3 ($B_{13}\rho,(\nu_{13})$), which is directly dependent upon the spectral energy density of the first laser, was varied while holding all other relationships between the levels constant. The de-excitation rates from the uppermost levels to one of the intermediate levels or from one of these intermediate levels to the ground level was set at $1.1 \times 10^8 \text{ s}^{-1}$ and all upwards excitation, in the absence of laser probing, was assumed to be negligible with respect to the other atomic processes. The rate of collisional exchange between the two intermediate levels was set at 1×10^7 and excitation into the ionization continuum was neglected. Figure 7-22 was generated while holding the spectral energy density of the first transition constant and varying the spectral energy density of the second excitation step.

In Figure 7-21, the relative population densities of the atomic levels quickly reach their steady state values, while in Figure 7-22, the relative population densities demonstrated a nonlinear response with increased spectral energy density of the laser responsible for the second excitation step while it did not appear that steady state values have been attained even at $1 \times 10^9 \text{ s}^{-1}$. This demonstrated the need for more laser power

of the second excitation step to achieve saturation conditions of the transitions corresponding to the wavelength of this excitation radiation.

CHAPTER 8 CONCLUSIONS

Fluorescence dip spectroscopy has been shown through the work presented in this dissertation to be greatly affected by the atom reservoir being implemented in the study as well as the collisional relationships within the analyte atom system itself. The changes in the fluorescence dip measurement can be related to the analyte type and atom source and yield information about both.

Unfortunately, the rate equations approximation was not sufficient to actually solve for physical parameters describing the relationship between the two excited state, intermediate levels in this case because there were simply too many unknown experimental parameters and physical constants for excited state transitions. It was, however, possible to study trends in the data as the atom system or atom source was changed, providing some information about both.

For the first time, the inverted fluorescence dip which was predicted through the rate equations approximation was seen in a low collisional environment with relatively large electronic spacing, as was expected. This type of fluorescence dip was only predicted when some sort of nonresonance fluorescence scheme was being studied for this theoretical treatment. The density matrix theoretical approach predicts negative fluorescence dips for resonance schemes, as well, through possible coherence effects. Since the atom sources implemented in this experimentation did not experience these

coherence effects, it was unnecessary to employ this much more complex theoretical treatment. The density matrix formalism would be necessary, however, if a lower collisional environment than those implemented in these studies was to be employed.

The implementation of this technique in other atom sources is a logical extension yielding further information about copper and silver in these atom reservoirs supplying more information about the atom systems, and, with additional information about the excited state transitions, perhaps resulting in values for the rates of exchange within these atom systems. Other atom systems could also be investigated using fluorescence dip spectroscopy, perhaps with different electronic spacing or losses to a metastable level or the ionization continuum. The latter of these suggestions (i.e. losses to a metastable or the ionization continuum) would require time dependent fluorescence dips to be monitored which was not possible with the instrumentation available in this laboratory. Time resolved fluorescence dips would yield more physical information than the steady state fluorescence dips, and this is definitely the direction of the natural progression of research in this field.

As was discussed earlier, two-step excitation and fluorescence schemes have been implemented more and more as fluorescence techniques are more frequently applied to chemical analysis. Two-step fluorescence techniques have shown remarkable improvement over comparable one-step techniques in both sensitivity and selectivity, but information must be known about the atom systems being studied in order to maximize these advantages. Collisions within the atom system induced by the atom source can greatly effect the fluorescence signal and, therefore, sensitivity. It is useful, then, to

understand these mechanisms for different atom systems in different atom reservoirs to properly choose the experimental conditions resulting in the desired information. It is, therefore, necessary to continue the implementation of fluorescence dip spectroscopy and other two-step excitation techniques as diagnostic tools providing necessary information about atom sources and the analytes investigated in them.

REFERENCE LIST

1. R.W. Wood, *Phil. Mag.*, 3, 128, 1902.
2. E.L. Nichols and H.L. Howes, *Phys. Rev.*, 23, 472, 1924.
3. C.Th.J. Alkemade, *Proc. Xth Spectrosc. Int.*, Spartan Books, Washington D.C., 1963.
4. J.D. Winefordner and T.J. Vickers, *Anal. Chem.*, 36, 161, 1964.
5. G.M. Hieftje, *Spectrochim. Acta*, 47B(1), 3, 1992.
6. N. Omenetto and J.D. Winefordner, Atomic Fluorescence Spectroscopy with Laser Excitation, N. Omenetto, Ed., John Wiley and Sons Publ., New York, 1979.
7. P.W.J.M. Boumans, *Spectrochim. Acta.*, 43B(1), 5, 1988.
8. N. Omenetto, *Spectrochim. Acta*, 43B(1), 5, 1988.
9. Alexander Scheeline, *Spectrochim. Acta*, 43B(1), 15, 1988.
10. J.M. Mermet, *Spectrochim. Acta*, 43B(1), 45, 1988.
11. C.J. Seliskar, *Spectrochim. Acta*, 43B(1), 51, 1988.
12. A.C.G. Mitchell and M.W. Zemansky, Resonance Radiation and Excited Atoms, The Macmillan Company, New York, 1934.
13. P. Pringsheim, Fluorescence and Phosphorescence, Interscience Publ. Inc., New York, 1949.
14. R.W. Wood, *Phil. Mag.*, 10(59), 513, 1905.
15. R.W. Wood and Fred L. Mohler, *Phys. Rev.*, 11, 70, 1918.
16. R.J. Strutt, *Proc. Roy. Soc.*, 91A, 511, 1914.

17. Proc. Roy. Soc., 96A, 272, 1919.
18. R.W. Wood and L. Dunoyer, Phil. Mag., 27, 1018, 1914.
19. Carl J. Christensen and G.K. Rollefson, Phys. Rev., 34, 1157, 1929.
20. R.W. Wood, Phil. Mag., 23, 689, 1912.
21. A. Bogros, Compt. Rend., 183, 124, 1926.
22. E.L. Nichols and H.L. Howes, Phys. Rev., 22, 425, 1923.
23. E.L. Nichols and H.L. Howes, Phys. Rev., 23, 472, 1924.
24. A.L. Boers, C.Th.J. Alkemade, and J.A. Smit, Physica, 22, 358, 1956.
25. J.D. Winefordner and R.A. Staab, Anal. Chem., 36(1), 165, 1964.
26. J.D. Winefordner and R.A. Staab, 36(7), 1367, 1964.
27. J.M. Mansfield and J.D. Winefordner, Anal. Chem., 37(8), 1050, 1965.
28. D.W. Ellis and D.R. Demers, Anal. Chem., 38(13), 1944, 1966.
29. D.N. Armentrout, Anal. Chem., 38(9), 1236, 1966.
30. Claude Veillon, J.M. Mansfield, M.L. Parsons, and J.D. Winefordner, Anal. Chem., 38(2), 204, 1966.
31. L.M. Fraser and J.D. Winefordner, Anal. Chem., 44(8), 1444, 1972.
32. N. Omenetto and J.D. Winefordner, Appl. Spectrosc., 26(5), 555, 1972.
33. V. Schyra, V. Svoboda, and I. Rubeska, Atomic Fluorescence Spectroscopy, Van Nostrand Reinhold Company Ltd., London, 1975.
34. A.C. Kolb and E.R. Streed, J. Chem. Phys., 20, 1872, 1952.
35. R. Klaus, Z. Klin. Chem., 4, 29, 1966.
36. V. Sychra and D. Kolihoiva, Third International Conference on Atomic Absorption and Atomic Fluorescence Spectroscopy, Paris, 1971.
37. H.T. Delves, Analyst, 95, 431, 1970.
38. J. Matousek and V. Sychra, Anal. Chim. Acta, 49, 175, 1970.

39. M.D. Amos, P.A. Bennett, K.G. Brodie, P.W.Y. Lung, and J.P. Matousek, *Anal. Chem.*, 43, 211, 1971.
40. R.M. Dagnall, M.R.G. Taylor, and T.S. West, *Lab. Pract.*, 20, 209, 1971.
41. G.F. Kirkbright, A.P. Rao, and T.S. West, *Anal. Letters*, 2, 465, 1969.
42. D.H. Cotton and D.R. Jenkins, *Spectrochim. Acta*, 25B, 283, 1970.
43. R.L. Miller, L.M. Fraser, and J.D. Winefordner, *Appl. Spec.*, 24, 477, 1971.
44. R.M. Dagnall, G.F. Kirkbright, T.S. West, and R. Wood, *Anal. Chem.*, 43, 1765, 1971.
45. V.I. Muscat, T.J. Vickers, and A. Andren, *Anal. Chem.*, 44, 218, 1971.
46. David Butcher, *Spectroscopy*, 8(2), 14, 1993.
47. N. Omenetto and J.D. Winefordner, Analytical Laser Spectroscopy, N. Omenetto, Ed., John Wiley and Sons Publ., New York, 1979.
48. M.B. Denton and H.V. Malmstadt, *Appl. Phys. Letters*, 18(11), 485, 1971.
49. L.M. Fraser and J.D. Winefordner, *Anal. Chem.*, 43(12), 1893, 1971.
50. J. Kuhl and G. Marowsky, *Optics Comm.*, 4(2), 125, 1971.
51. J. Kuhl, G. Marowsky, and R. Torge, *Anal. Chem.*, 44(2), 375, 1972.
52. E.H. Piepmeier, *Spectrochim. Acta*, 27B, 431, 1972.
53. L.M. Fraser and J.D. Winefordner, *Anal. Chem.*, 44(8), 1972.
54. N. Omenetto, N.N. Hatch, L.M. Fraser, and J.D. Winefordner, *Spectrochim. Acta*, 28B, 65, 1973.
55. N. Omenetto, N.N. Hatch, L.M. Fraser, and J.D. Winefordner, *Anal. Chem.*, 45(1), 1973.
56. N. Omenetto, P. Benetti, L.P. Hart, J.D. Winefordner, and C.Th.J. Alkemade, *Spectrochim. Acta*, 28B, 289, 1973.
57. G.D. Boutilier, M.B. Blackburn, J.M. Mermet, S.J. Weeks, H. Haraguchi, J.D. Winefordner, and N. Omenetto, *Appl. Opt.*, 17(15), 2291, 1978.
58. S.J. Weeks, H. Haraguchi, and J.D. Winefordner, *Anal. Chem.*, 50(2), 360, 1978.

59. S. Neumann and M. Kriese, *Spectrochim. Acta*, 29B, 127, 1974.
60. F.R. Preli, Jr., J.P. Dougherty, and R.G. Michel, *Anal. Chem.*, 59, 1784, 1987.
61. M. Leong, J. Vera, B.W. Smith, N. Omenetto, and J.D. Winefordner, *Anal. Chem.*, 60, 1605, 1988.
62. M.A. Bolshov, A.V. Zybin, V.G. Koloshnikov and I.I. Smirenkina, *Spectrochim. Acta*, 43B(4/5), 519, 1988.
63. N. Omenetto, B.W. Smith, and J.D. Winefordner, *Spectrochim. Acta*, 43B(9/11), 1111, 1988.
64. A. Montaser and V.A. Fassel, *Anal. Chem.*, 48(11), 1490, 1976.
65. D.R. Demers, *Spectrochim. Acta*, 40B(1/2), 93, 1985.
66. B.D. Pollard, M.B. Blackburn, S. Nikdel, A. Massoumi, and J.D. Winefordner, *Appl. Spectrosc.*, 33(1), 5, 1979.
67. M.S. Epstein, S. Nikdel, J.D. Bradshaw, M.A. Kosinski, J.N. Bower, and J.D. Winefordner, *Analytica Chim. Acta*, 113, 221, 1980.
68. N. Omenetto, H.G.C. Human, P. Cavalli, and G. Rossi, *Spectrochim. Acta*, 39B(1), 115, 1984.
69. X. Huang, J. Lanauze, and J.D. Winefordner, *Appl. Spectrosc.*, 39(6), 1042, 1985.
70. B.W. Smith, N. Omenetto, and J.D. Winefordner, *Spectrochim. Acta*, 39B, 1389, 1984.
71. B.M. Patel and J.D. Winefordner, *Spectrochim. Acta*, 41B, 469, 1986.
72. M.A. Kosinski, H. Uchida, and J.D. Winefordner, *Talanta*, 30, 339, 1983.
73. C.A. Van Dijk, P.J.Th. Zeegers, G. Nienhuis, and C.Th.J. Alkemade, *J. Quant. Spectrosc. Radiat. Transfer*, 20, 55, 1978.
74. A.W. Miziolek and R.J. Willis, *Optics Letters*, 6(11), 528, 1981.
75. M.O. Rodgers, J.D. Bradshaw, K. Liu, and D.D. Davis, *Optics Letters*, 7(8), 359, 1982.
76. M. Leong, J. Vera, B.W. Smith, N. Omenetto, and J.D. Winefordner, *Anal. Chem.*, 60, 1605, 1988.

77. M.Alden, H.Edner, P. Grafstrom, and S. Svanberg, *Optics Comm.*, 42(4), 244, 1982.
78. S. Agrup, U. Westblom, and M. Alden, *Chem. Phys. Letters*, 170(4), 406, 1990.
79. R.P. Lucht, J.T. Salmon, G.B. King, D.W. Sweeny, and N.M. Larendeau, *Optics Letters*, 365, 8(7), 1983.
80. A.W. Miziolek and M.A. DeWilde, *Optics Letters*, 9(9), 390, 1984.
81. J.E.M. Goldsmith, R.J.M. Anderson, and L.R. Williams, *Optics Letters*, 15(1), 78, 1990.
82. J.E.M. Goldsmith and N.M. Larandeau, *Optics Letters*, 15(10), 576, 1990.
83. N. Omenetto, B.W. Smith, L.P. Hart, P. Cavalli, and G. Rossi, *Spectrochim. Acta*, 40B(10/12), 1411, 1985,
84. R.M. Measures, *J. Appl. Phys.*, 39(11), 5232, 1968.
85. D.J. Kalnicky, R.N. Kniseley, and V.A. Fassel, *Spectrochim. Acta*, 30B, 511, 1975.
86. R.M. Barnes and J.L. Genna, *Spectrochim. Acta*, 36B, 299, 1981.
87. T. Edmonds and G. Horlick, *Appl. Spectroscopy*, 31, 536, 1977.
88. R.N. Savage and G.M. Hieftje, *Anal. Chem.*, 52, 1267, 1980.
89. J. Jarosz, J.M. Mermet, and J.P. Robin, *Spectrochim. Acta*, 33B, 55, 1978.
90. N.Furuta and G. Horlick, *Spectrochim. Acta*, 37B, 53, 1982.
91. G.R. Kornblum and L.deGalan, *Spectrochim. Acta*, 32B, 71, 1977.
92. J.F. Alder, R.M. Bombelka, and G.F. Kirkbright, *Spectrochim. Acta*, 35B, 163, 1980.
93. G.R. Kornblum and L. deGalan, *Spectrochim. Acta*, 29B, 249, 1974.
94. H. Uchida, K. Tanabe, Y. Nojiri, H. Haraguchi, and K. Fuwa, *Spectrochim. Acta*, 35B, 881, 1980.
95. H.R. Griem, Plasma Spectroscopy, McGraw-Hill, New York, 1864.
96. U. Westblom and S. Svanberg, *Physica Scripta*, 31, 31, 1985.

97. T.V. George and L.J. Denes, *Appl. Phys. Letters*, 26(1), 1, 1975.
98. J.D. Hey, *J. Quant. Spectrosc. Radiat. Transfer*, 17, 721, 1977.
99. G. Gillson and G. Horlick, *Spectrochim. Acta*, 41B, 1323, 1986.
100. H. Uchida, M.A. Kosinski, N. Omenetto, and J.D. Winefordner, *Spectrochim. Acta*, 39B, 63, 1984.
101. W.P. Townsend, D.S. Smyly, P.J.Th. Zeegers, V. Svoboda, and J.D. Winefordner, *Spectrochim. Acta*, 26B, 595, 1971.
102. M. Norton and A. Gallagher, *Phys. Rev. Ser. 3A*, 3, 915, 1971.
103. M. Kwaitkowski, G. Micali, K. Werner, and P. Zimmermann, *J. Phys. B : At. Mol. Phys*, 15, 4357, 1982.
104. H. Kerkhoff, M. Schmidt, U. Teppner, and P. Zimmermann, *J. Phys. B : Atom. Mol. Phys.*, 13, 3969, 1980.
105. P. Benetti, M. Broglia, and P. Zampetti, *Optics Comm.*, 36(3), 218, 1981.
106. J.M. Gagne, B. Mongeau, Y. Demers, and P. Pianarosa, *J. Opt. Soc. Am.*, 71(9), 1140, 1981.
107. U. Nielson, O. Poulsen, L. Young, *Optics Letters*, 10(12), 591, 1985.
108. H.B. Lim, R.S. Houk, M.C. Edelson, and K.P. Carney, *J. of Analyt. Atom. Spectrom.*, 4, 365, 1989.
109. W.B. Whitten, L.B. Koutny, T.G. Nolan, J.M. Ramsey, *Anal. Chem.*, 59, 2203, 1987.
110. M.Alden, H.Edner, P. Grafstrom, and S. Svanberg, *Optics Comm.*, 42(4), 244, 1982.
111. S. Agrup, U. Westblom, and M. Alden, *Chem. Phys. Letters*, 170(4), 406, 1990.
112. R.P. Lucht, J.T. Salmon, G.B. King, D.W. Sweeny, and N.M. Larendeau, *Optics Letters*, 365, 8(7), 1983.
113. A.W. Miziolek and M.A. DeWilde, *Optics Letters*, 9(9), 390, 1984.
114. J.E.M. Goldsmith, R.J.M. Anderson, and L.R. Williams, *Optics Letters*, 15(1), 78, 1990.

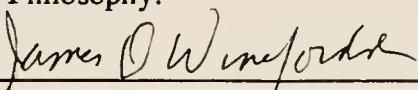
115. J.E.M. Goldsmith and N.M. Laroche, *Optics Letters*, 15(10), 576, 1990.
116. T. Ebata, N. Mikami, and M. Ito, *J. Chem. Phys.*, 78, 1132, 1983.
117. Y. Anezaki, T. Ebata, N. Mikami, and M. Ito, *Chem. Phys.*, 89, 103, 1984.
118. Y. Anezaki, T. Ebata, N. Mikami, and M. Ito, *Chem. Phys.*, 97, 153, 1985.
119. K.D. Pedrotti, *Optics Comm.*, 62(4), 250, 1987.
120. J.T. Salmon and N.M. Laroche, *Optics Letters*, 11(7), 419, 1986.
121. J.T. Salmon and N.M. Laroche, *Appl. Optics*, 26(14), 2881, 1987.
122. K.D. Bonin, M. Gatzke, C.L. Collins, and M.A. Kader-Kallen, *Phys. Rev. A*, 39(11), 1989.
123. R.H. Pogo and C.S. Gudeman, *J. Opt. Soc. Am. B*, 7(9), 1761, 1990.
124. O. Axner, M. Norberg, and H. Rubinsztein-Dunlop, *Spectrochim. Acta*, 44B(7), 693, 1989.
125. L. Xu, Y. Zhan, G. Wang, M. He, and Z. Wang, *J. Opt. Soc. Am. B*, 9(7), 1017, 1992.
126. J.B. Simeonsson, K.C. Ng, and J.D. Winefordner, 1992.
127. J.B. Simeonsson, B.W. Smith, J.D. Winefordner, and N. Omenetto, *Appl. Spectrosc.*, 45(4), 521, 1991.
128. W. Demtroder, *Laser Spectroscopy*, Springer-Verlag, Berlin, Heidelberg, 1981.
129. J.D. Ingle and S.R. Crouch, *Spectrochemical Analysis*, Prentice Hall, Englewood Cliffs, N.J., 1988.
130. J.D. Winefordner and R. Smith, *Atomic Flame Spectroscopy, Selected Topics*, R. Mavrodineau, Ed.,
131. M.A. Bolshov, A.V. Zybin, L.N. Kolonina, I.A. Majorov, I.I. Smirenkina, and O.A. Shiryayeva, *Zh. Anal. Khim.*, 39, 320, 1984.
132. P.W.J.M. Boumans, *Inductively Coupled Plasma Emission Spectroscopy - Part 1*, Wiley-Interscience, Publ., New York, 1987.
133. M.S. Hendrick, M.D. Seltzner, and R.G. Michel, *Spectrosc. Letters*, 19, 141, 1985.

134. M.S. Hendrick, M.D. Seltzer, and R.G. Michel, *Spectrochim. Acta*, 41B, 335, 1986.
135. T. Berthoud, P. Mauchien, A. Vian, and P. LeProvost, *Appl. Spectrosc.*, 41, 913, 1987.
136. D.J. Butcher, J.P. Dougherty, F.R. Preli, A.P. Walton, G.T. Wei, R.L. Irwin, and R.G. Michel, *J. of Anal. At. Spectrom.*, 3, 1059, 1988.
137. N. Omenetto, *Anal. Chem.*, 48, 75A, 1976.
138. J.W. Daily, *Appl. Opt.*, 16, 2322, 1977.
139. J.W. Daily, *Appl. Opt.*, 17, 225, 1978.
140. N. Omenetto, G.C. Turk, M. Rutledge, and J.D. Winefordner, *Spectrochim. Acta*, 42B, 807, 1987.

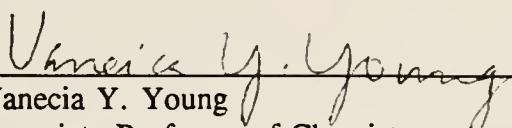
BIOGRAPHICAL SKETCH

Donna Jean Robie was born on July 12, 1966, in Toledo, Ohio. After living in Ohio for thirteen years, she moved to Orlando, FL with her family. She attended Seminole Community College from August 1984 to December 1986 from where she received her A.A. degree. She then attended the University of Central Florida from January 1987 to April 1989 and was awarded a B.S. degree in chemistry. She attended the University of Florida where she received her Ph.D., working under J.D. Winefordner from August 1989 to August 1993. She has accepted a position as a Research Food Chemist with Kellogg's in Battle Creek, MI.

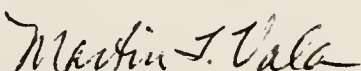
I certify that I have read this study and that in my opinion it conforms to acceptable standards of scholarly presentation and is fully adequate, in scope and quality, as a dissertation for the degree of Doctor of Philosophy.


James D. Winefordner, Chair
Graduate Research Professor of Chemistry

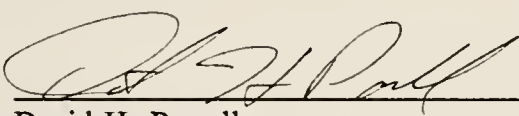
I certify that I have read this study and that in my opinion it conforms to acceptable standards of scholarly presentation and is fully adequate, in scope and quality, as a dissertation for the degree of Doctor of Philosophy.


Vanecia Y. Young
Associate Professor of Chemistry


I certify that I have read this study and that in my opinion it conforms to acceptable standards of scholarly presentation and is fully adequate, in scope and quality, as a dissertation for the degree of Doctor of Philosophy.


Martin T. Vala
Professor of Chemistry

I certify that I have read this study and that in my opinion it conforms to acceptable standards of scholarly presentation and is fully adequate, in scope and quality, as a dissertation for the degree of Doctor of Philosophy.


David H. Powell
Associate Professor of Chemistry

I certify that I have read this study and that in my opinion it conforms to acceptable standards of scholarly presentation and is fully adequate, in scope and quality, as a dissertation for the degree of Doctor of Philosophy.


Robert P. Bates
Professor of Food Science and Human
Nutrition

This dissertation was submitted to the Graduate Faculty of the Department of Chemistry in the College of Liberal Arts and Sciences and to the Graduate School and was accepted as partial fulfillment of the requirements for the degree of Doctor of Philosophy.

December 1993

Dean, Graduate School

UNIVERSITY OF FLORIDA



3 1262 08556 8623